Dissolved oxygen fluxes and ecosystem metabolism in an eelgrass (*Zostera marina*) meadow measured with the novel eddy correlation technique

Andrew Christer Hume
Alexandria, Virginia

B.A. Environmental Science, University of Virginia, 2005

A thesis presented to the Graduate Faculty
of the University of Virginia in Candidacy for the Degree of
Master of Science

Department of Environmental Science

University of Virginia
May 2008

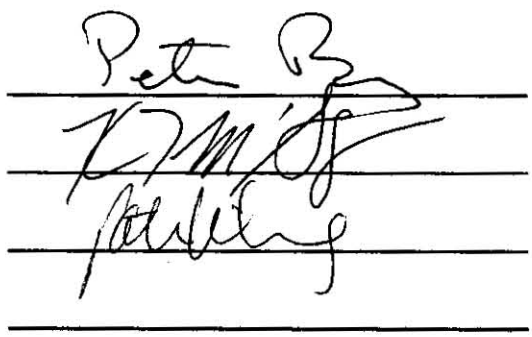

Abstract:

Community metabolism was measured using the novel *in situ* eddy correlation technique in a restored eelgrass (*Zostera marina*) meadow and a nearby bare sediment substrate, located in a coastal bay off the eastern shore of Virginia, USA. Dissolved oxygen (DO) fluxes were measured at 64 Hz (64 times per second) and cumulative fluxes were calculated at 15-min intervals. High variations in these measurements indicate the importance of measuring ecosystem metabolism under natural environmental conditions. Multiple linear regressions of environmental variables show significant relationships between hourly DO fluxes and photosynthetically active radiation (PAR) and significant wave height for both the seagrass-dominated and the bare sediment community. This study is the first to report a significant relationship between DO fluxes and significant wave height over a seagrass-dominated sediment. Mean hourly DO fluxes from multiple eddy correlation deployments were used to calculate community respiration (R), gross primary production (GPP), and net ecosystem metabolism (NEM) during the study period. Rates of seagrass-dominated community R, GPP and NEM were: -120.0 ± 39.2, 143.2 ± 33.2 and 23.2 ± 29.9 mmol O_2 m^{-2} d^{-1}, respectively. The nearby bare sediment R, GPP and NEM were: -64.5 ± 28.7, 25.3 ± 15.8 and -39.2 ± 13.1 mmol O_2 m^{-2} d^{-1}, respectively. Estimates of C cycling suggest that the bare sediment is a net source of C while the vegetated substrate was a net sink. N assimilation calculations based on the C metabolism indicate an increased assimilation and temporary retention of N in the benthic community as it shifts from bare to algal-dominated and ultimately seagrass-dominated substrate with the successful seagrass restoration efforts. A comparison was made

between the eddy correlation technique and the conventional open-water technique using a water quality datasonde. Our results indicates that the eddy correlation technique has significant advantages over this, and other, conventional techniques in that it: 1) captures short-term variability in oxygen metabolism that result from environmental variations in light, current, and wave energy; 2) accurately integrates over a large area and thus captures small-scale heterogeneity; 3) is non-invasive and allows for true *in situ* light and hydrodynamic conditions; and 4) can be used over topographically complex substrates where conventional methods may fail.

Acknowledgments:

This research would not be possible without imagination and persistence of my major advisors, Peter Berg and Karen McGlathery. Their dedication, advice and generosity have made this experience truly extraordinary. I would also like to thank Pat Wiberg for her synthesis of ideas throughout this project. I'd like to thank the staff of the University of Virginia ABCRC/LTER field station for all their logistical support. A special thanks goes to my REU Josh Richards for his assistance in the field. I would also like to acknowledge the 1972 Aquasport for allowing me to carry on the tradition and not giving up on me (mostly). Lastly, I would like to thank my parents for introducing me to and inspiring my curiosity in the natural world. This research was funded by National Science Foundation grant DEB-0621014 to the Virginia Coast Reserve LTER. Some of the data used in this publication were provided by the Virginia Coastal Reserve LTER project, which was supported by National Science Foundation grants BSR-8702333-06, DEB-9211772, DEB-9411974 and DEB-0080381 and DEB-0621014.

Table of Contents:

List of Tables

List of Figures

Introduction:

Rates of community respiration (R) and net production (P) are used commonly as measures of gross primary production (GPP) and net ecosystem metabolism (NEM), and provide valuable information about ecosystem function in coastal environments (e.g. Caffrey 2004). Seagrasses are known to inhabit approximately 10% of shallow coastal environments around the world (Charpy-Roubaud and Sournia 1990, Larkum et al. 2006). Seagrass-dominated ecosystems serve many functions such as baffling wave energy and stabilizing sediments (Fonseca 1989, Fonseca and Kenworthy 1987, Fonseca and Cahalan 1992, Madsen et al. 2001), improving water clarity (Madsen et al. 2001, Agawin and Duarte 2002), providing refuge for fauna (Bostrom et al. 2002, Hovel et al. 2002, Hovel 2003), acting as nutrient filters (Bricker and Stevenson 1996, D'Avanzo et al. 1996, Welsh et al. 2000, Kemp et al. 2005), sequestering carbon (Duarte 2002), and serving as biological indicators of ecosystem health (Fourqurean et al. 1997, Bostrom et al. 2002, Lee et al. 2004, Orth et al. 2006). Seagrass-dominated environments are thought to be among the most productive ecosystems in the world and represent importance parameters in global C and N models (Kemp et al. 1997). With the pressure of eutrophication from anthropogenic sources in response to coastal development, understanding seagrass-dominated ecosystem metabolism is essential to accurately predict responses to increased pollution (Orth and Moore 1983, Short et al. 1995, Hauxwell et al. 2003).

Background: In 2003, Berg et al. demonstrated the successful application of a commonly used atmospheric technique based on eddy correlation to measure dissolved oxygen (DO) fluxes from the sediment-water interface. This technique exploits the relationship between simultaneous measurements of eddy turbulence and solute concentration at a single point to calculate a flux (Wyngaard 1989) on the same high temporal resolution as the turbulent eddies. With recent advances in marine instrumentation, adaptation of the eddy correlation technique to marine environments has become relatively simple and elegant. The *in situ*, and more importantly, non-intrusive nature of the technique alleviates many of the problems associated current DO flux measurements. Because of its passive sampling without disturbance of the sediment, the measurements represent a true flux as influenced by natural variations in the environment, including light availability, currents and wave energy. This technique can be used over substrates that include vegetation, benthic fauna and bare substrate. As Berg et al (2007) demonstrate, the "footprint" that contributes to the flux measurements is predictable and integrates over a larger area than benthic chambers, on the scale of 100 m^2 compared < 1 m^2 that is typical of chamber measurements. This effectively eliminates the potential sampling bias associated with the small-scale heterogeneity that is typical in these systems (Jorgensen and Revsbech 1985, Fenchel and Glud 2000, Wenzhöfer et al. 2004, Thouzeau 2007). To date, the technique has only been used to measure DO fluxes over cohesive and permeable bare sediments (Berg et al. 2003, Kuwae et al. 2006). This study represents the first application of this technique to vegetated marine sediments.

Many different methods have been used to determine rates of aquatic ecosystem metabolism including photosynthesis-irradiance (P-I) curves (e.g. Kraemer and Alberte

1993), labeled isotopes tracers (e.g. Lindeboom and deBree 1982), primary production biomass and growth (e.g. Hasegawa et al. 2007), mass balance models (e.g. Kemp et al. 1997, Kaldy et al. 2002), and diurnal fluxes of DO and dissolved inorganic carbon (DIC) (Odum 1956). The DO flux approach is arguably the most commonly used method because it is relatively inexpensive and simple to perform. Currently, the most common approaches for measuring DO fluxes are either continuous measurements in the water column or discrete measurements from *in situ* benthic chambers or laboratory incubations of substrate cores. Open-water measurements estimate DO fluxes based on changes in DO concentrations over a diurnal cycle (Odum 1956, Seeley 1969), and are performed commonly with water quality datasondes or periodic water sampling. The open-water approach has been used widely in coastal bays (e.g. Nixon and Oviatt 1972, Moriarty et al. 1990, Marino and Howarth 1993, D'avanzo et al. 1996, Ziegler and Benner 1998, Caffrey 2004), including seagrass-dominated environments (Murray and Wetzel 1987, Martin et al. 2005). *In situ* benthic chambers and laboratory incubations calculate rates of ecosystem metabolism based on DO fluxes within the microcosm measured in the light and dark (e.g. Odum 1957, Pamatmat 1968, Lindeboom and DeBree 1982, Jahnke 1989, Pinckney and Zingmark 1991, Malan & McLachlan 1991, Erftemeijer et al. 1993, Glud et al. 1999, Hansen et al. 2000, McGlathery et al. 2001, Wenzhofer & Glud 2004). Because of the dynamic physical nature of coastal environments, accurate measurements of DO fluxes are difficult with these microcosm methods (Kemp and Boynton 1980).

A number of environmental variables are known to influence DO flux dynamics. Over bare sediments DO fluxes can be influenced by horizontal pressure differences due to flows over microtopography (Forster et al. 1996, Roy et al. 2002, Huettel et al. 2003,

Roy et al. 2005), bioroughness (Huettel and Gust 1992, Ziebis et al. 1996), bioirrigation (Berg et al. 2001, Meysman et al. 2005), decreasing diffusion boundary layer thickness with increasing flow (Jorgensen and Revsbech 1985, Berninger and Huettel 1997), wave action (Prech and Huettel 2003, Prech and Huettel 2004, Prech et al. 2004), phytoplankton advection and degradation in the sediment (Huettel and Rusch 2000, Ehrenhauss and Huettel 2004, Franke et al. 2006), and the effects of variable light on benthic primary producers (Pinckney and Zingmark 1991, Stutes et al. 2006). These variations in DO fluxes can in turn influence ecosystem metabolism.

Previous studies using open-water, benthic *in situ*, and laboratory cores in seagrass-dominated ecosystems have explained some of the variation in ecosystem metabolism with several physical variables including photosynthetically active radiation (PAR) (Moncreiff et al. 1992, Ziegler and Benner 1998), water temperature (Moriarty et al. 1990, Moncreiff et al. 1992, Ziegler and Benner 1998, Plus et al. 2001, Caffrey 2004) and current flow (Nixion and Oviatt 1972, Fonseca and Kenworthy 1987, Koch 1994, Binzer et al. 2005, Abdelrhman 2007).

Current flow is one physical parameter that is suspected to influence seagrass community metabolism in several ways. It is hypothesized that the increased light availability that results from the settling of suspended particles as the seagrass blades attenuate current flow increases seagrass photosynthesis (Fonseca & Kenworthy 1987, Koch 2001, Agawin & Duarte 2002). Different unidirectional flow regimes also can change seagrass canopy morphology and ultimately influence seagrass photosynthesis. With increasing flows, the canopy moves from an erect state to gentle swaying to coherent swaying (monami) (Ghisalberti and Nepf 2002, Ackerman and Okubo 1993)

and finally to canopy compression ((Fonseca & Kenworthy 1987) (Nepf and Vivoni 2000). When the canopy becomes compressed, reduced within-canopy mixing and increased self-shading have been shown to decrease seagrass photosynthesis (Nepf 1999, Fonseca et al. 1982). In contrast, the swaying from surface waves and monami is hypothesized to enhance within canopy mixing and increase seagrass photosynthesis (Grizzle et al. 1996, Koch & Gust 1999). At the leaf surface, decreases in the diffusive boundary layer with increasing current flow are known to enhancing nutrient uptake and gas exchange, both of which may enhance seagrass photosynthesis (Fonseca & Kenworthy 1987, Gambi et al. 1990, Koch 1994).

If environmental variables are known to strongly influence DO fluxes and ecosystem metabolism, it is reasonable to ask how accurate are the conventional DO flux methods? Comparative studies have shown that open-water measurements of ecosystem metabolism tend to be higher than benthic chamber, and it has been suggested that this difference is due to the influence of physical forcing on open-water measurements (Kemp and Boynton 1980, Ziegler and Benner 1998).

Purpose: The purpose of this research was to utilize the eddy correlation technique to measure DO fluxes and to calculate ecosystem metabolism from a recently restored seagrass-dominated site and an adjacent bare sediment site in a temperate coastal bay off the eastern shore of Virginia, USA. These results were compared to concurrent open-water datasonde measurements. Because of the high temporal resolution of the eddy correlation technique, correlations between DO fluxes and several environmental variables were made to explain observed variations in DO fluxes. Assumptions that go

into measuring DO fluxes and calculating ecosystem metabolism with the eddy correlation technique are reviewed and compared with current approaches. Finally, rates of N assimilation and implications for ecosystem function and seagrass recolonization are considered. This research provides the first glimpse of short-term temporal dynamics of oxygen exchange from seagrass and bare sediment substrates under true *in situ* environmental conditions.

Materials and Methods:

Site description: South Bay (37º 15'13.86" N, 75º 48'43.70" W) is a typical coastal bay located on the mid-Atlantic east coast of North America. South Bay is within the Virginia Coastal Reserve (VCR) and is part of the Long Term Ecological Research (LTER) site network. It is exposed to the north and south by coastal inlets (Figure 1) and is bordered by the Delmarva Peninsula to the west and barrier islands to the east. South Bay is shallow (average depth <1 m at MLW) and has a semi-diurnal tidal range of ~ 1.5 m. South Bay is fed by a small watershed of approximately 571 ha on the Delmarva, of which approximately 50% was agricultural in 1995 (Arnold et al. 2004). Historically, the coastal lagoons of the Delmarva Peninsula flourished with meadows of eelgrass (*Zostera marina*), but these fell victim to the marine slime mold *Labyrinthula zosterae* in the 1930s (Orth and Moore 1983, Moore et al. 1996, McGlathery et al 2001, Orth et al. 2006). The combined effects of the *L. zosterae* pandemic and a powerful hurricane in 1933 caused the local extinction of *Z. marina* in the region (Orth et al. 2006). After the discovery of natural patches of *Z. marina* in South Bay in the late 1990's, large restoration efforts by seeding were conducted in South Bay from 2001 through 2004 (Orth et al. 2003) and have recently shown significant success (Orth et al. 2006). By 2003, over 150 ha of restored seagrass habitat was mapped in the Virginia coastal bays. The seagrass meadows sampled in this study were approximately 5 years old at the time of sampling. The permeable sediments were composed of fine sands, with <10 % mud (Lawson 2008).

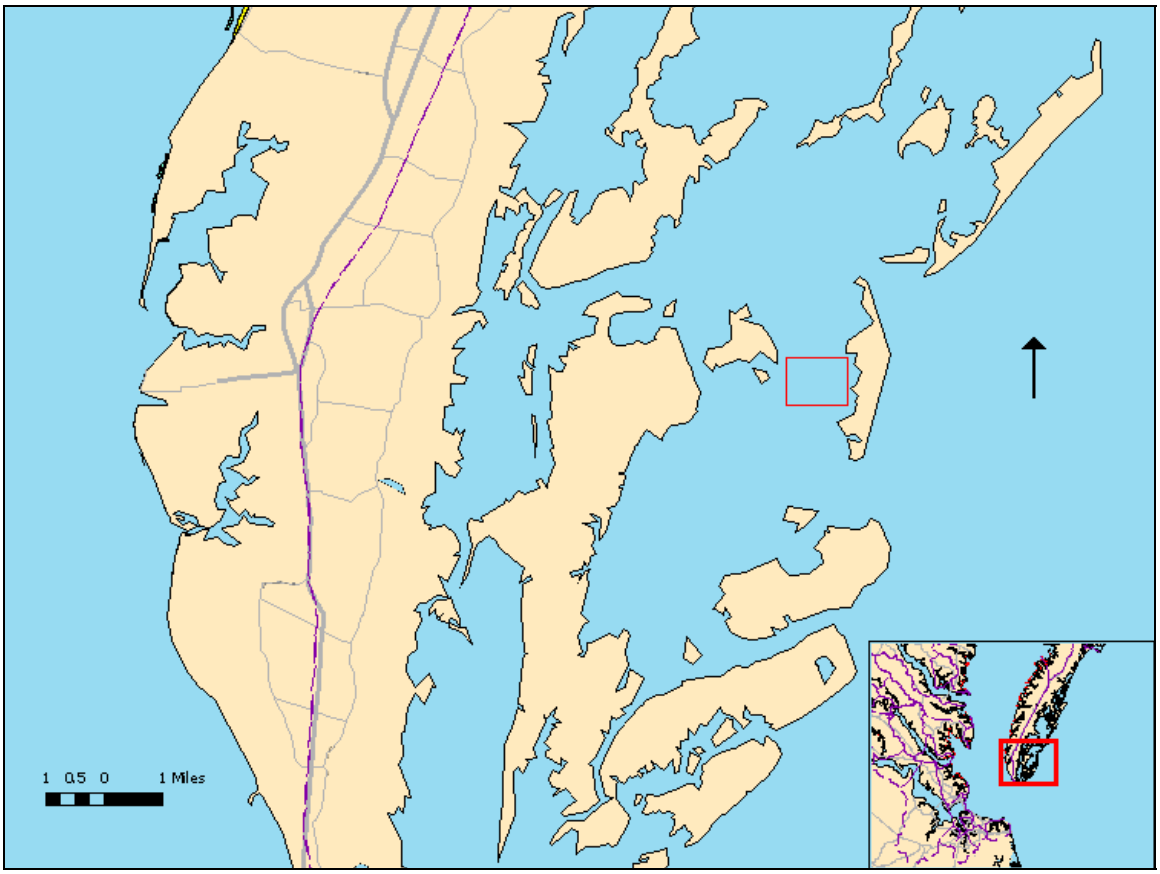

Figure 1. Site map of the coastal lagoons off the Delmarva Peninsula (inset). South Bay is highlighted by the red square.

Site selection: Two sampling sites were established within South Bay. The first site, referred to as the vegetated site, was in a 0.4 ha *Z. marina* meadow restored in 2002 (Orth et al. 2006). The second site, referred to as the bare sediment site, was a bare permeable sediment substrate with an area of approximately 0.3 ha approximately 200 m east of the vegetated site. Sites were marked with a physical marker and GPS to ensure accurate replication of deployments.

Site characterization: Six 10 ml sediment cores were taken on July 9th, 2007 of the upper 3 cm of sediment surface from both sites, homogenized and kept frozen and in the dark until analyzed. The cores were analyzed for porosity, organic matter and benthic chlorophyll a on 4 replicate samples from each core. Benthic chlorophyll a concentrations were determined following the methods described by McGlathery et al. (2001). Seagrass canopy height was measured *in situ* at 50 randomly selected locations within the vegetated site. Shoot density was randomly measured *in situ* by counting all the shots within a 0.25 m^2 quadrant at 6 locations within the vegetated site.

Eddy correlation technique: An eddy correlation system similar to the one used by Berg et al. (2003) was developed as a prototype commercial product (Unisense A/S, Denmark). In short, a Vector acoustic Doppler velocimeter (ADV) (Nortek AS, Norway) was modified to interface with a Clark-type microelectrode through a picoamplifier (Unisense A/S, Denmark). Fabrication of this prototype was a collaborative effort between the respective companies and the Max Plank Institute for Marine Microbiology, Germany and the University of Virginia, USA. The sensors were mounted on a custom-

built stainless steel tripod frame with the ADV vertically aligned facing the sediment surface and the microelectrode and picoamplifier positioned at approximately a 45° angle (Figure 2) with the microelectrode tip on the edge of the ADV measuring volume downstream of the ADV (Figure 3).

DO fluxes were measured over diurnal cycles from June 18 – July 19, 2007 at the vegetated and bare sediment sites. A total of 12 deployments were made, alternating between the two sites. Concurrent deployments with a water quality datasonde (YSI Inc., Yellow Springs, Ohio) were made at each site to compare the two techniques for calculating DO fluxes and ecosystem metabolism (Figure 2). The eddy correlation system was always deployed with a northerly orientation at low tide. Eddy correlation measurements were made at 64 Hz for 14.5 min with a 0.5-min "sleep" period for approximately 24 hr. Because of the fragile nature of the microelectrode, some deployments were truncated due to a broken microelectrode. The eddy correlation system was positioned to measure DO fluxes approximately 15 cm above the sediment surface at the bare sediment site. At the vegetated site, the eddy correlation system was positioned to measure at the top of the seagrass canopy (approximately 25 cm above the sediment surface). DO also was measured with a handheld YSI 550A membrane probe DO meter (YSI Inc., Yellow Springs, Ohio) at the beginning and end of each eddy correlation deployment to calibrate the microelectrode.

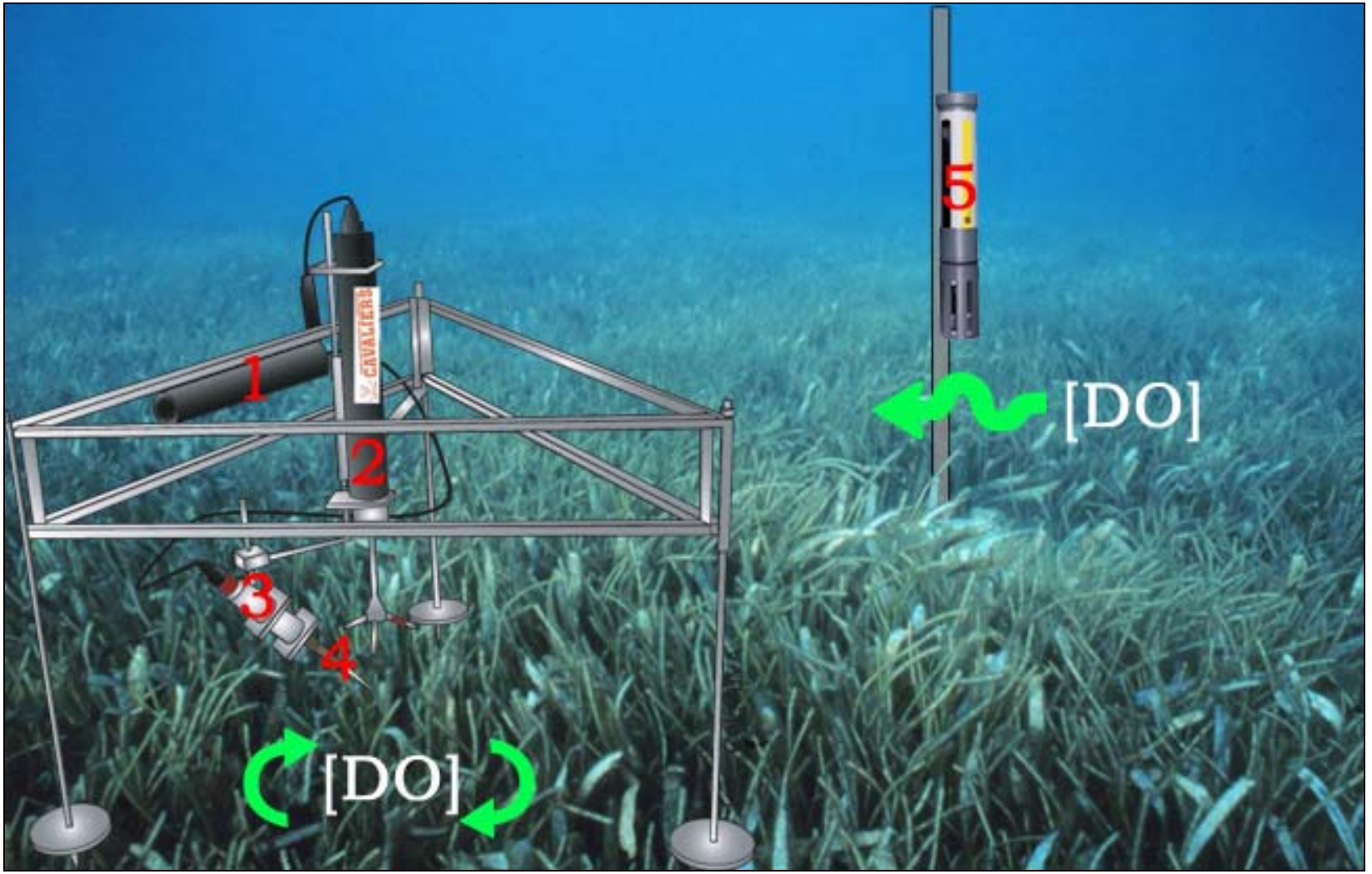

Figure 2: Schematic of DO Flux measurements: Eddy-correlation sensors assembled on stainless steel tripod frame: 1) External battery housing; 2) acoustic Doppler velocimeter; 3) O_2 Picoamplifier; 4) Oxygen microelectrode. Open-water method: 5) water quality datasonde.

Eddy correlation system:

Acoustic Doppler velocimeter (ADV): A bistatic sonar ADV equipped with an internal data logger modified to interface with the O_2 picoamplifier was used for this study. While the external sensors were logged at a user-defined frequency (≤ 64 Hz), the ADV sampled velocities at a higher internal ping rate (100 – 250 Hz) and logs an average value (Vector User Manual p.24, Nortek AS, Norway). When used for eddy-correlation measurements, the ADV and microelectrode are oriented so that the tip of the microelectrode rests on the edge of the 1.5 cm x 1.5 cm cylindrical measuring volume located 14.9 cm below the center of the ADV center sensor (Figure 3).

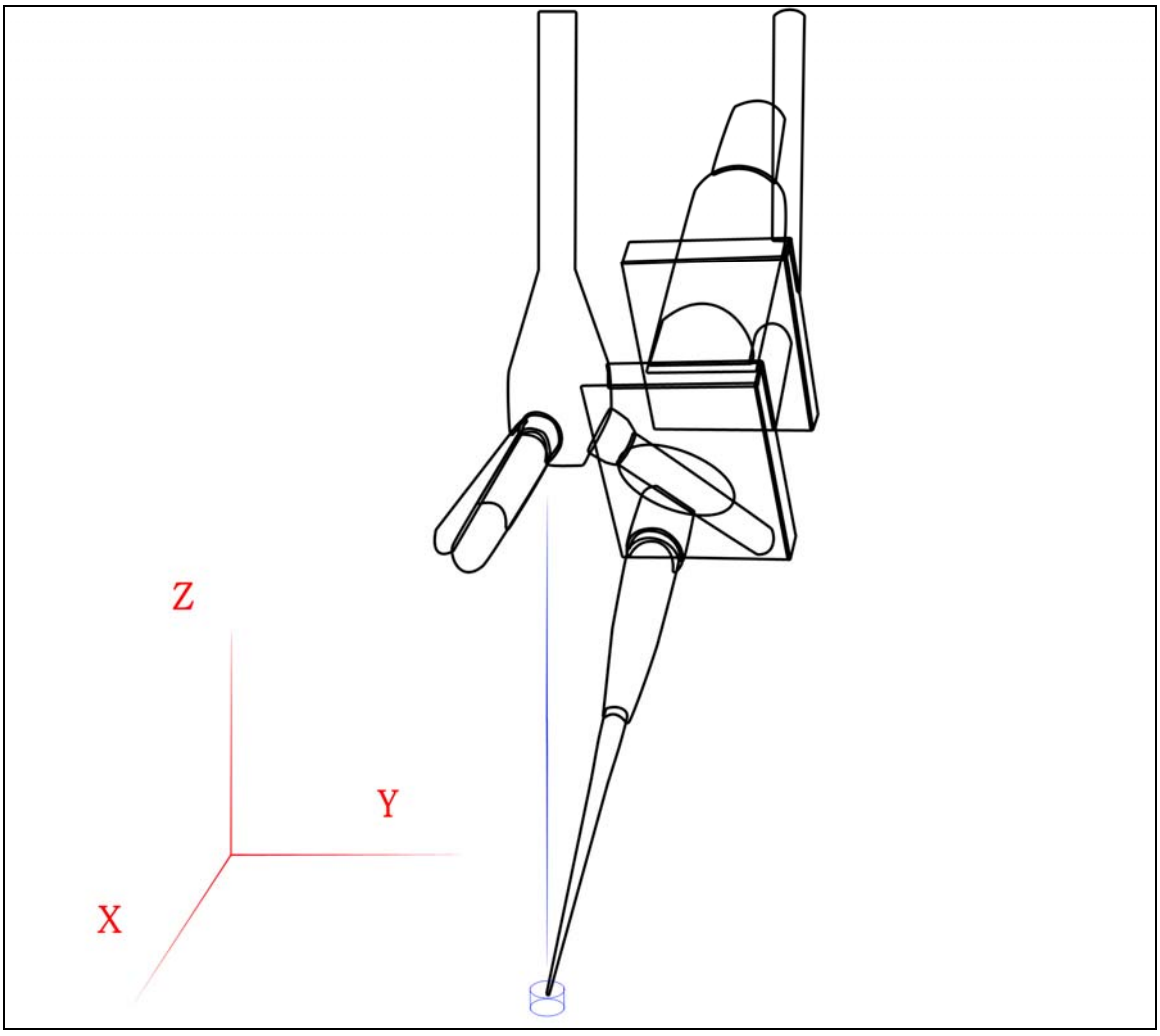

Figure 3: Three-dimensional field orientation of the ADV and microelectrode with respect to the ADV's measuring volume (blue cylinder).

Oxygen picoamplifier: Oxygen microelectrodes require a constant source of negative electronic potential to measure DO. This is supplied by the picoamplifier while it simultaneously measures the reduction of DO on the microelectrode's cathode (in picoamps). A submersible picoamplifier custom built at the Max Planck Institute for Marine Microbiology, Germany was used in this study. The picoamplifier outputs three analog signals (Max Planck Institute for Marine Microbiology, Germany):

1. ALL: Voltage equivalent of the measurement current in the sensor.
   Calibration: 10mV per 1pA sensor current
2. AC: Voltage equivalent of the of the AC component in the sensor.
   Calibration: 100mV per 1pA sensor current.
3. DC: Voltage equivalent of the of the DC component in the sensor.
   Calibration: 10mV per 1pA sensor flow.

The AC and ALL signals are logged by the ADV's data logger simultaneously within the three-dimensional velocity field. In order for the ADV to log the voltage signals, they are first converted into a universal 16-bit integer proprietary to ADV referred to as Counts (Vector User Manual p.33, Nortek AS, Norway). The voltage, U (in millivolts), is converted into counts using the following equation:

$$Counts = 32768 + \frac{65535 - 32768}{2500} U \qquad (1)$$

Oxygen microelectrode: Clark-type oxygen microelectrodes (Figure 4) measure DO based on an electrical current generated by the oxidation of DO on the cathode of the microelectrode. The current produced (in picoamps) is linearly related to the oxygen partial pressure in the surrounding environment. Microelectrodes used in this study were fitted with guard cathodes that oxidize diffused oxygen present in the electrolyte behind the measuring cathode (Revsbech 1989). Prior to deployments, microelectrodes were polarized at –0.8 V overnight to ensure there was no drift in the signal as a result of residual DO in the electrolyte. Microelectrodes were attached to the picoamplifier via an Impulse waterproof miniature high-density connector (Impulse Enterprise, Inc. USA). A brass cone-shaped fitting screws over top of the microelectrode and holds it in place. Desiccant material was placed inside the brass electrode holder to keep the connections dry. Finally, silicone aquarium sealant was used to make a watertight seal around the shaft of the microelectrode and the electrode holder (Figure 4). Oxygen microelectrodes used in this study were custom built to have a fast response time of approximately 0.2s.

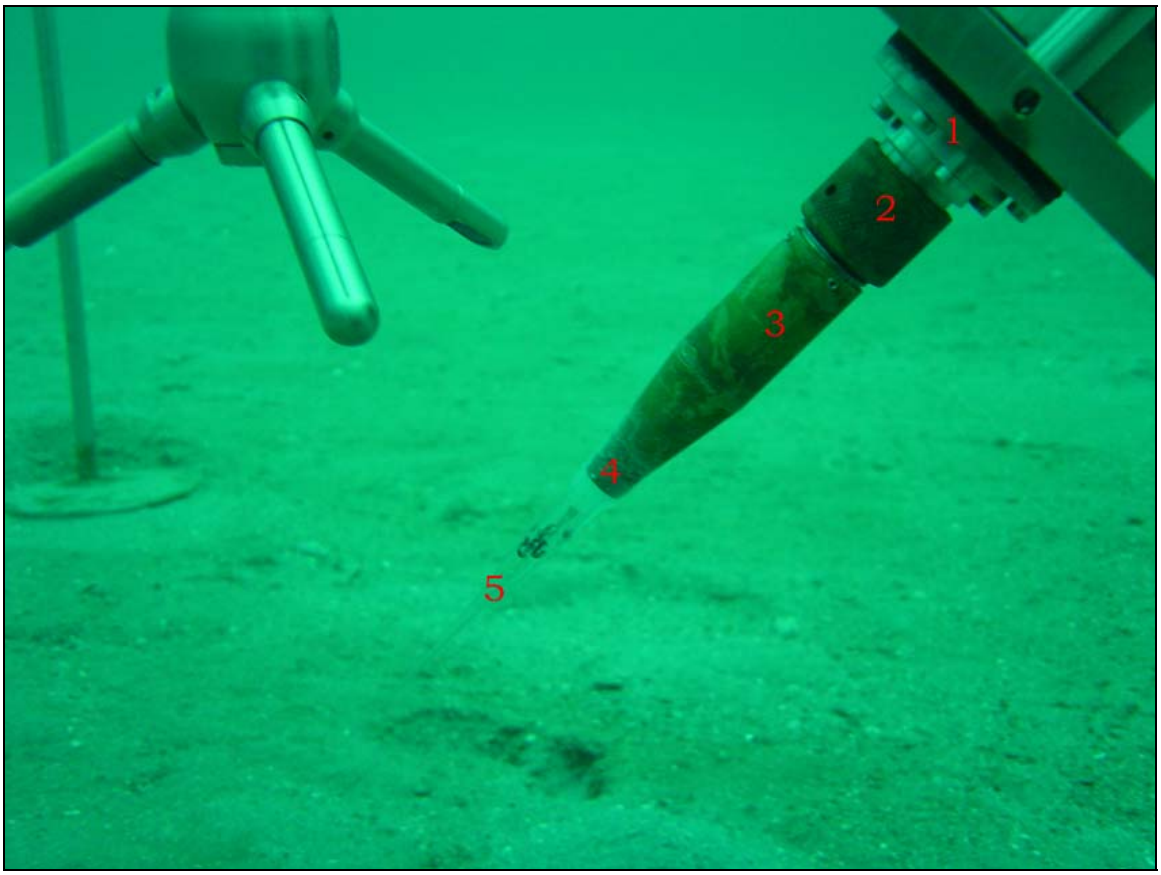

Figure 4: Example of eddy correlation system microelectrode interface with picoamplifier: (1) picoamplifier; (2) Impulse connector; (3) brass electrode holder; (4) silicone sealant; (5) microelectrode.

Environmental variables: Three HOBO pendant temperature-light data loggers (Onset Computer Corporation, USA) were attached to the top of the eddy correlation system tripod to sample light intensity (lum m^{-2}) every 0.5 min. Significant wave height and current direction were calculated from the ADV using the PUV method based on an 8.5-min energy spectrum using QuickWave Software (Nortek AS, Norway) and are reported as mean values for each 15 min measurement period. The ADV also measured water temperature and depth at 1 Hz and 64 Hz respectively. Wind speed was collected from a propeller anemometer mounted approximately 4 m above sea level on a meteorological tower on Hog Island and extrapolated from hourly measurements to 15 min using MATLAB (MathWorks, Inc., USA). Photosynthetically active radiation (PAR) data was also collected from the meteorological tower using a LI-COR 190 quantum sensor (LI-COR Biosciences) measuring every minute and expressed as hourly sums. The anemometer and quantum sensor data are part of the LTER meteorological network (http://www.vcrlter.virginia.edu/data/metdata/index.html).

Eddy correlation DO flux calculations: The vertical flux of any scalar (C) in a turbulent flow can be expressed as:

$$Flux = u_Z C - D\frac{dC}{dz} \qquad (2)$$

where u_Z is the vertical component of the three-dimensional velocity field and D is the molecular diffusivity of the solute in seawater. Since advection is the dominant transport process in turbulent flows above the diffusive boundary layer, molecular diffusion can be neglected. Using Reynolds decomposition, u_Z and C can be split into its two components, a

mean component and a fluctuating component (i.e. $u_Z = \overline{u_Z} + u'_Z$, where $\overline{u_Z}$ is the mean vertical velocity and u'_Z is the turbulent fluctuation around the mean).

In order to calculate u'_Z and C', the means $\overline{u_Z}$ and $\overline{C}$ must be defined. This can be a challenge in dynamic systems like shallow coastal bays where environmental variability is often observed. Linear detrend and a running averaging were used to define $\overline{u_Z}$ and $\overline{C}$ (Stull 1988). Linear detrend defines $\overline{u_Z}$ and $\overline{C}$ as the linear least squares regression fit to u_Z or C. In dynamic systems $\overline{C}$ may behave linearly over a few minutes, but is typically nonlinear over 0.5 to 1 hr. To account for the nonlinear nature of $\overline{C}$, a running averaging was also used. A running average produces a dynamic mean that reflects fluctuations in the ambient value larger than the applied averaging window. The averaging window used for calculating $\overline{u_Z}$ and $\overline{C}$ during this study was held constant at 3481 samples, equivalent to 1 min at 64 Hz.

The decompositions of u_Z and C are substituted into Equation 2 and the result is averaged over time. The averages of u'_Z and C' equal zero. Because of the relationship between u'_Z and C' (i.e. the eddy correlation), the average of their product is non-zero. Assuming the mean vertical velocity, $\overline{u_Z}$ is equal to zero, the time-averaged flux of C can be expressed as:

$$\overline{Flux} = \overline{u'_Z C'} \qquad (3)$$

Eddy correlation DO flux data treatment: Fifteen min averages of the DO flux using the running averaging and linear detrend were calculated from the raw data (Figure 5). These were related to the following environmental variables, also averaged over 15-min: water temperature, the three-dimensional velocity field, water column DO concentrations measured with the microelectrode, significant wave height, current

direction, and light intensity. Any DO fluxes that deviated considerably from neighboring values were examined more closely for unnatural disturbance from the measured environmental variables for the respective 15-min average. DO fluxes found to be unnaturally influenced were removed from further analysis.

Eddy correlation DO flux software: Measuring with the eddy correlation system at 64 Hz for of 24 hr resulted in over 5.5 million measures of the three-dimensional velocity field and simultaneous DO concentrations per deployment. To expedite the calculations of the DO fluxes, software was developed by Peter Berg at the University of Virginia. Software input parameters can be found in Tables A1 and A2 of the Appendix. For more thorough explanations of eddy correlation DO flux calculations, see Stull (1988), Berg et al. (2003) and Kuwae et al (2006).

Eddy correlation metabolism: Fifteen-min averages of running average and linear detrend DO fluxes and associated environmental variables were group into hourly averages and paired with the measured values of PAR. These hourly averages of the running average and linear detrend DO fluxes were used to calculate metabolism rates of R, GPP and NEM as shown below. Three or more 15-min DO fluxes were used to calculate hourly means (Figure 5). When two or fewer 15-min DO fluxes were present within an hour (due to removal during data treatment), then neighboring 15-min DO fluxes and PAR were used to interpolate an hourly average. These interpolated hourly DO fluxes were only used to estimate ecosystem metabolism.

Hourly DO fluxes were separated into light (>10,000 μEin m^{-2}) and dark (<10,000 μEin m^{-2}) periods. Averages of the DO flux with units of mmol O_2 m^{-2} d^{-1} were reduced to hourly rates (mmol O_2 m^{-2} hr^{-1}). This allowed a weighting of the ecosystem

metabolism parameters based on number of hours of dark and light periods with unequal length during the summer in the northern hemisphere. R was calculated as the sum of all hourly DO fluxes measured in the dark plus the mean of all hourly DO fluxes measured in the dark multiplied by the number of hours of daylight, as follows:

$$R = \sum(Flux_{DARK}) + \overline{Flux}_{DARK} h_{LIGHT} \quad (4)$$

where $Flux_{DARK}$ is hourly DO fluxes measured in the dark, $\overline{Flux}_{DARK}$ is the mean DO flux in the dark, and h_{LIGHT} is the number of hours of light. P was calculated as the sum of all hourly DO fluxes in the light, as follows:

$$P = \sum(Flux_{LIGHT}) \quad (5)$$

where $Flux_{LIGHT}$ is hourly DO fluxes measured in the light. GPP was calculated as the sum of hourly fluxes measured in the light plus the mean of all hourly fluxes measured in the dark multiplied by the number of hours of daylight:

$$GPP = \sum(Flux_{LIGHT}) + \overline{Flux}_{DARK} h_{LIGHT} \quad (6)$$

NEM was calculated as the sum of all hourly DO flux measurements over 24 hours, as follows:

$$NEM = \sum(Flux_{LIGHT}) + \sum(Flux_{DARK}) \quad (7)$$

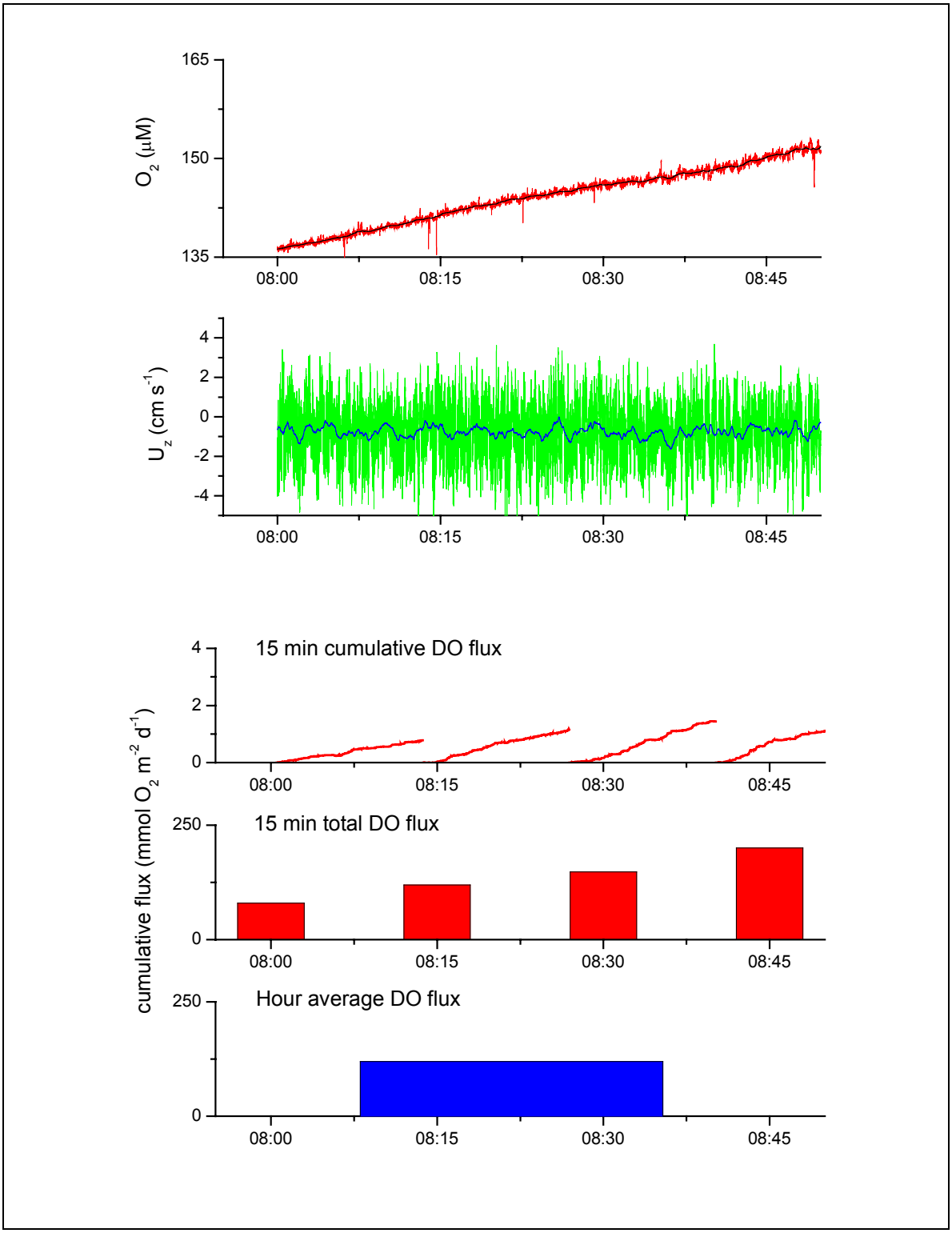

Figure 5: Example of conversion of raw data (DO and U_Z) (top) to 15-min cumulative DO fluxes, 15-min total DO fluxes, and hour average DO flux.

Open-water datasonde measurements: Open-water measurements were made with a YSI 66000 V2 datasonde (YSI Inc., Yellow Springs, Ohio). A single deployment with the datasonde for both the vegetated and bare sediment sites (July 10th and July 11th, 2007) was made concurrently with deployment 5 of the eddy correlation system at the vegetated site and deployment 4 of the eddy correlation system at the bare sediment site. Additional open-water measurements with the datasonde were not made because of instrument malfunction. The datasonde measured DO, water column chlorophyll concentration, pH, turbidity, salinity, water temperature, and photosynthetic active radiation (PAR) at a 0.5 min intervals for the duration of each eddy correlation system deployment. The datasonde was mounted approximately 20 cm above the substrate surface onto fixed PVC poles located less than 10 m to the northwest of each eddy correlation system deployment location. The datasonde was equipped with optical DO, water column chlorophyll, and turbidity sensors with anti-fouling mechanisms. All calibrations were performed before each deployment following specifications in the user manual.

Open-water datasonde DO flux: Rates of open-water DO change measured with the datasonde were calculated as the difference between two consecutive DO measurements divided by the change in time, and multiplied by the mean depth (Ziegler and Benner 1998, Gazeau et al. 2005, Caffery 2004, Nagel 2007):

$$F = \overline{h}\left(\frac{(C_{n+1} - C_n)}{\bar{t}}\right) \qquad (8)$$

where F is the open-water DO 'flux' expressed in units of mass per area per time. C is the concentration of DO at time steps n and n+1, $\bar{t}$ is the mean adjusted time, and $\overline{h}$ is the

mean water depth expressed in meters. Rates of DO change were then corrected for the influence of air-water exchange based on the equation from Liss and Slater (1974):

$$f = k(C_{WATER} - C_{SAT}) \quad (9)$$

where f is the air-water exchange flux expressed in units of mass per area per time. C_{WATER} and C_{SAT} are the mean concentration and saturation concentration of DO and k is the piston velocity expressed in units of cm h^{-1}. Equation 9 assumes that the concentration of oxygen above the air-water interface is equal to the saturation concentration of DO in solution in seawater (D'Avanzo et al. 1996).

The piston velocity, k, was calculated using an empirical model from Marino and Howarth (1993):

$$\ln(k) = 0.920 + 0.237u \quad (10)$$

where u is the wind speed in m s^{-1} and k is in cm h^{-1}. This empirical model is based on published data from lakes, rivers, estuaries, and the open ocean (Marino and Howarth 1993). The model includes the Schmidt number (Sc) raised to the –1/2 power, which has been shown to represent a piston velocity for air-water interfaces where non-whitecapping waves are present (Wanninkhof 1992). These are valid assumptions for South Bay, which typically has small non-breaking waves (personal observation). By assuming the horizontal flux of DO to be zero, the difference in the air-water exchange and the change in DO is a measure of DO exchange from the sediment-water interface. While this value is comparable to the DO flux measured with the eddy correlation technique, it is not a true DO flux because the datasonde is not capable of distinguishing changes in DO concentration from the turbulent transport of DO.

The environmental variables measured by the datasonde and the calculated sediment-water interface DO change were synchronized to the ADV-derived data using MATLAB. A quality control of all apparent sediment-water interface flux outliers was performed based on neighboring flux values and environmental variables. Sediment-water interface flux estimates that were unnaturally biased were removed from further analysis.

Open-water datasonde metabolism calculations: To compare open-water datasonde metabolism calculations with the eddy correlation technique and published studies, rates of DO change and metabolism were estimated using the popular diel curve method (Odum 1956). Rates of P and R were calculated as the mean of all rates of DO change from the light and dark, respectively. A second calculation of P and R was performed following the removal of anomalous rates of DO change observed during both the light and dark. Rates of GPP were calculated as the sum of the absolute values of P and R. NEM was calculated as the difference between the absolute values of GPP and R (Ziegler and Benner 1998, Caffrey 2004).

Statistical analysis: Stepwise multiple linear regressions were performed with the measured environmental variables on DO fluxes combined by site using SAS (SAS Inc, USA). Hourly mean running average and linear detrend DO fluxes were used as dependant variables. The independent environmental variables included photosynthetically active radiation (PAR), mean current flow (U_{MEAN}), water depth (Depth), significant wave height (Hs), water temperature (Temp), mean DO concentration (O_2Mean), and current direction (CurDir). Entry and remove criteria for the models were set at 0.05. Autocorrelation among independent variables was tested using

variance inflation factors. Variables with a variance inflation factor over 10 were considered autocorrelated and removed from the model (Cody and Smith 2006). The same stepwise multiple linear regressions were also performed for individual deployments at both sites.

Results:

The 12 deployments made with the eddy correlation system resulted in approximately 55 million measurements of DO and the three-dimensional velocity field or a combined sum of over 165 million measurements. Five of the deployments from the vegetated site and three from the bare sediment site were used for further analysis. The remaining four deployments were removed from further analysis due to sampling problems and/or system errors (Table 2).

Site characterization: Seagrass density was 257 ± 25 shoots m^{-2} (standard error, n = 5) and seagrass canopy height was approximately 25 cm. Sediment organic matter was 0.8 ± 0.02 % and 1.0 ± 0.06 % for the vegetated and bare sediment sites, respectively. Benthic chlorophyll a was 32.9 ± 1.6 mg m^{-2} for the bare sediment site and 32.6 ± 1.7 mg m^{-2} for the vegetated site. Porosity was 0.379 and 0.385 for the vegetated and bare sediment sites, respectively (Table 1).

Eddy correlation: DO fluxes calculated from the two methods (running average and linear detrend) produced similar results (Tables A3a – A3h). Unlike the running average method, the linear detrend method accounts for changes in eddy size thus reducing the risk of underestimating DO fluxes. Unless otherwise noted the linear detrend DO flux is the default flux reported throughout this study.

Co-spectral analysis of U_z' and C' from selected 15-min intervals at both sites under similar conditions reveals the eddy sizes that contribute to DO fluxes.

Approximately 90% of the DO flux for the bare sediment site for the sample period was due to the influence of eddies ranging from 100 s (0.01 Hz) to 10 s (0.1 Hz) (Figure 6a). In contrast, approximately 80% of the DO flux for the vegetated site for the sample period was due to the influence of eddies with a 1.6 - 2 s (0.5 – 0.6 Hz) frequency. (Figure 6b)

Hourly averages of current flow and direction, significant wave height, water depth and temperature, and DO concentration for individual deployment DO fluxes highlights the dynamic nature of South Bay and the variability in DO fluxes. Understanding how DO fluxes vary in response to environmental variables is essential for understanding how the environment functions and making accurate calculations of ecosystem metabolism. Water temperature varied from approximately 24 to 30° C during the sampling period (Figures 7b – 14b). The average water depth ranged from 0.32 m to 1.8 m during the study (Figures 7b – 7b). The hourly mean current ranged from < 1 cm s^{-1} to 18 cm s^{-1} over the bare sediment site and < 1 cm s^{-1} to 10 cm s^{-1} over the vegetated site (Figures 7a – 14a). Water column chlorophyll, pH, salinity, turbidity and DO measured with the datasonde over the vegetated and bare sediment site can be seen in Figures A3a&b.

	OM %	Benthic Chl a mg m^{-2}	Porosity
Vegetated	0.8 ± 0.02	32.6 ± 1.7	0.379
Bare Sediment	1.0 ± 0.06	32.9 ± 1.6	0.385

Table 1. Sediment core characterizations for the vegetated and bare sediment sites. Ranges given are standard error based on n = 24.

Deployment	Date	Start time 0000- 2400	Duration min	Notes
Bare Sediment Site				
1	June 18-19, 2007	0800	1057	No light data
	(Deployment 1 not used in analysis)			
2	June 20-21, 2007	0900	1252	
3	July 9-10, 2007	1100	1342	
4	July 11-12, 2007	1300	1282	Concurrent Datasonde Deployment
5	July 17-18, 2007	1900	292	
	(Deployment 5 not used in analysis)			
Vegetated Site				
3	June 25-26, 2007	1200	1282	
4	June 26-27, 2007	1330	1177	No light data
5	July 10-11, 2007	1330	1237	Concurrent Datasonde Deployment
6	July 16-17, 2007	1800	1282	
7	July 18-19, 2007	1900	1267	

Table 2: Details of eddy correlation deployments from this study.

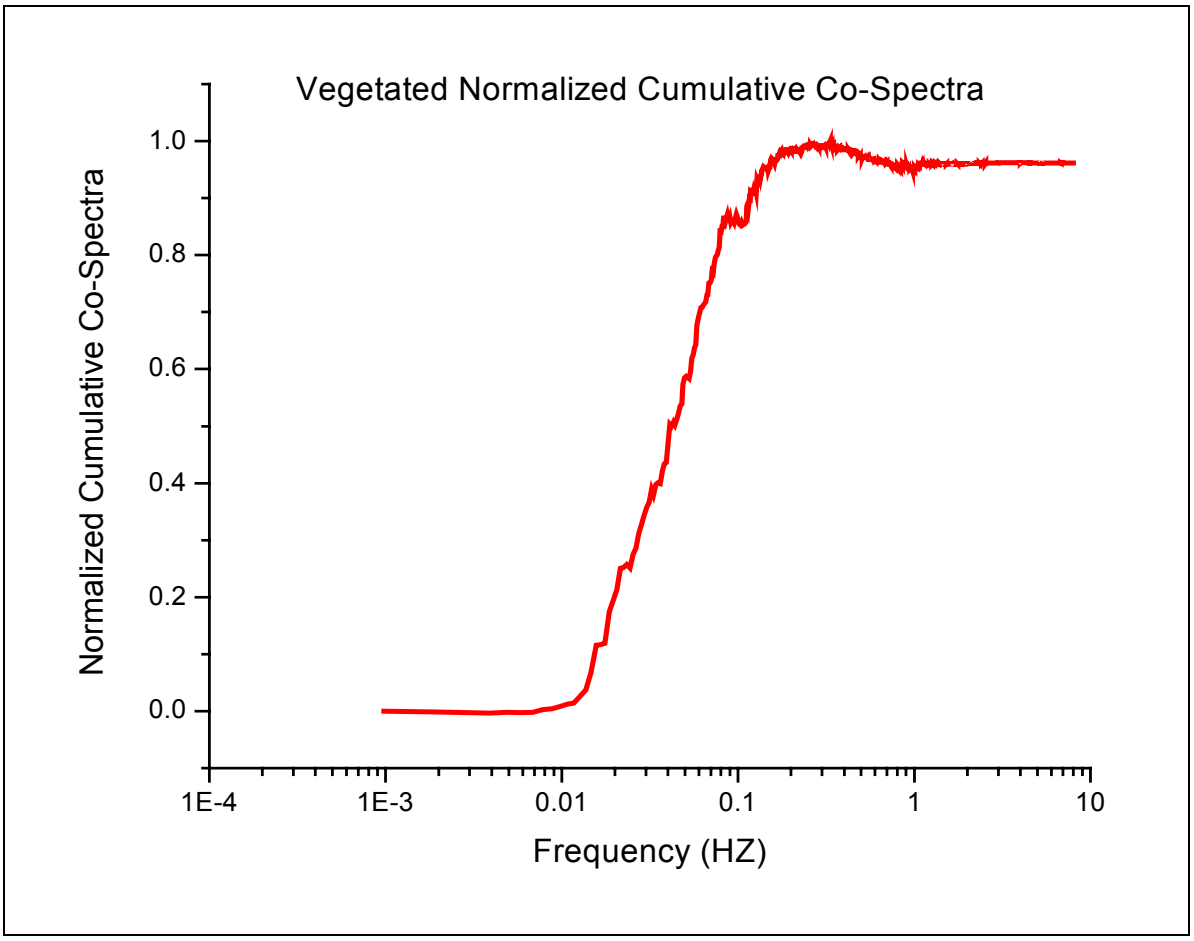

Figure 6a: Normalized cumulative co-spectra of the DO flux for a 15-min interval from a eddy correlation deployment at the vegetated site

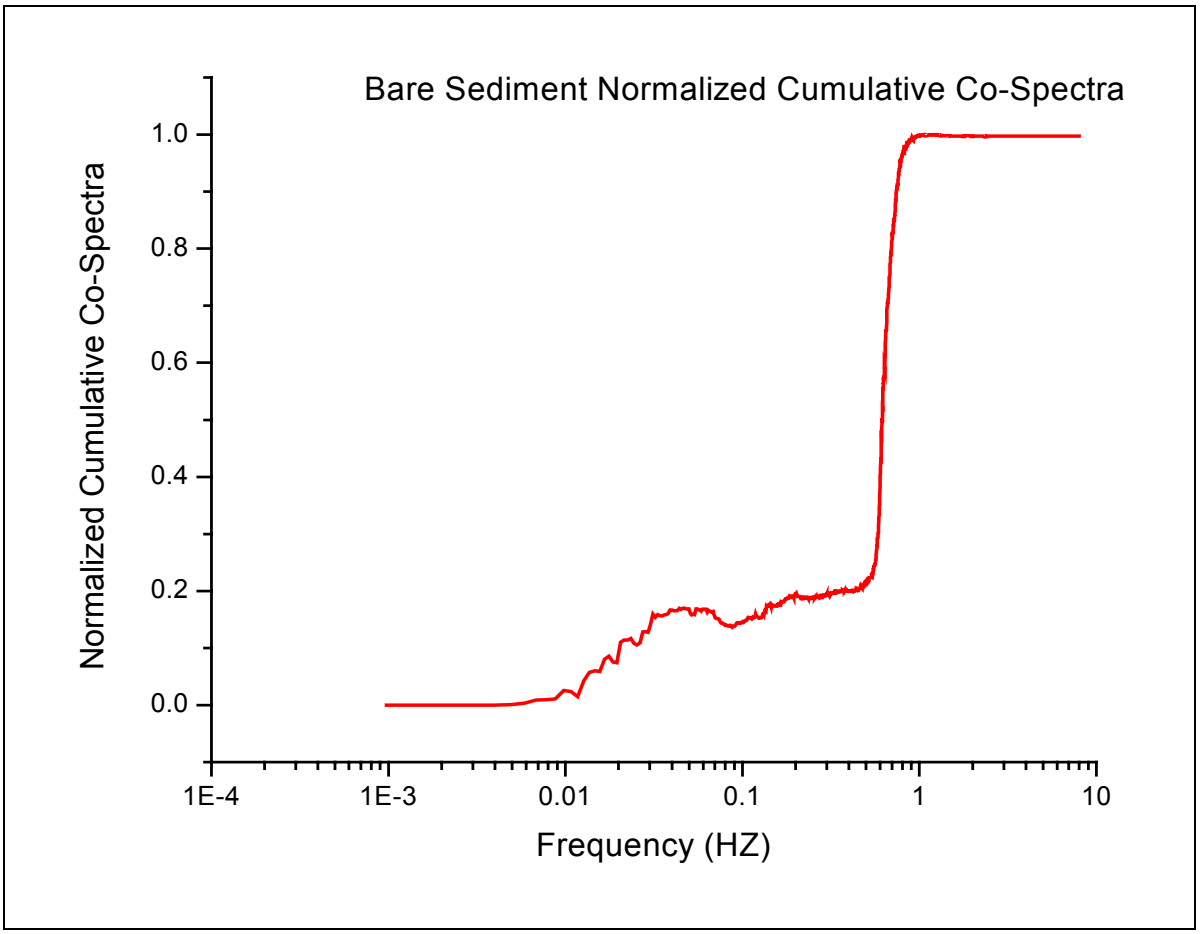

Figure 6b: Normalized cumulative co-spectra of the DO flux for a 15-min interval from a eddy correlation deployment at the bare sediment site

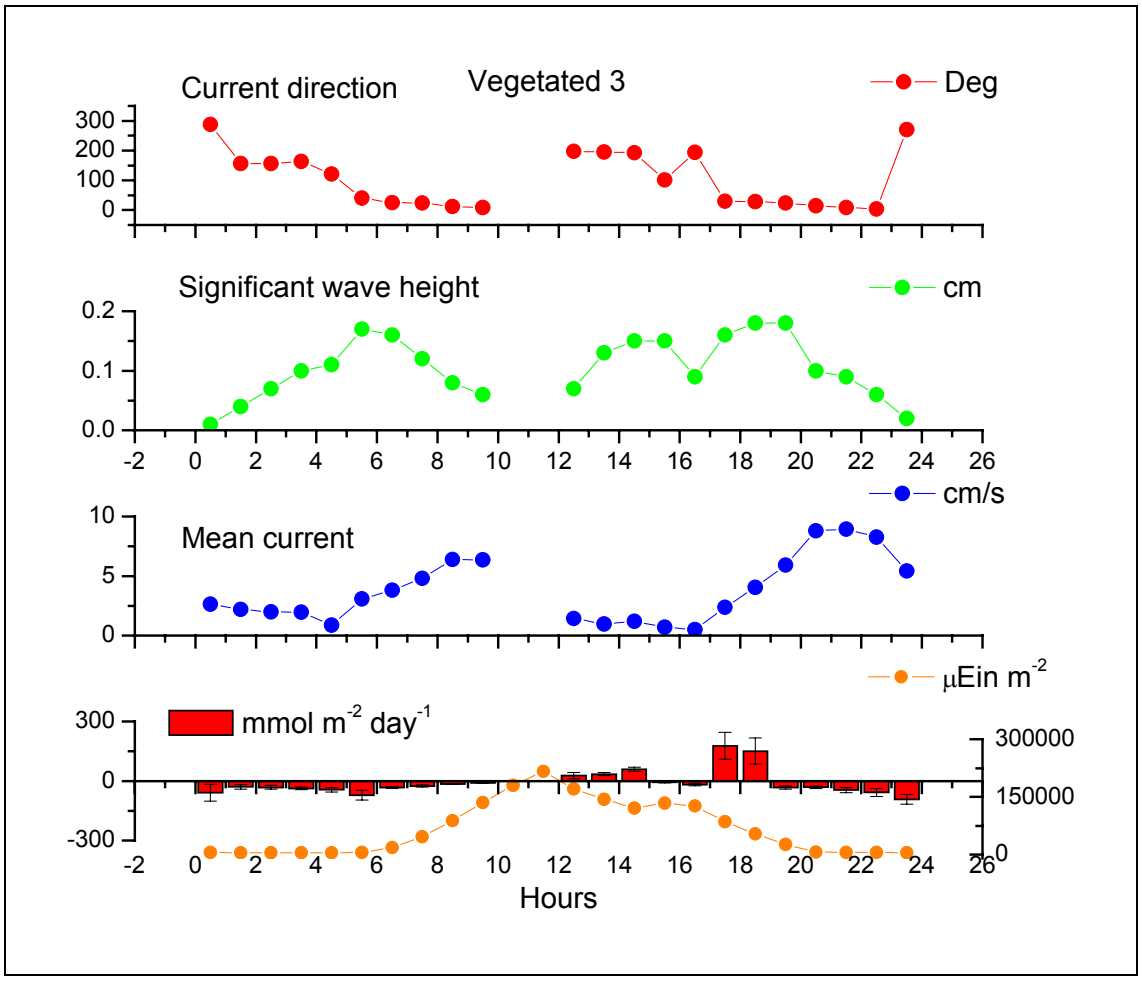

Figure 7a. Hourly measures from top to bottom of current direction (degrees), significant wave height (cm), mean current (cm s^{-1}) and DO flux (mmol O_2 m^{-2} d^{-1}) from vegetated 3 deployment.

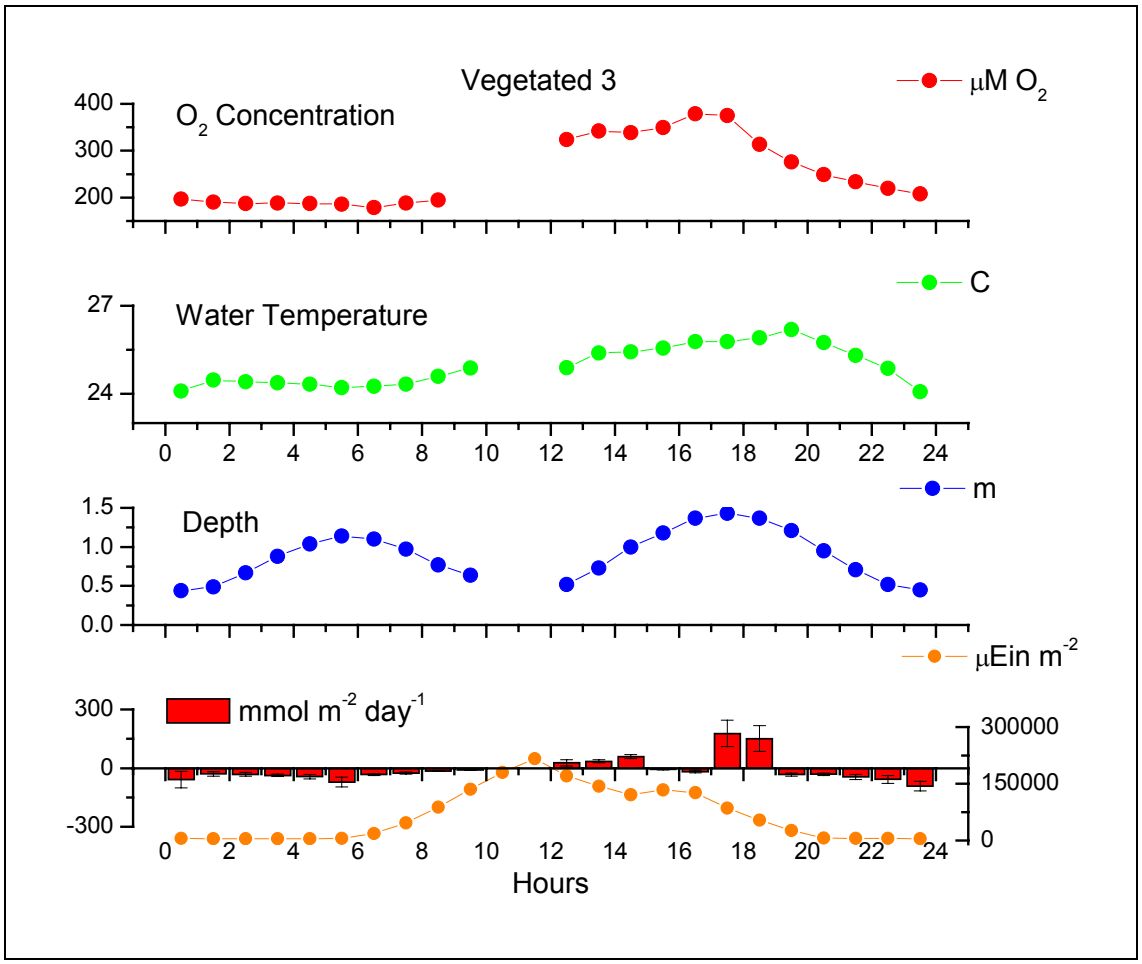

Figure 7b. Hourly measures from top to bottom of O_2 concentration (μM), water temperature (C), water depth (m) and DO flux (mmol O_2 m^{-2} d^{-1}) from vegetated 3 deployment.

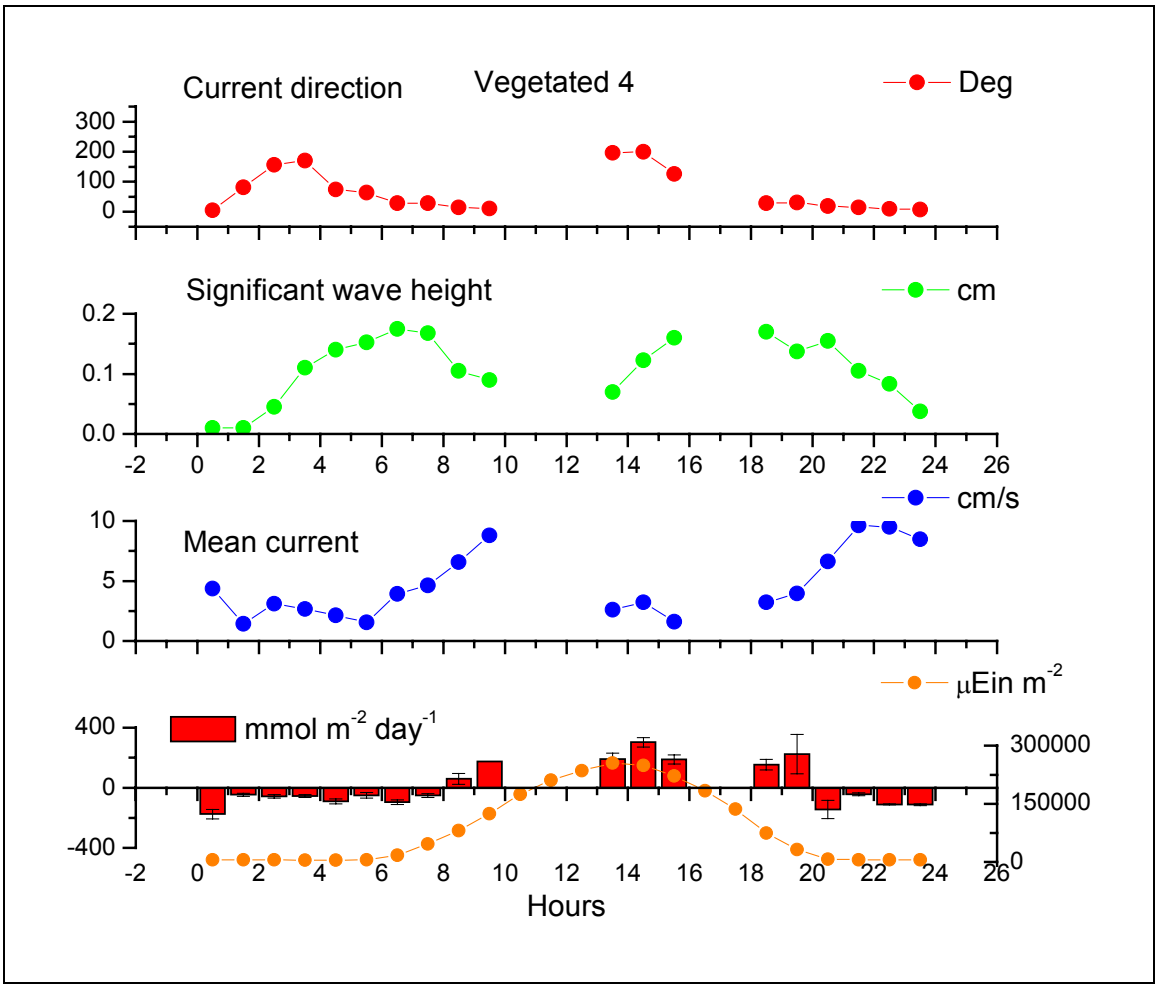

Figure 8a. Hourly measures from top to bottom of current direction (degrees), significant wave height (cm), mean current (cm s^{-1}) and DO flux (mmol O_2 m^{-2} d^{-1}) from vegetated 4 deployment.

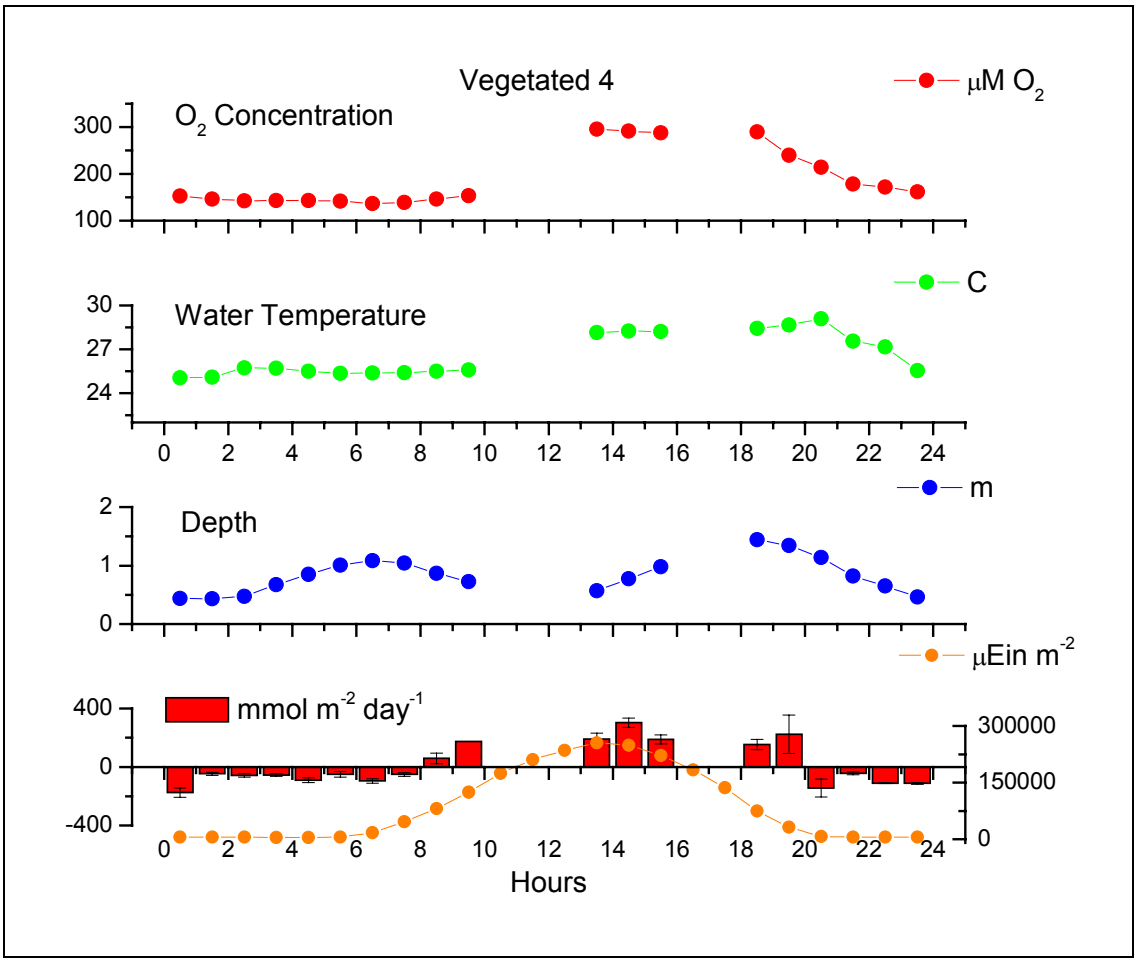

Figure 8b. Hourly measures from top to bottom of O_2 concentration (μM), water temperature (C), water depth (m) and DO flux (mmol O_2 m^{-2} d^{-1}) from vegetated 4 deployment.

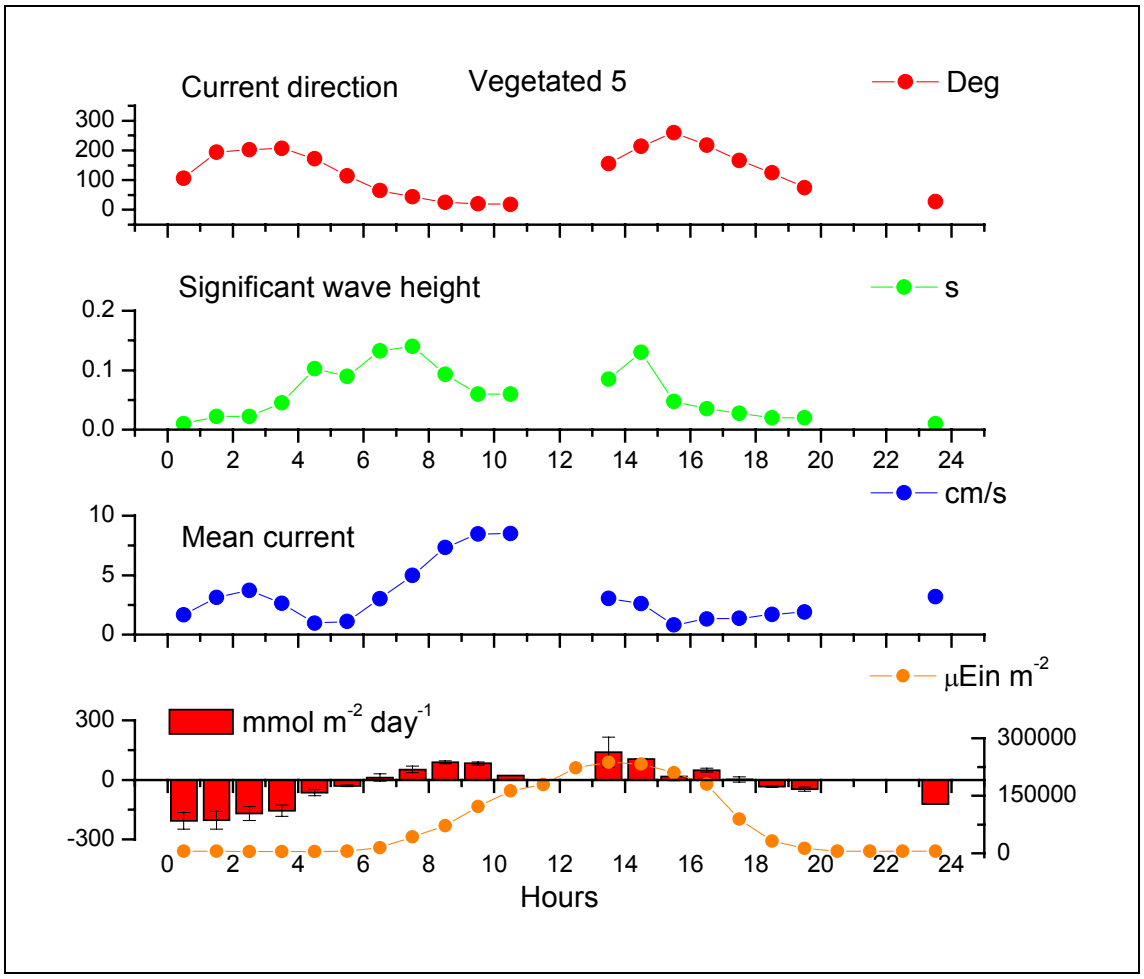

Figure 9a. Hourly measures from top to bottom of current direction (degrees), significant wave height (cm), mean current (cm s^{-1}) and DO flux (mmol O_2 m^{-2} d^{-1}) from vegetated 5 deployment.

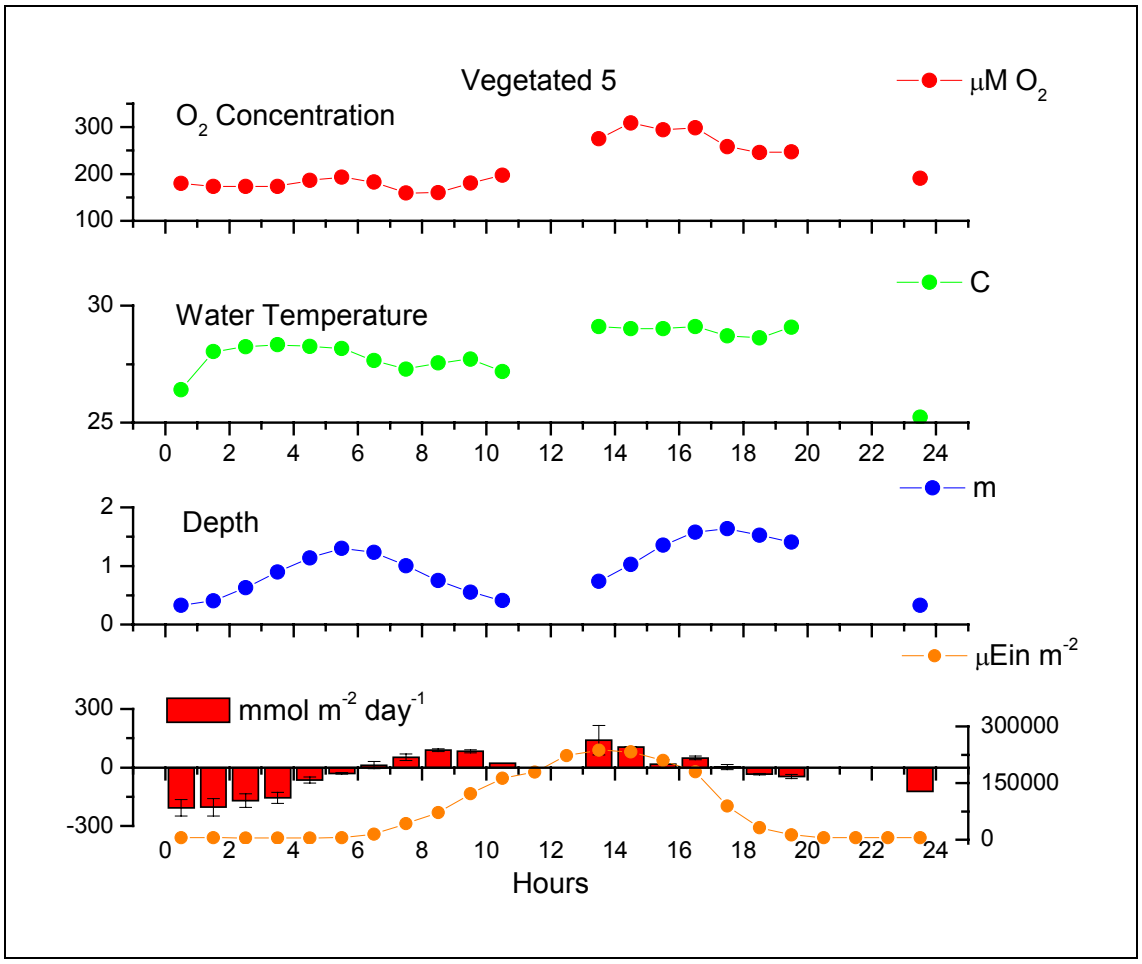

Figure 9b. Hourly measures from top to bottom of O_2 concentration (μM), water temperature (C), water depth (m) and DO flux (mmol O_2 m^{-2} d^{-1}) from vegetated 5 deployment.

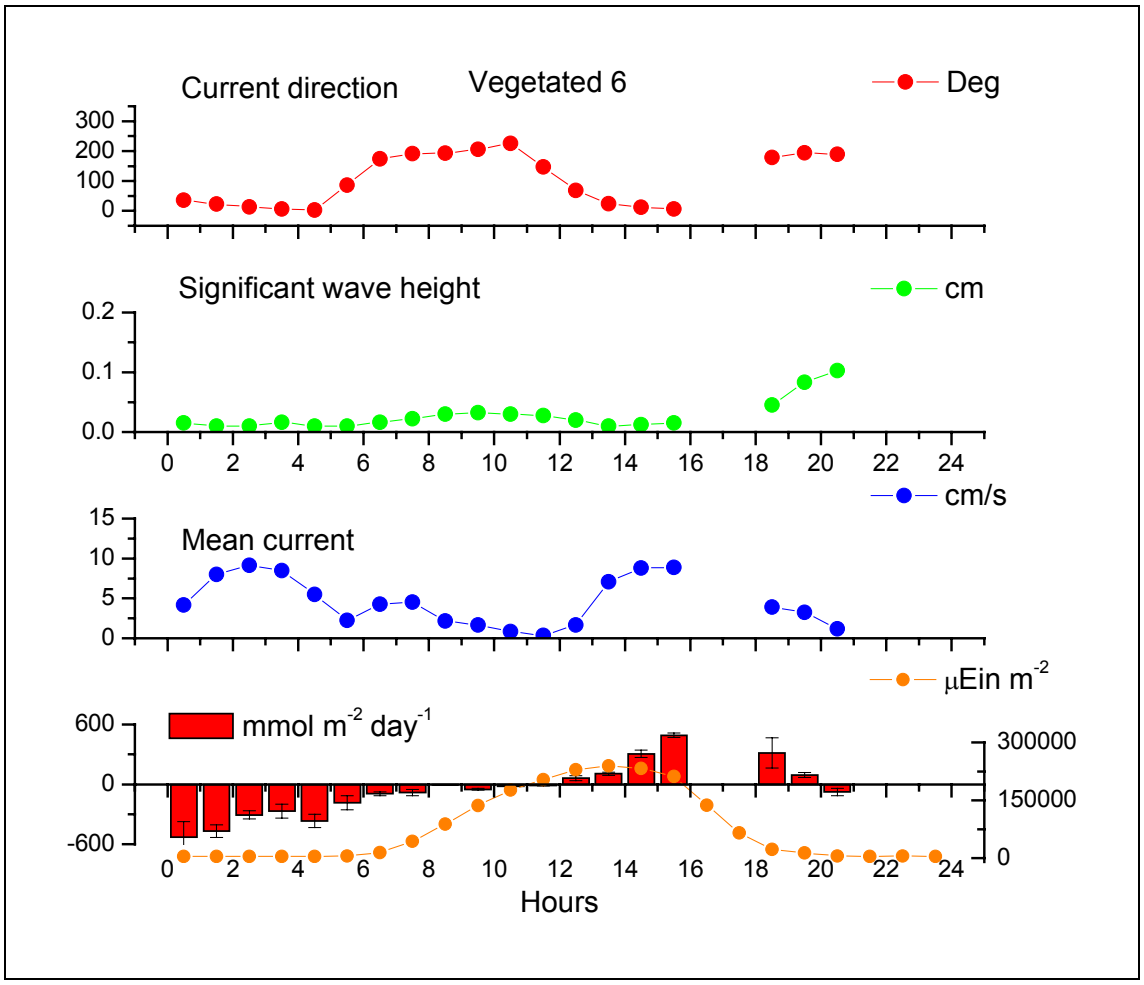

Figure 10a. Hourly measures from top to bottom of current direction (degrees), significant wave height (cm), mean current (cm s^{-1}) and DO flux (mmol O_2 m^{-2} d^{-1}) from vegetated 6 deployment.

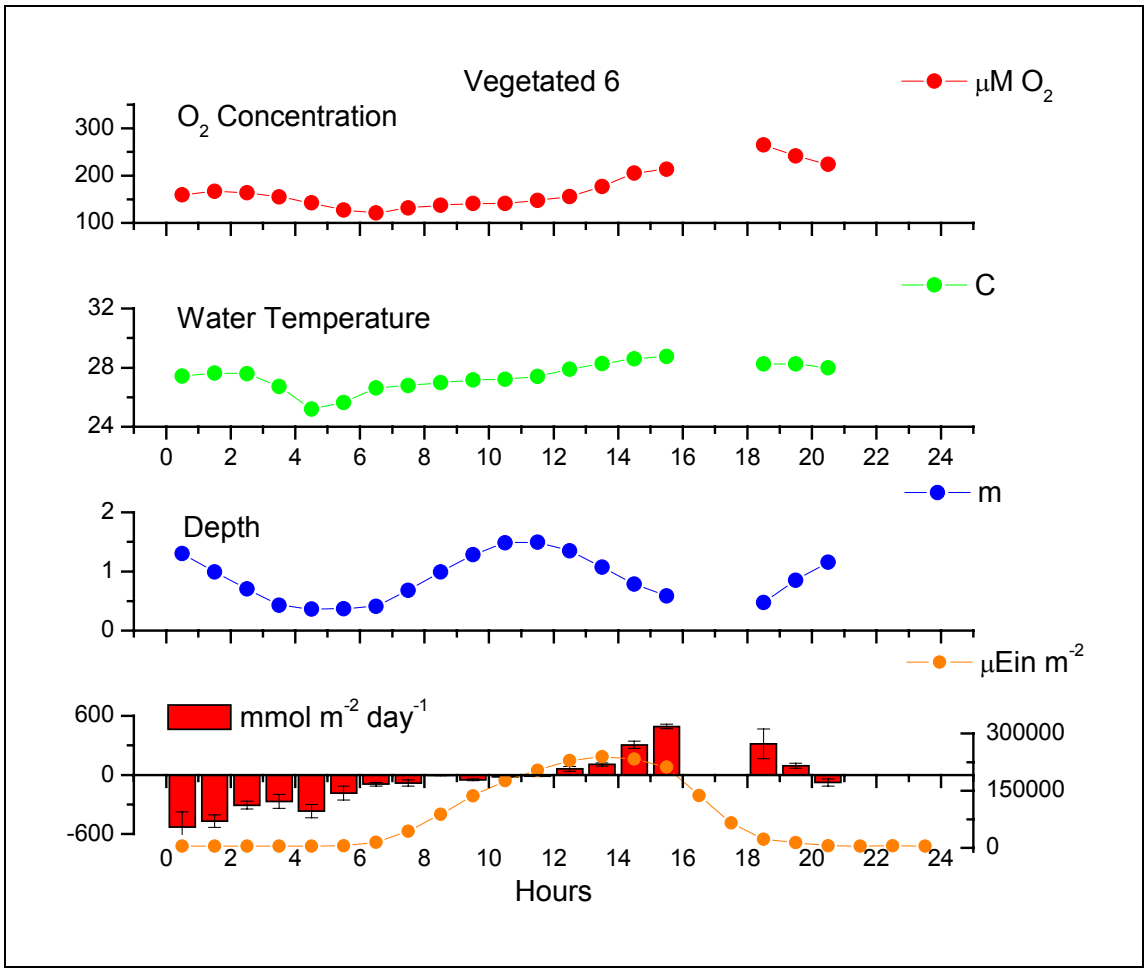

Figure 10b. Hourly measures from top to bottom of O_2 concentration (μM), water temperature (C), water depth (m) and DO flux (mmol O_2 m^{-2} d^{-1}) from vegetated 6 deployment.

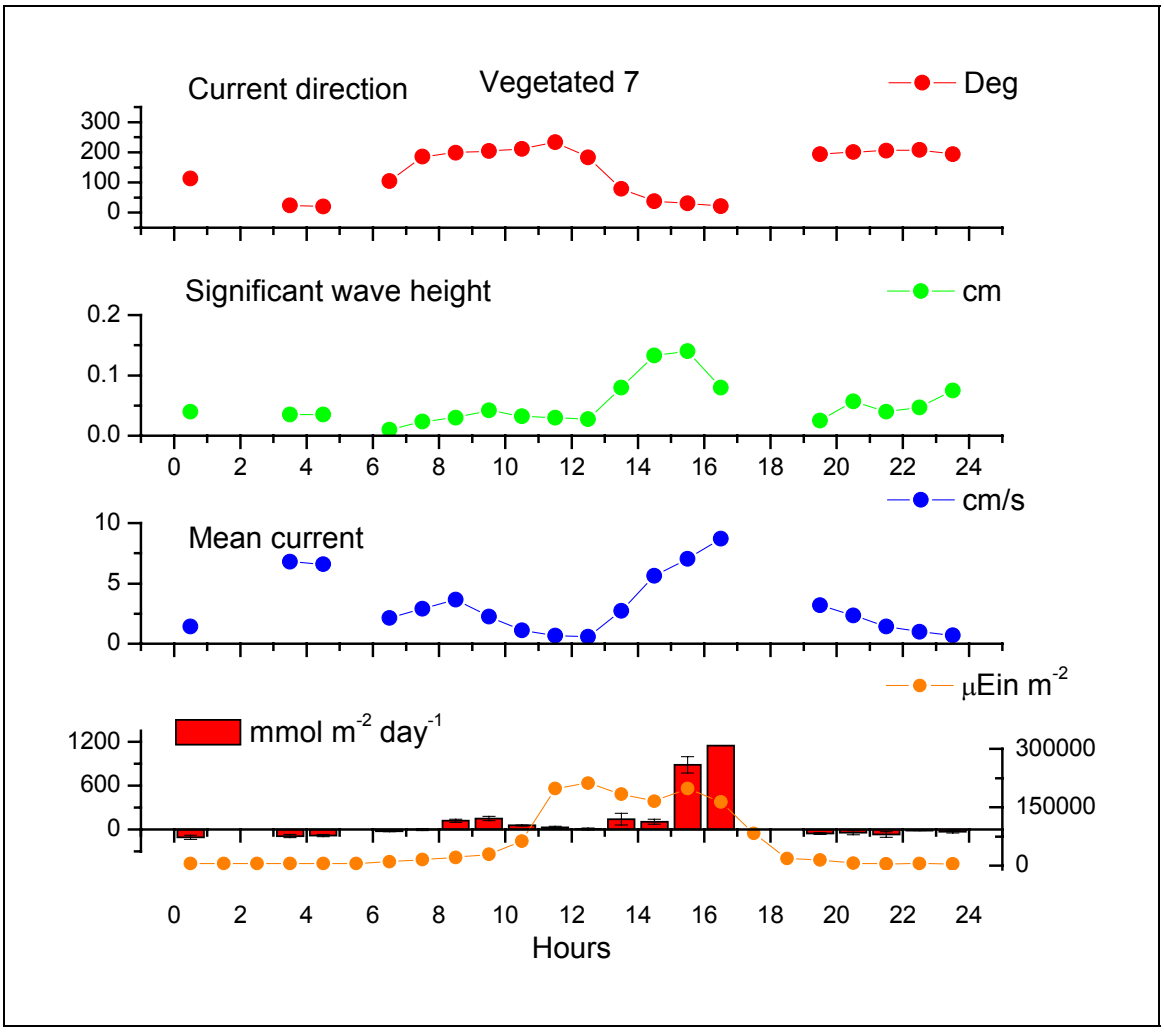

Figure 11a. Hourly measures from top to bottom of current direction (degrees), significant wave height (cm), mean current (cm s^{-1}) and DO flux (mmol O_2 m^{-2} d^{-1}) from vegetated 7 deployment.

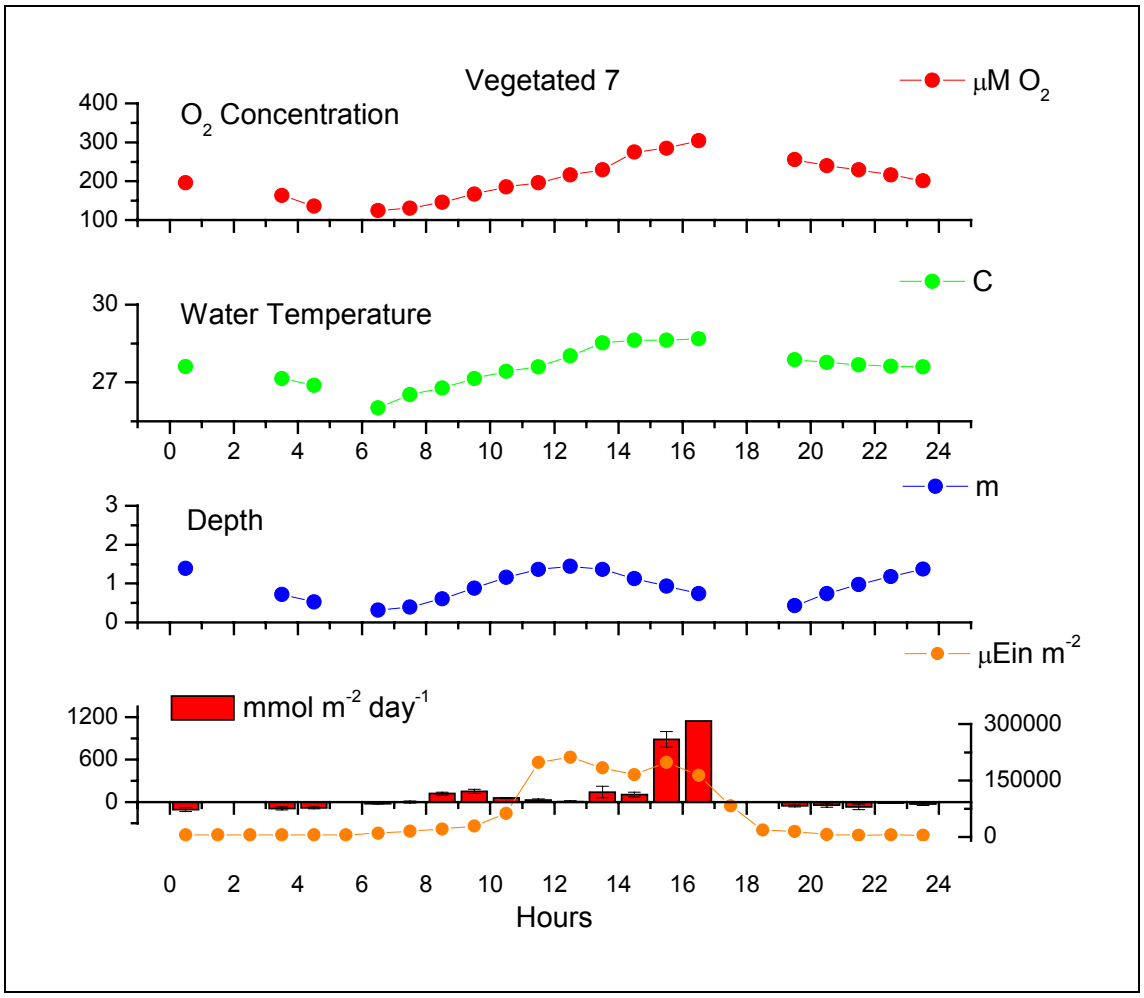

Figure 11b. Hourly measures from top to bottom of O_2 concentration (μM), water temperature (C), water depth (m) and DO flux (mmol O_2 m^{-2} d^{-1}) from vegetated 7 deployment.

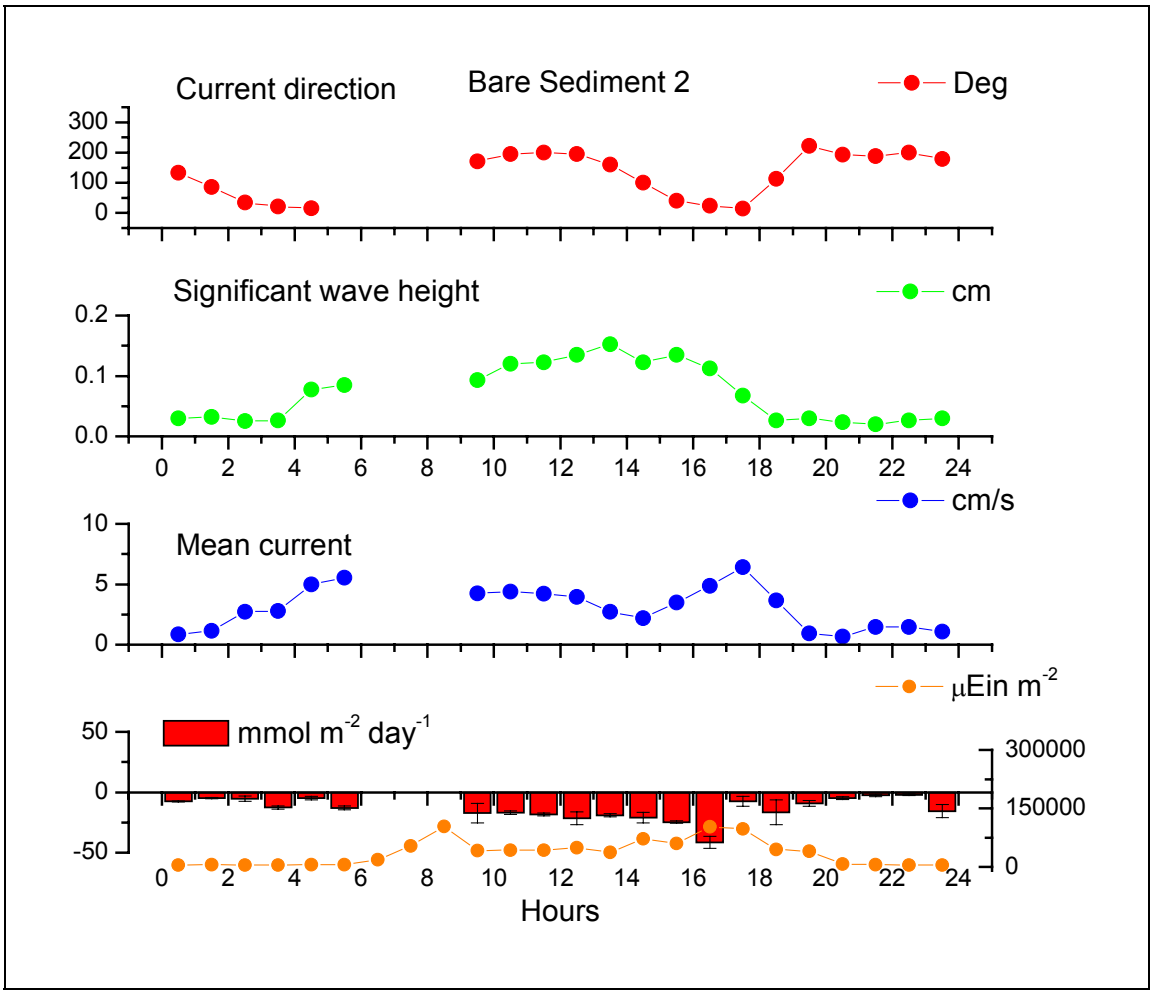

Figure 12a. Hourly measures from top to bottom of current direction (degrees), significant wave height (cm), mean current (cm s^{-1}) and DO flux (mmol O_2 m^{-2} d^{-1}) from bare sediment 2 deployment.

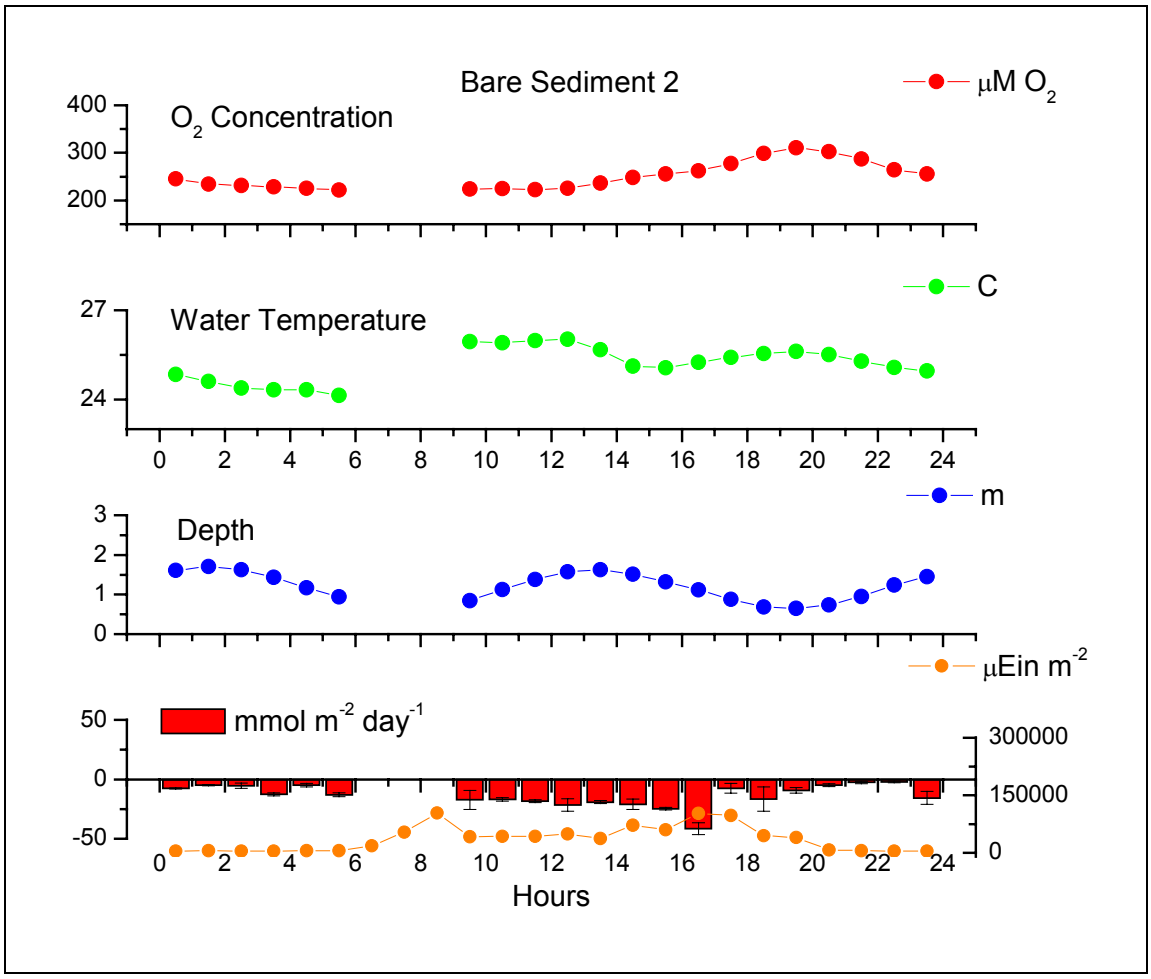

Figure 12b. Hourly measures from top to bottom of O_2 concentration (μM), water temperature (C), water depth (m) and DO flux (mmol O_2 m^{-2} d^{-1}) from bare sediment 2 deployment.

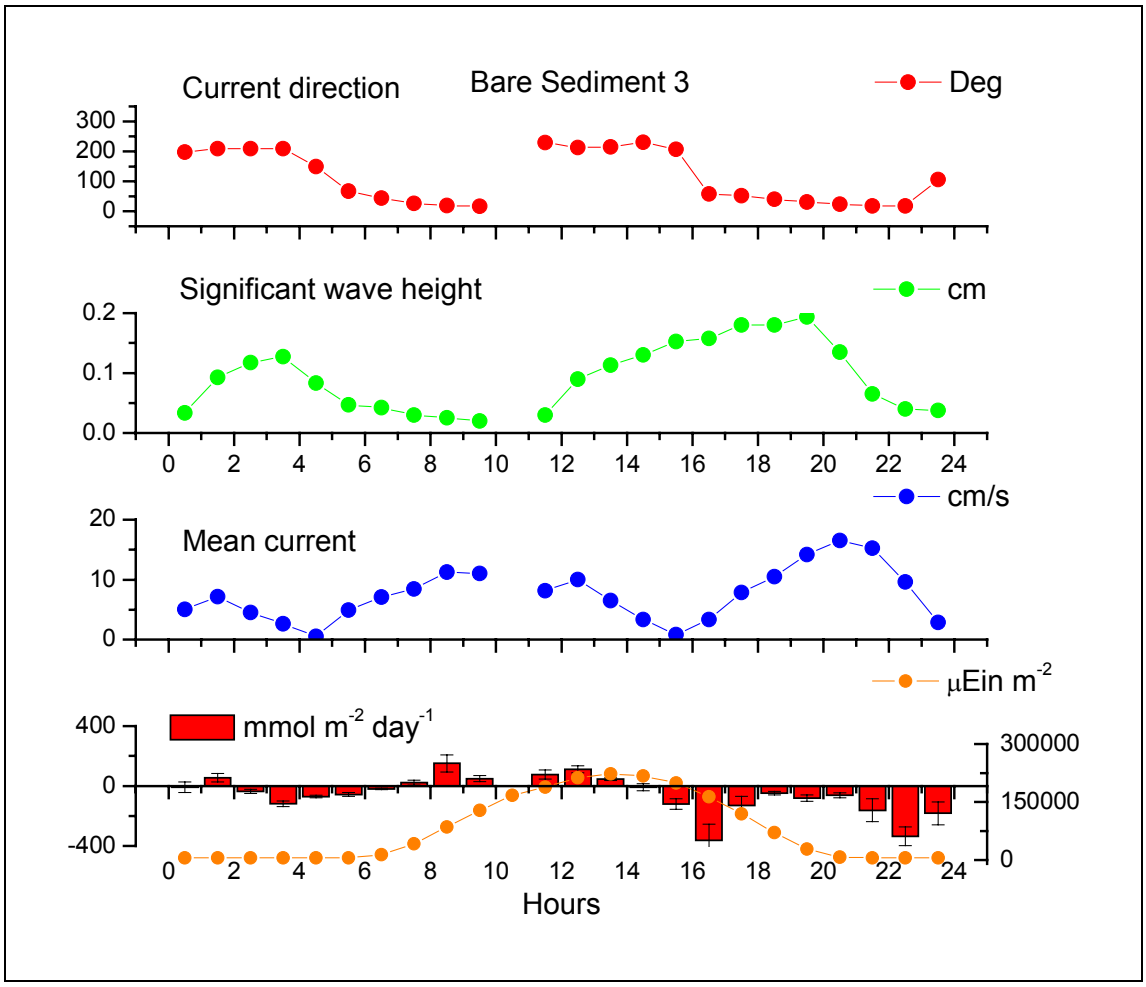

Figure 13a. Hourly measures from top to bottom of current direction (degrees), significant wave height (cm), mean current (cm s^{-1}) and DO flux (mmol O_2 m^{-2} d^{-1}) from bare sediment 3 deployment

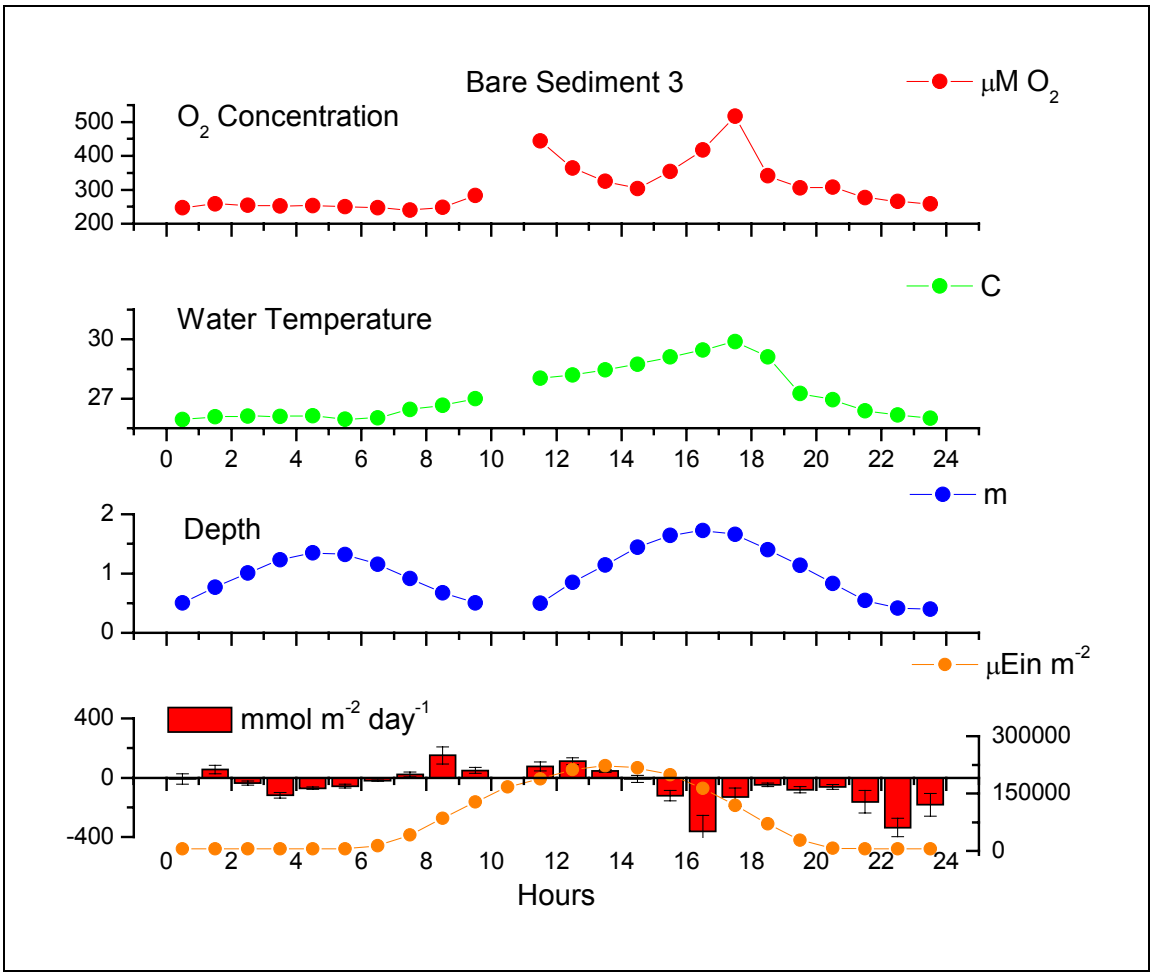

Figure 13b. Hourly measures from top to bottom of O_2 concentration (μM), water temperature (C), water depth (m) and DO flux (mmol O_2 m^{-2} d^{-1}) from bare sediment 3 deployment.

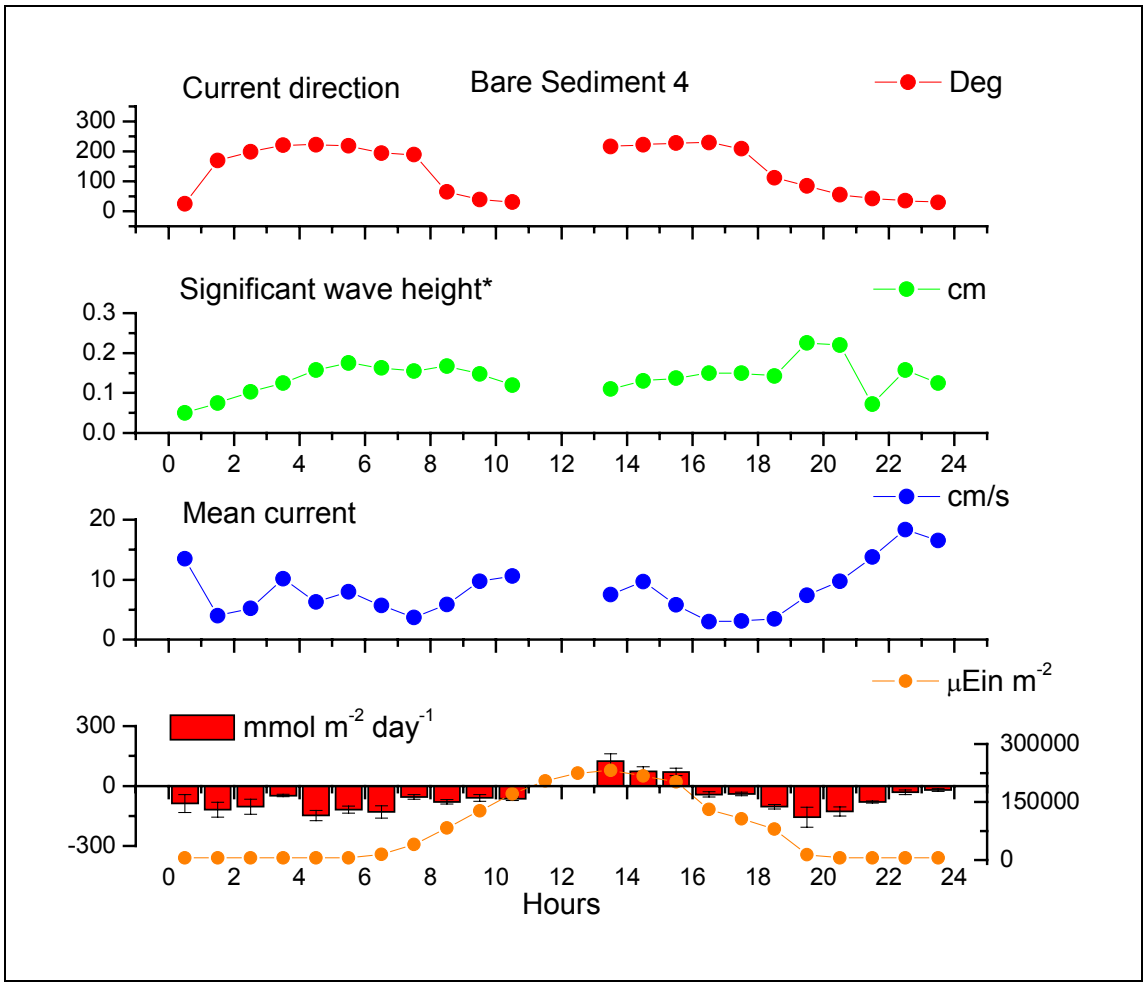

Figure 14a. Hourly measures from top to bottom of current direction (degrees), significant wave height (cm), mean current (cm s^{-1}) and DO flux (mmol O_2 m^{-2} d^{-1}) from bare sediment 4 deployment. *denotes change in scale.

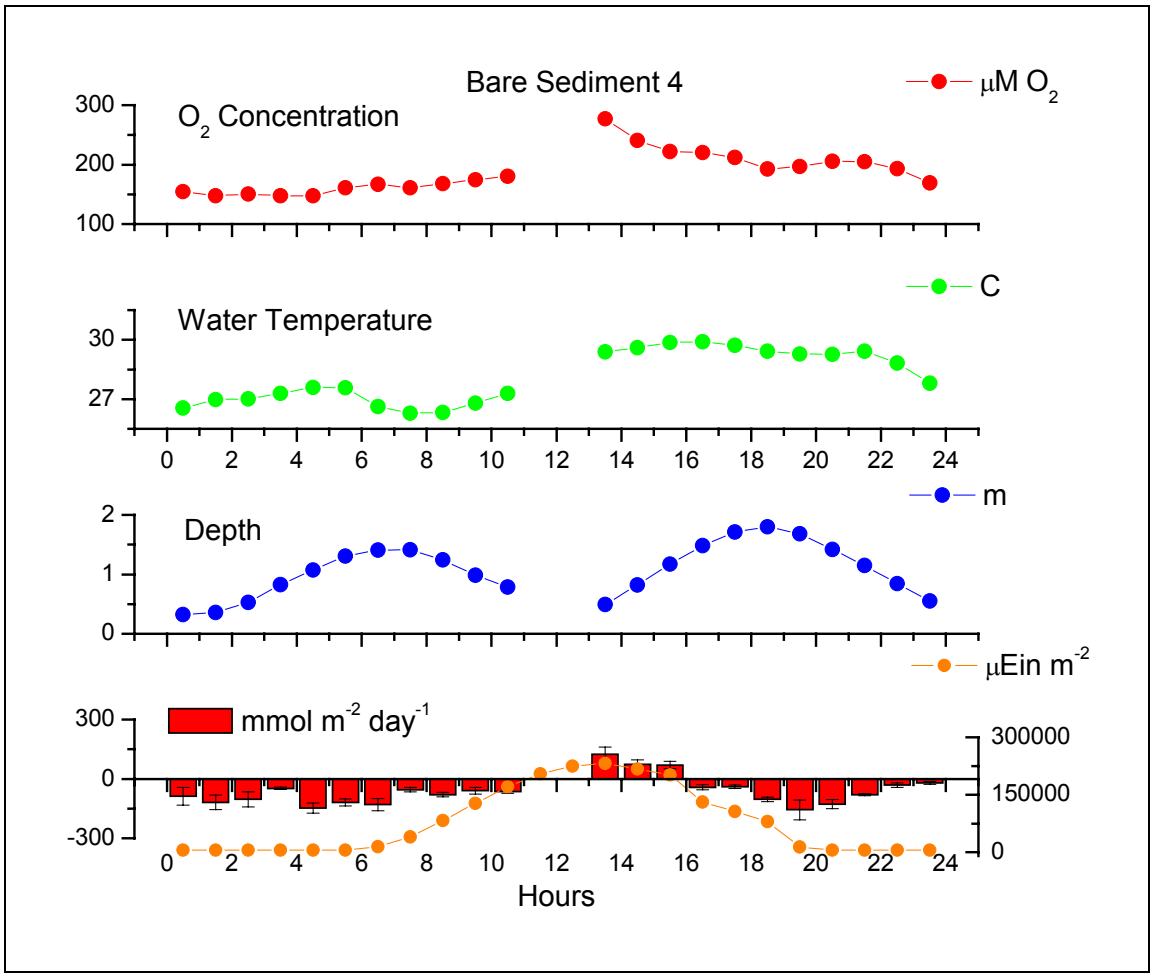

Figure 14b. Hourly measures from top to bottom of O_2 concentration (μM), water temperature (C), water depth (m) and DO flux (mmol O_2 m^{-2} d^{-1}) from bare sediment 4 deployment.

Site DO flux variation: Results of the stepwise multiple linear regressions of DO fluxes versus environmental variables for all deployments give a model R^2 of 0.34 and 0.40 for the running average and linear detrend DO fluxes, respectively, (as dependent variables) for all eddy correlation vegetated deployments (Table 3). The two models both include PAR as a significant environmental variable. The running average DO flux model also included significant wave height. The linear detrend DO flux included mean current and mean DO concentration as additional significant environmental variables. Variance inflation factors were around 1.0 for all significant variables in all models. Least squares linear regressions were performed the three significant variables, PAR, 15-min mean DO concentration, and significant wave height, for the two sites (Figures 15 – 17). All regression showed positive relationships except that of significant wave height and hourly DO fluxes for the bare sediment site, which was negative.

Model R^2 values of 0.24 and 0.22 were calculated for all deployments at the bare sediment site using the running average and linear detrend DO fluxes, respectively. Both models included PAR and significant wave height as significant environmental variables (Table 3). The linear detrend DO flux model also included mean DO concentration as a significant environmental variable. Variance inflation factors were around 1.0 for all significant variables in all models.

Stepwise multiple linear regressions for the running average and linear detrend DO fluxes for individual eddy correlation deployments from both sites showed similar results to the site based regression models (Table 3). Vegetated deployments 4, 5, and 6 had high R^2 values of 0.82, 0.94, and 0.98 respectively for the running average DO flux (Table 4). The same three deployments also had high R^2 values with the linear detrend

DO flux (Table 5). PAR and water depth were included in all three models for both fluxes for the three vegetated deployments. In addition, significant wave height was included in vegetated deployments 4 and 5 running average DO flux models and in deployment 4 linear detrend DO flux model. Current direction was included in vegetated deployments 5 and 6 for both DO flux models. Mean current flow was only significant for vegetated deployment 7 with both DO flux models. Bare sediment deployments 2 and 4 had high R^2 values of 0.62 and 0.83 respectively for the running average DO flux (Table 4) and were also high for the linear detrend DO flux (Table 5). Significant wave height was the only included environmental variable for bare sediment deployment 2 for the linear detrend DO flux model. PAR was consistently the largest contributor for all individual deployment models from both sites, ranging in partial-R^2 values of 0.19 to 0.67.

	Vegetated (n = 97)				Bare sediment (n = 66)			
	RA		LD		RA		LD	
	R^2	Prob > F	R^2	Prob > F	R^2	Prob > F	R^2	Prob > F
PAR	0.29	<0.0001	0.33	<0.0001	0.14	0.0011	0.07	0.0223
Umean			0.05	0.0038				
Depth								
Hs	0.05	0.0062			0.1	0.0104	0.07	0.0290
Temp								
O_2Mean			0.05	0.0050			0.08	0.0183
CurDir								
Model	0.34		0.44		0.24		0.22	

Table 3. Results from stepwise multiple linear regressions of DO fluxes calculated with a running average (RA) and linear detrend (LD) on environmental variables pooled by site. Independent variables include photosynthetically active radiation (PAR), mean current flow (U_{MEAN}), water depth (Depth), significant wave height (Hs), water temperature (Temp), mean DO concentration (O_2Mean), and current direction (CurDir). Entry and remove criterion for the model were set at 0.05.

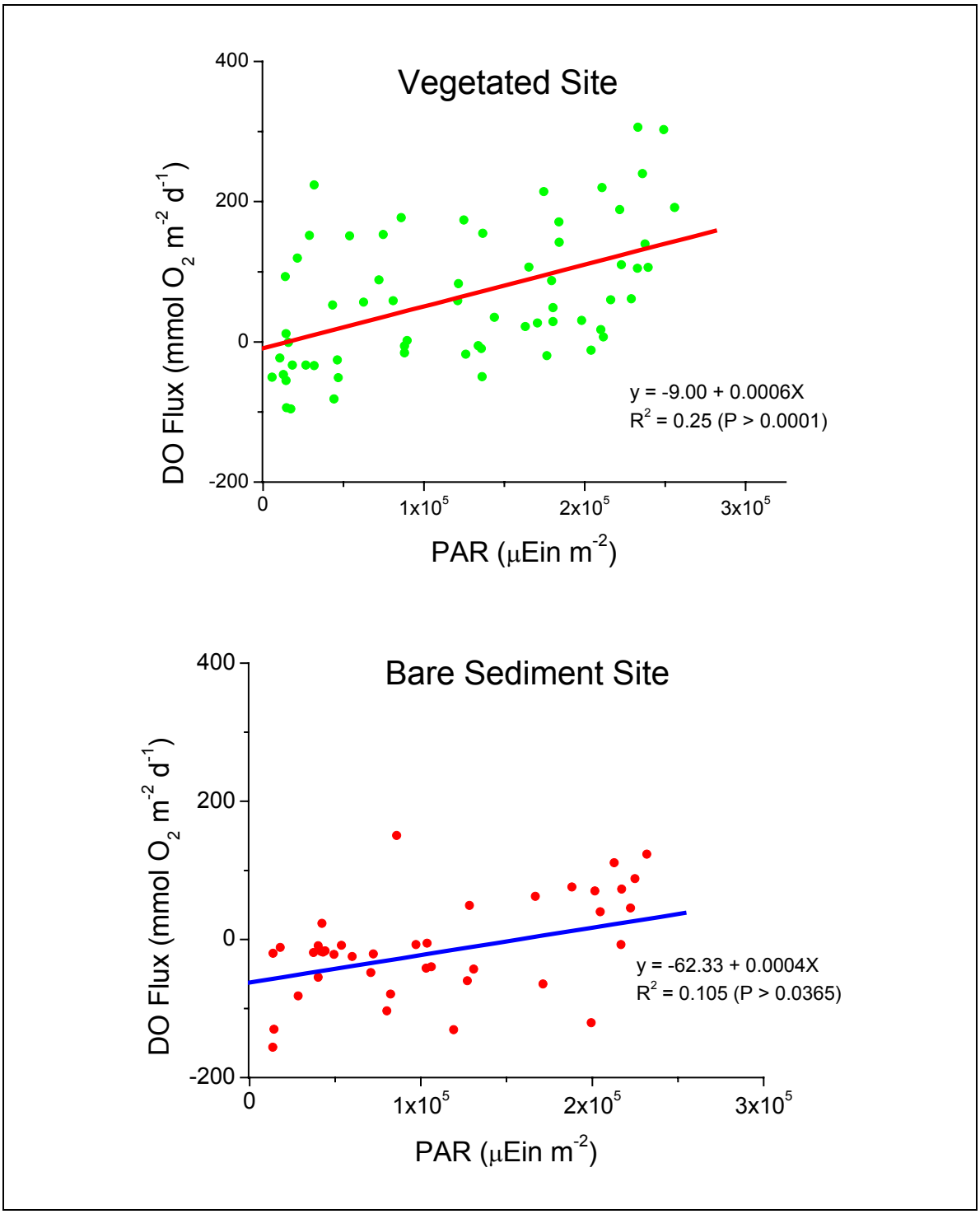

Figure 15: least squares linear regressions of PAR to hourly DO fluxes for the vegetated site (top) and bare sediment site (bottom).

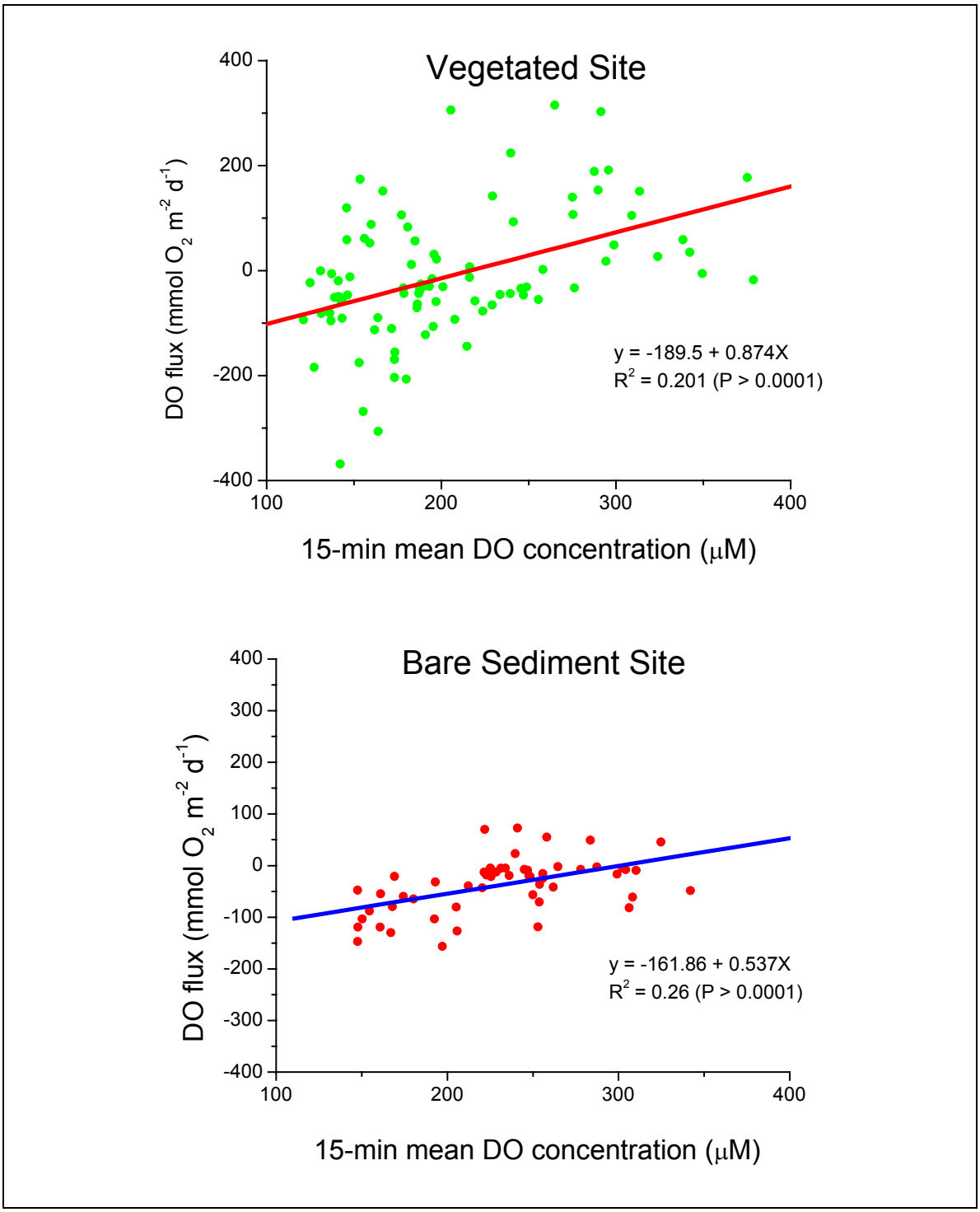

Figure 16: least squares linear regressions of 15-min mean DO concentration to hourly DO fluxes for the vegetated site (top) and bare sediment site (bottom).

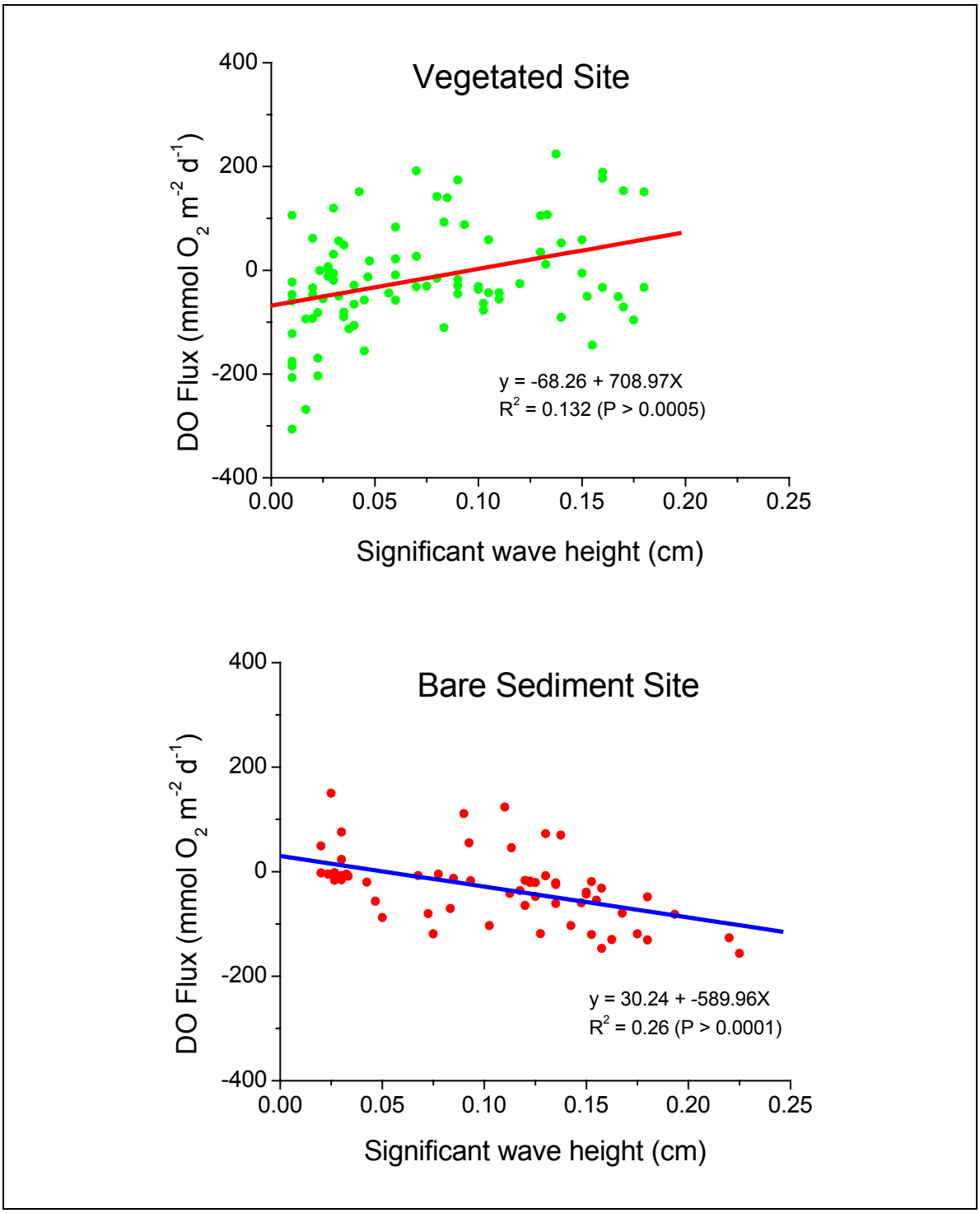

Figure 17: least squares linear regressions of significant wave height to hourly DO fluxes for the vegetated site (top) and bare sediment site (bottom).

		PAR	Umean	Depth	Hs	Temp	O_2Mean	CurDir	Model R^2	Prob>F
Vegetated										
3 (n = 21)	6/25/2007						0.47		0.47	0.0006
4 (n = 19)	6/26/2007	0.67		0.08	0.07				0.82	<0.0001
5 (n = 19)	7/10/2007	0.54		0.11	0.20			0.09	0.94	<0.0001
6 (n = 19)	7/16/2007	0.40		0.12			0.28	0.18	0.98	<0.0001
7 (n = 19)	7/18/2008	0.19	0.40						0.59	0.0008
Bare										
2 (n = 21)	6/18/2007	0.50			0.12				0.62	<0.0001
3 (n = 22)	7/9/2007									0.0206
4 (n = 21)	7/11/2007	0.61	0.10					0.12	0.83	<0.0001

Table 4. Results from stepwise multiple linear regressions of DO fluxes calculated with a running average on environmental variables for individual deployments. Independent variables include photosynthetically active radiation (PAR), mean current flow (U_{MEAN}), water depth (Depth), significant wave height (Hs), water temperature (Temp), mean DO concentration (O_2Mean), and current direction (CurDir). Entry and remove criterion for the model were set at 0.05.

		PAR	Umean	Depth	Hs	Temp	O_2Mean	CurDir	Model R^2	Prob>F
Vegetated										
3 (n = 21)	6/25/2007						0.53		0.53	0.0002
4 (n = 19)	6/26/2007	0.63		0.08	0.11				0.83	<0.0001
5 (n = 19)	7/10/2007	0.66		0.12				0.09	0.88	<0.0001
6 (n = 19)	7/16/2007	0.38		0.13			0.30	0.18	0.98	<0.0001
7 (n = 19)	7/18/2008	0.19	0.40						0.59	0.0008
Bare										
2 (n = 21)	6/18/2007				0.58				0.58	<0.0001
3 (n = 22)	7/9/2007						0.24		0.24	0.0206
4 (n = 21)	7/11/2007	0.58		.13				0.07	0.78	<0.0001

Table 5. Results from stepwise multiple linear regressions of DO fluxes calculated with a linear detrend on environmental variables for individual deployments. Independent variables include photosynthetically active radiation (PAR), mean current flow (U_{MEAN}), water depth (Depth), significant wave height (Hs), water temperature (Temp), mean DO concentration (O_2Mean), and current direction (CurDir). Entry and remove criterion for the model were set at 0.05.

Site DO fluxes: Figures 18a and 18b show the variation in hourly DO fluxes over the two sites. A diurnal cycle of DO fluxes was observed during the majority of deployments, where hourly DO fluxes were mostly positive during light conditions and mostly negative during dark conditions. Considerable variation among hourly DO fluxes was also observed within deployments at each site. There was also variation between deployments, highlighted by the significantly lower DO fluxes from deployments 2 and 3 for the bare sediment and vegetated sites relative to the remaining deployments at each site. Anomalous DO fluxes were observed in several deployments, including a large increase in DO fluxes around sunset (see Appendix for further discussion). A lag in maximum positive DO fluxes associated with primary production photosynthesis and maximum PAR was also observed in several deployments.

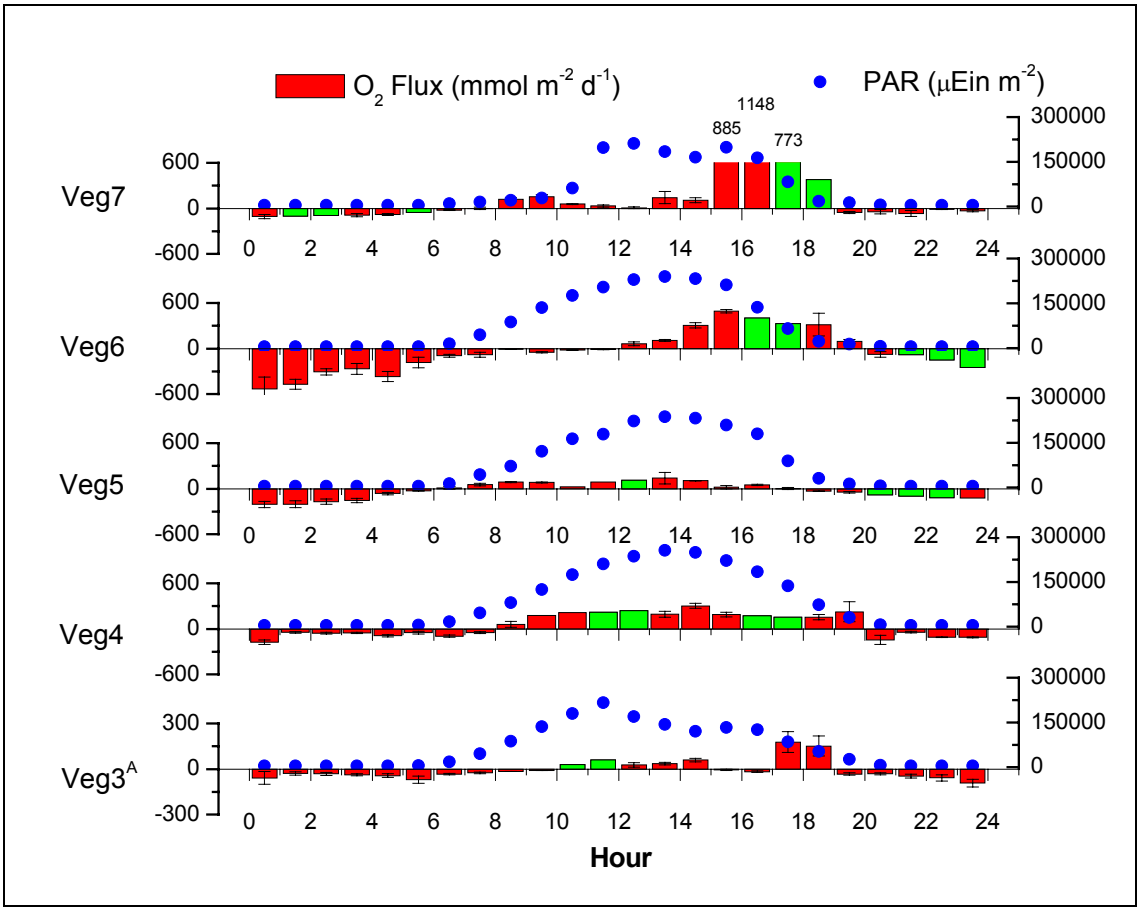

Figure 18a. Hourly vegetated DO flux results with the eddy correlation technique for each deployment. Hourly DO fluxes out of range are given above the flux. Red bars are measured DO fluxes with the eddy correlation system. Green bars are interpolated DO fluxes. Closed blue circles are hourly sums of PAR.
[A] Indicates a different scale than the rest of the deployments.

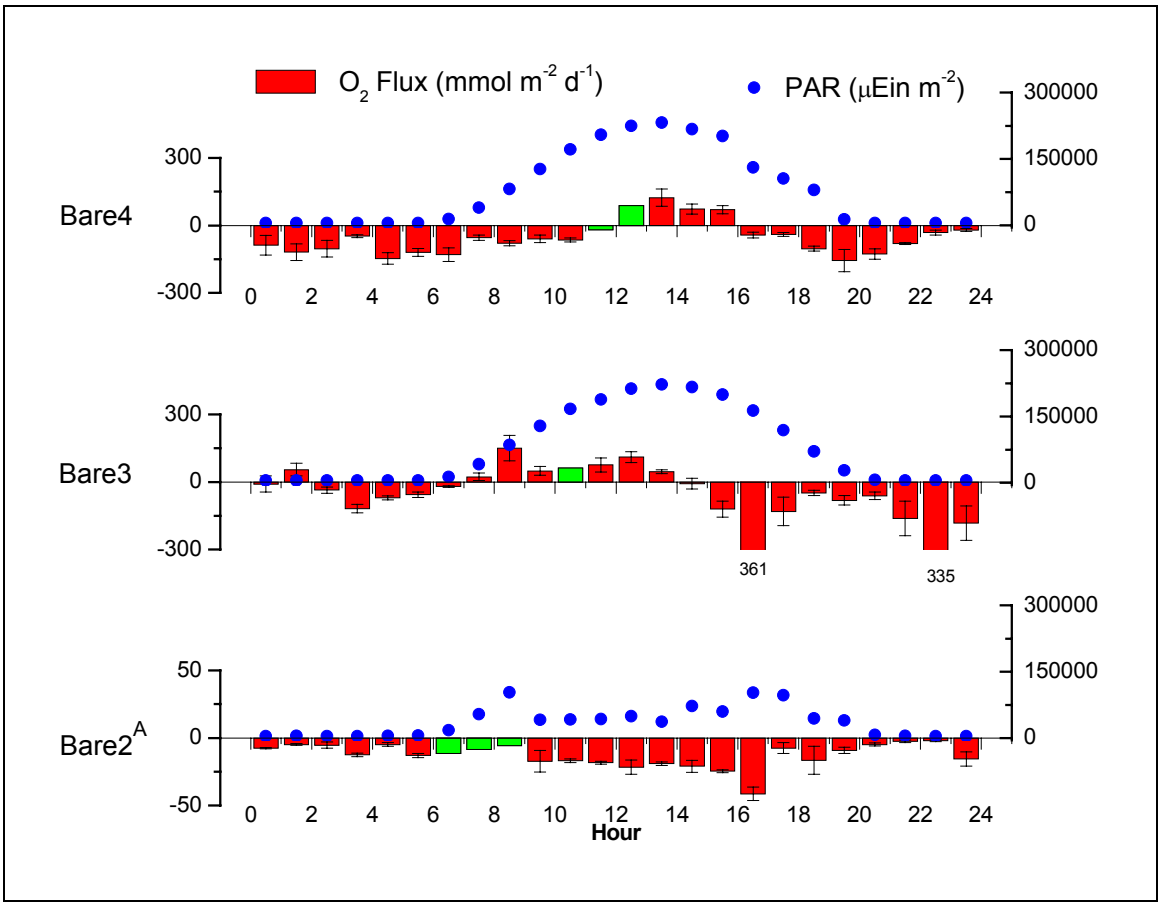

Figure 18b. Hourly bare sediment DO flux results with the eddy correlation technique for each deployment. Hourly DO fluxes out of range are given above the flux. Red bars are measured DO fluxes with the eddy correlation system. Green bars are interpolated DO fluxes. Closed blue circles are hourly sums of PAR.
[A] Indicates a different scale than the rest of the deployments.

Eddy correlation metabolism: The mean R over the vegetated site and bare sediment site was -155.6 ± 36.5 and -83.38 ± 35.0 mmol O_2 m^{-2} d^{-1}, respectively. Vegetated and bare sediment GPP was calculated to be 171.7 ± 24.9 and 18.00 ± 17.6 mmol O_2 m^{-2} d^{-1}, respectively. Vegetated and bare sediment NEM was calculated to be 16.1 ± 29.6 and -65.3 ± 26.9 mmol O_2 m^{-2} d^{-1}, respectively. DO flux calculations from individual eddy correlation deployments from the vegetated site were both net autotrophic and net heterotrophic, suggesting the site was nearly in metabolic balance, while all deployments at the bare sediment site were net heterotrophic (Table 6). Rates of R and GPP for the vegetated site were nearly twice as large as the bare sediment site (Figure 19).

Site & Deployment	Date	R	GPP	NEM	Trophic State	R	GPP	NEM	Trophic State
Flux Type:		RA	RA	RA		LD	LD	LD	
Vegetated									
3	6/25/2007	-50.0	45.7	-4.3	Hetero	-89.4	79.3	-10.1	Hetero
4	6/26/2007	-88.7	141.2	52.5	Auto	-103.5	191.1	87.7	Auto
5	7/10/2007	-124.7	101.4	-23.3	Hetero	-232.3	177.1	-55.2	Hetero
6	7/16/2007	-268.6	233.2	-35.4	Hetero	-256.2	229.3	-26.9	Hetero
7	7/18/2008	-68.0	194.6	126.5	Auto	-96.7	181.7	85.0	Auto
Mean		-120.0	143.2	23.2	Auto	-155.6	171.7	16.1	Auto
SE (n = 5)		39.2	33.2	29.9		36.5	24.9	29.6	
Sonde	7/10/2007	-34.9	88.1	53.1	Auto	-34.9	88.1	53.1	Auto
Bare Sediment									
2	6/18/2007	-7.3	-5.7	-13.0	Hetero	-14.2	-9.3	-23.5	Hetero
3	7/09/2007	-97.7	46.4	-51.3	Hetero	-127.8	12.3	-115.4	Hetero
4	7/11/2007	-88.4	35.0	-53.3	Hetero	-107.9	51.0	-56.9	Hetero
Mean		-64.5	25.3	-39.2	Hetero	-83.3	18.0	-65.3	Hetero
SE (n = 3)		28.7	15.8	13.1		35.0	17.6	26.9	
Sonde	7/11/2007	-18.6	40.0	21.4	Auto	-18.6	40.0	21.4	Auto

Table 6. Respiration (R), gross primary production (GPP) and net ecosystem metabolism (NEM) for individual eddy correlation calculated from a running average (RA) (right) and linear detrend (LD) (left) and datasonde deployments
Units mmol O_2 m^{-2} day^{-1}.

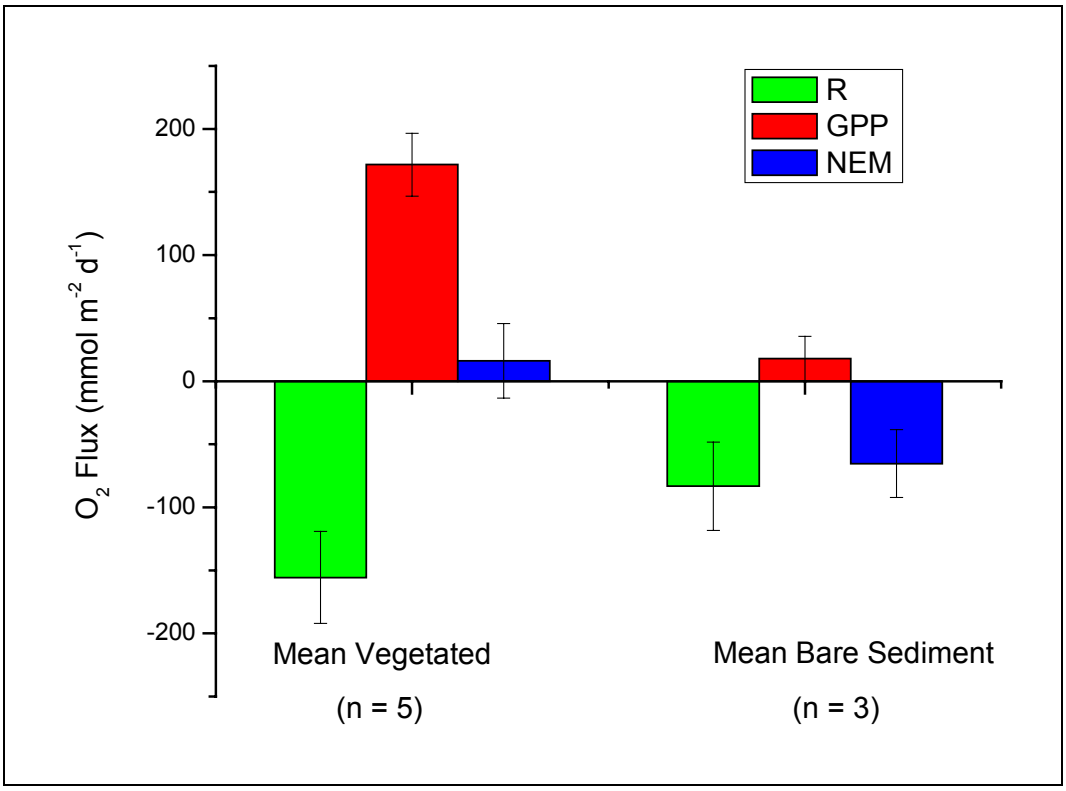

Figure 19. Mean respiration (R), gross primary production (GPP) and net ecosystem metabolism (NEM) for the vegetated site (left) and bare sediment site (right).

Open-water datasonde: DO change calculated from datasonde data was significantly lower than the concurrent eddy correlation deployment DO fluxes at both sites (Figure 20). Air-water exchange appeared to have a strong influence on 15-min average DO change. Diurnal variations of DO fluxes observed with the eddy correlation is not as evident in DO change variation with the datasonde deployments.

Trophic state varied depending on the criteria for calculating DO change with the datasonde. The datasonde data indicated net autotrophic ecosystem states during the deployments at both sites following the removal of anomalous rates of DO change observed in the light and dark. In contrast, using a simple mean of all rates of DO change during light and dark predicted net autotrophic state for the vegetated site, but predicted a negative GPP for the bare sediment site (Figure 21). The eddy correlation technique calculated net heterotrophic states for the comparable deployments. Rates of R calculated from the open water datasonde deployments were –34.93 and –18.58 mmol O_2 m^{-2} d^{-1} for the vegetated and bare sediment sites, respectively (Table 6). The comparable eddy correlation system deployments calculated rates of R to be -232.2 and –107.9 mmol O_2 m^{-2} d^{-1}. Rates of GPP calculated with the datasonde were 88.1 and 40.0 mmol O_2 m^{-2} d^{-1} for the vegetated and bare sediment sites, respectively. The comparable eddy correlation technique rates of GPP were 177.1 and 51.0 mmol O_2 m^{-2} d^{-1}. NEM determined from the datasonde for the vegetated and bare sediment sites was 53.1 and 27.4 mmol O_2 m^{-2} d^{-1}, respectively. This can be compared to a calculated NEM of –55.2 and –56.9 mmol O_2 m^{-2} d^{-1} estimated with the eddy correlation technique (Figure 22).

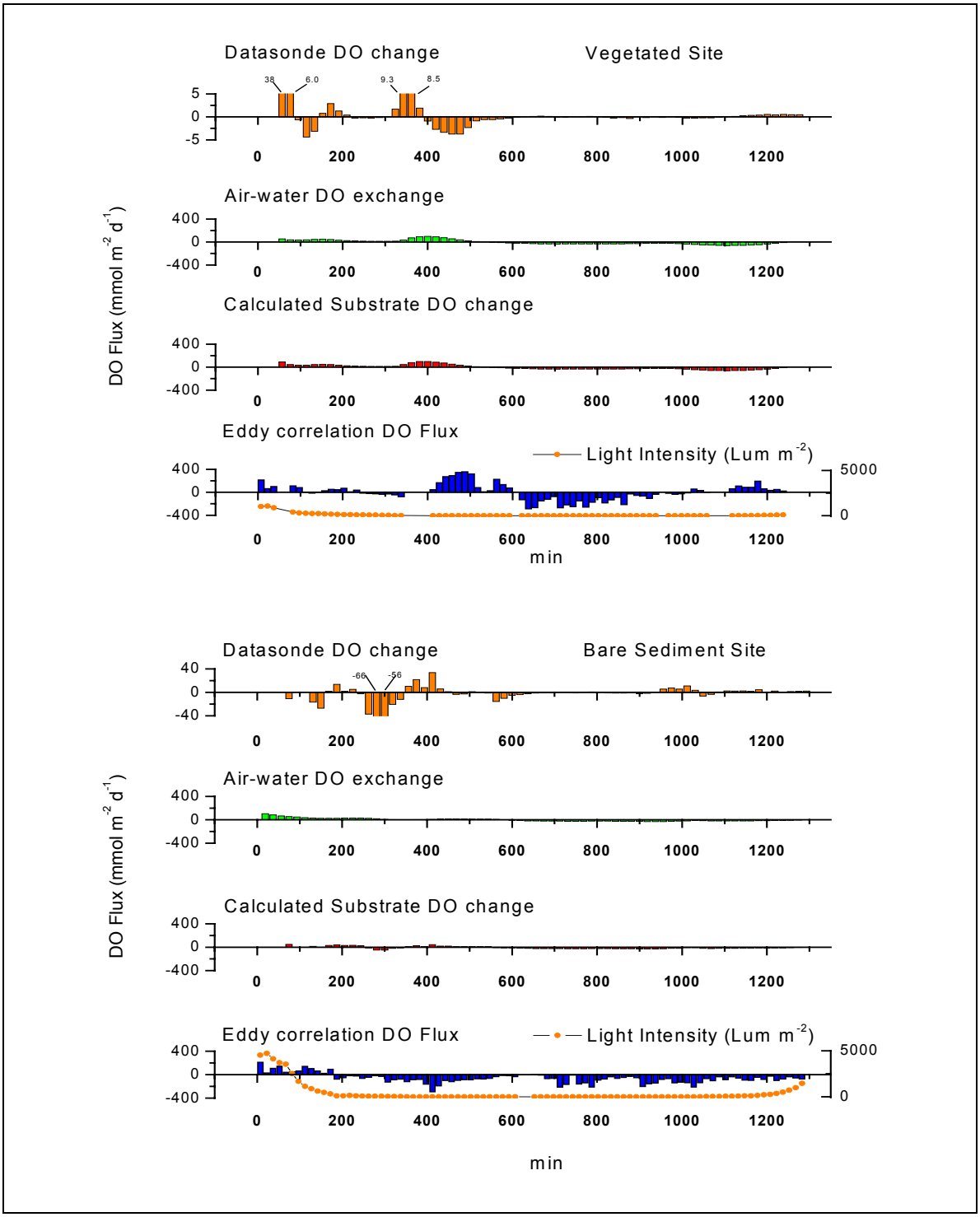

Figure 20. Top figure for vegetated site. Bottom figure for bare sediment site. From top to bottom: 15-minute DO change calculated from the datasonde, air-water DO exchange, calculated substrate-water interface DO change and respective eddy correlation substrate-water interface DO flux for comparison. Note different scales on graphs.

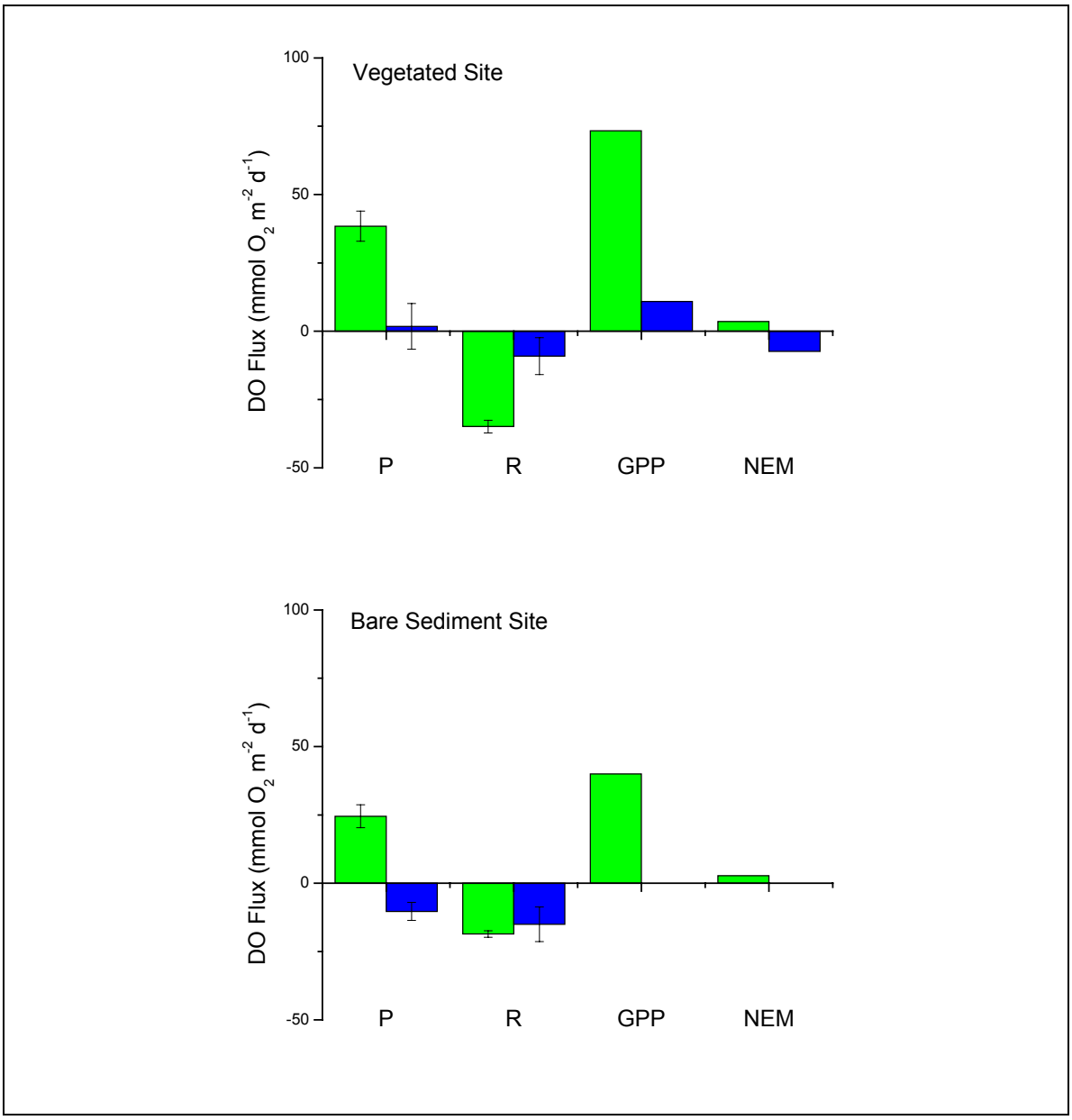

Figure 21: Ecosystem metabolism parameters calculated from rates of DO change from the datasonde data as calculated after the removal of anomalous rates of DO change from the light and dark (green) and mean of all rates of DO change from light and dark (blue) for the vegetated site (top) and the bare sediment site (bottom).

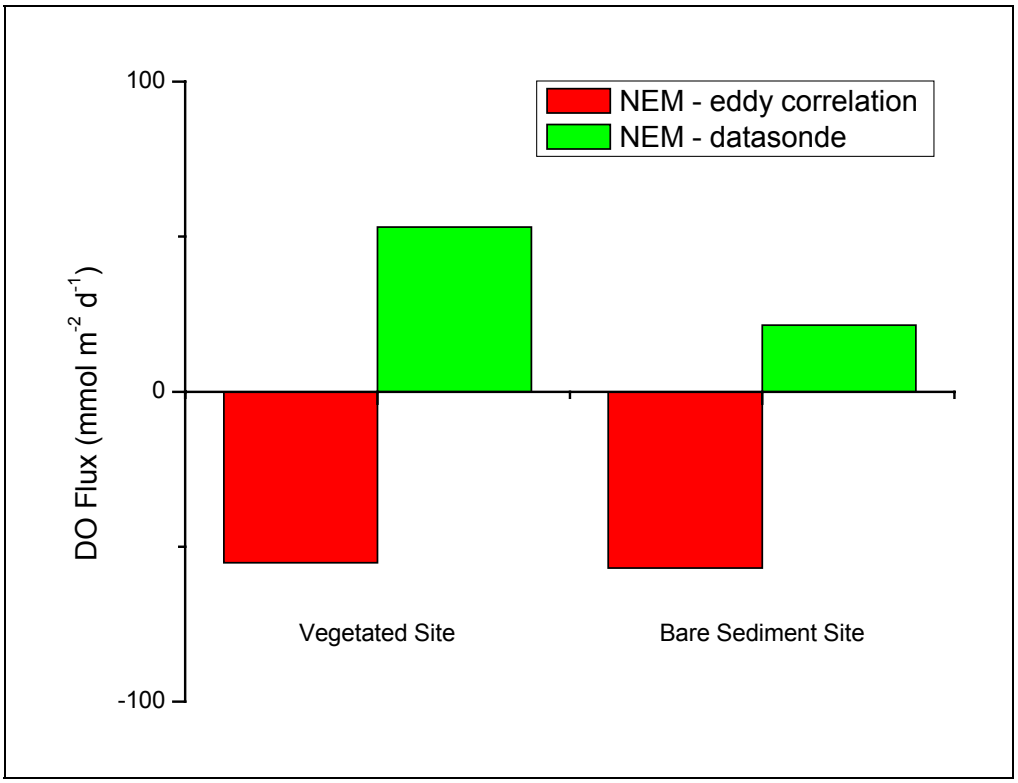

Figure 22. Comparison of NEM calculated with the eddy correlation system (red) and open-water datasonde measurements (green) for the vegetated deployment 5 (left) and bare sediment deployment 4 (right).

Discussion:

Eddy correlation method considerations: Measurements made with the eddy correlation technique can be conceptualized as the flux across the top of a control volume that sits between the sediment surface and the height of the ADV measuring volume. It is assumed that the flux across the top of this control volume is representative of flux at the substrate-water interface. In order for this to be true, it must be assumed that the storage of DO in the control volume is negligible. Changes in water temperature and water column metabolism can have an influence on DO storage. To correct for DO storage in this study, the size of the control volume was kept at a minimum by sampling as close as possible to the substrate surface. The eddy correlation technique also assumes that molecular diffusion within the control volume is negligible. This assumption is nearly always valid in coastal environments where turbulent mixing prevents large DO concentration gradients from establishing, and thus molecular diffusion is generally orders of magnitude smaller than advective transport.

The eddy correlation technique also assumes that the three-dimensional velocity field is not disturbed. However, changes in current direction can create situations where the flow is perturbed by unnatural structures like the legs of eddy correlation system tripod. Great care was taken in designing a tripod that would have minimum influence on local hydrodynamics including narrow legs. Since individual deployments were made with the same orientation relative to the sites, the argument could be made that a correlation between the DO fluxes and current direction for all deployments at a site may be an indication of an obstruction. Neither regression model from the two sites included

current direction as a significant variable, suggesting that the frame did not influence DO flux measurements.

Several sources of error could potentially come from the ADV, including inaccurate calibration or obstruction of the ADV measuring volume (Figure 3). The most likely causes for an obstruction of the measuring volume are suspended debris floating through the measuring volume or blades of seagrass waving in an out of the measuring volume under different current speeds. Had a large obstruction passed through the measuring volume it would show as an outlier DO flux and be removed from further analysis during quality checking. In addition, the tip of the oxygen microelectrode is so fragile that any debris passing through the measuring volume will likely break the microelectrode. A third possible obstruction would be the oxygen microelectrode itself. If the microelectrode is placed too far within the measuring volume then it could potentially corrupt ADV measurements. A test of the signal to noise ratio (SNR) with and without the microelectrode tip present in the measuring volume confirmed that in water with a background noise greater than 15 dB, the microelectrode tip has no influence on the ADV's performance (Atle Lohrmann, personal communication, March 20, 2007). Background noise from all eddy correlation system deployments in South Bay was greater than 15 dB due to high concentrations of suspended solids. In addition, the tip of the microelectrode was carefully positioned outside the measuring volume before each deployment.

Another potential source of error is the placement of the microelectrode's tip too far from the measuring volume. Depending on current direction and flow conditions, a spatial discrepancy between the measurements of vertical velocity and DO concentration

could result in a time lag between the two variables. This time lag would produce an underestimation of the DO flux based on a weakening of the correlation between the two variables.

Current direction can have a significant influence on the DO flux due to heterogeneity of the substrate and shifting of the eddy correlation footprint (Kuwae et al 2006, Berg et al. 2007). Because of the constant orientation of the eddy correlation system and the fact that current direction was not included as a significant environmental variable in the multiple regression models from either site suggests that substrate heterogeneity may not an issue during this study (Table 3).

Perhaps the most challenging aspect of the eddy correlation technique is determining the best method for calculating the flux. The cannon of literature on the subject is extensive and beyond the scope of this study. However it should be noted that the running average and linear detrend methods used in this study yielded very similar metabolic rates (Table 6). This suggests that over 15 min, water column concentrations of DO can generally be described linearly. Any variation in estimates between the two methods is the result of nonlinear changes in the concentration of DO over the 15 min.

To reduce the complexity of the data analysis in this study, a constant averaging window of 3841 (~ 1 min at 64 Hz) was used to calculate the running average DO flux for all deployment. Thus, the assumption is implicitly made that during a deployment the eddies contributing to the vertical flux have frequencies higher than 1 min. Clearly, tides and surface gravity waves can have strong influences on eddy size, making the use of a constant window size problematic. For example, increased water depths during high tides will allow eddies to grow much larger than during low tides.

Defining the averaging window too small or large can filter out eddies or include dynamic changes not associated with the turbulent transport, respectively. This problem is highlighted in Figure 23, which demonstrates how sensitive the DO flux can be to increasing the average window size (open black circles). The initial decrease in the DO flux largely coincides with a jump in the normalized cumulative co-spectra (red and blue lines respectively) at approximately 1.6 s (0.6 Hz). This decrease contributes approximately 60 - 80% of the total DO flux and is the result of surface gravity waves. An averaging window of 1 min (0.016 Hz) will then encompass these eddies. However, a second decrease in the DO fluxes coincides with a decrease of the normalized cumulative co-spectra at approximately 2.7 min (0.006 Hz) and contributes an additional 10 - 20% of the total DO fluxes. The averaging window of 1 min failed to capture these "slower" eddies and underestimated the DO flux by 10 - 20% for this 15-min burst. However, additional co-spectra analysis from each site does not include the observed lower frequency oscillations, and the ~1 min averaging window encompasses the total DO flux (Figures 6a&b).

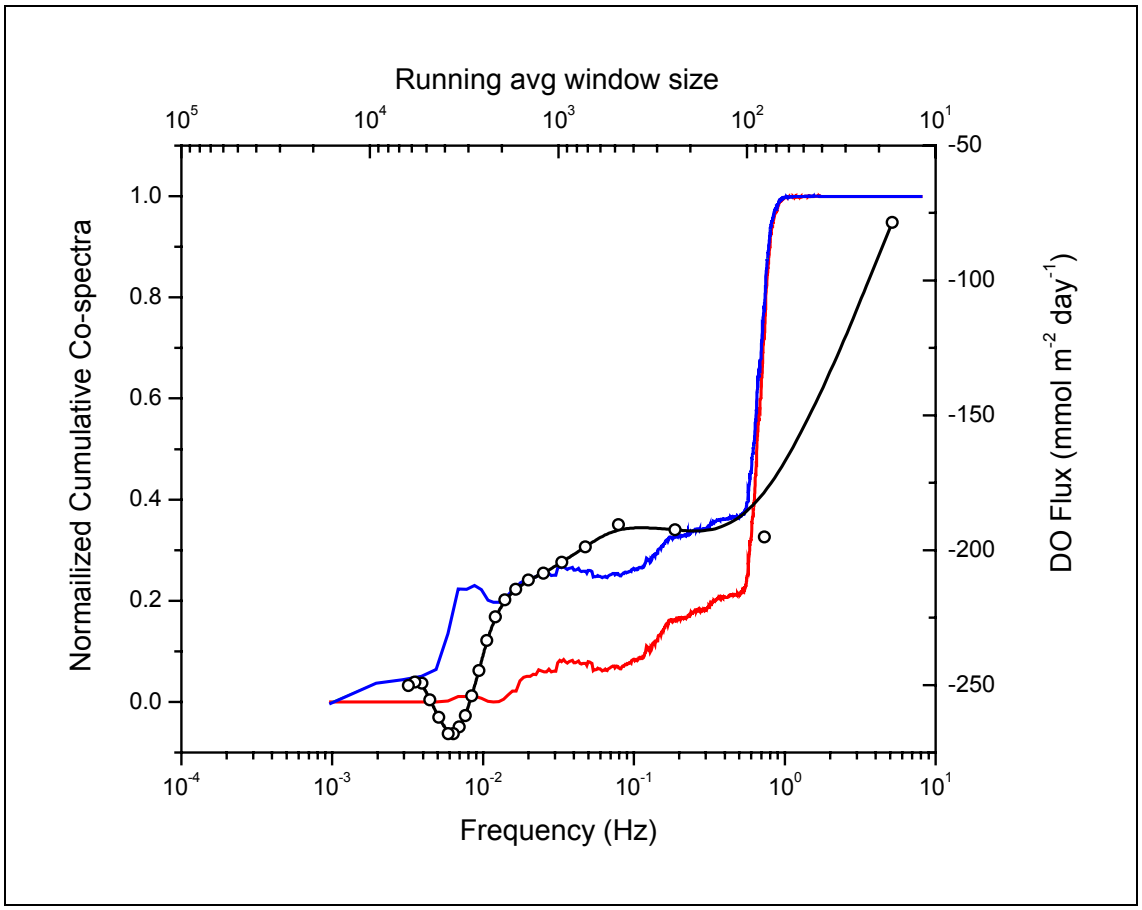

Figure 23: Changes in the O_2 eddy flux based on the running average window size (black open circles) overtop of the normalized cumulative co-spectra using the two methods for calculating the flux; running average (red) and linear detrend (blue).

Despite the assumptions associated with the eddy correlation technique, the standard errors of R, GPP and NEM (Figures 18a&b, Table 6) are similar to published results from benthic chambers (Ziegler 1998, Hansen et al. 2000), open-water measures (Ziegler 1998, Caffrey 2004) and previous eddy correlation system deployments (Kuwae et al. 2006, Berg et al. 2003). This suggests that the collective influence of the eddy correlation technique sources of error is tolerable. Perhaps the two biggest advantages of the eddy correlation technique are the high-temporal resolution and non-invasive integrated measurements. Measurements with the eddy correlation technique are not only non-invasive, but integrate over a relatively large area (Figure 24). The eddy correlation footprint is the area that lies upstream of the eddy correlation system and can be estimated based on the measurement height above the substrate, the surface roughness height (Z_0), and water depth (Berg et al. 2007). For example, eddy correlation measurements made 15 cm above a substrate with a surface roughness height of 0.01 m (rough bare sediment) in 1 m of water will have a footprint of approximately 40 m^2. The advantage of measurements being made upstream and integrated over a large area is that true *in situ* environmental conditions will exist and measurements can be made over many types of substrate. As this study shows, environments with substrate heterogeneity can be accurately integrated into ecosystem scale calculations. Based on the results from this and other aquatic eddy correlation studies, it can be seen that the advantages of the eddy correlation technique clearly outweigh the potential errors.

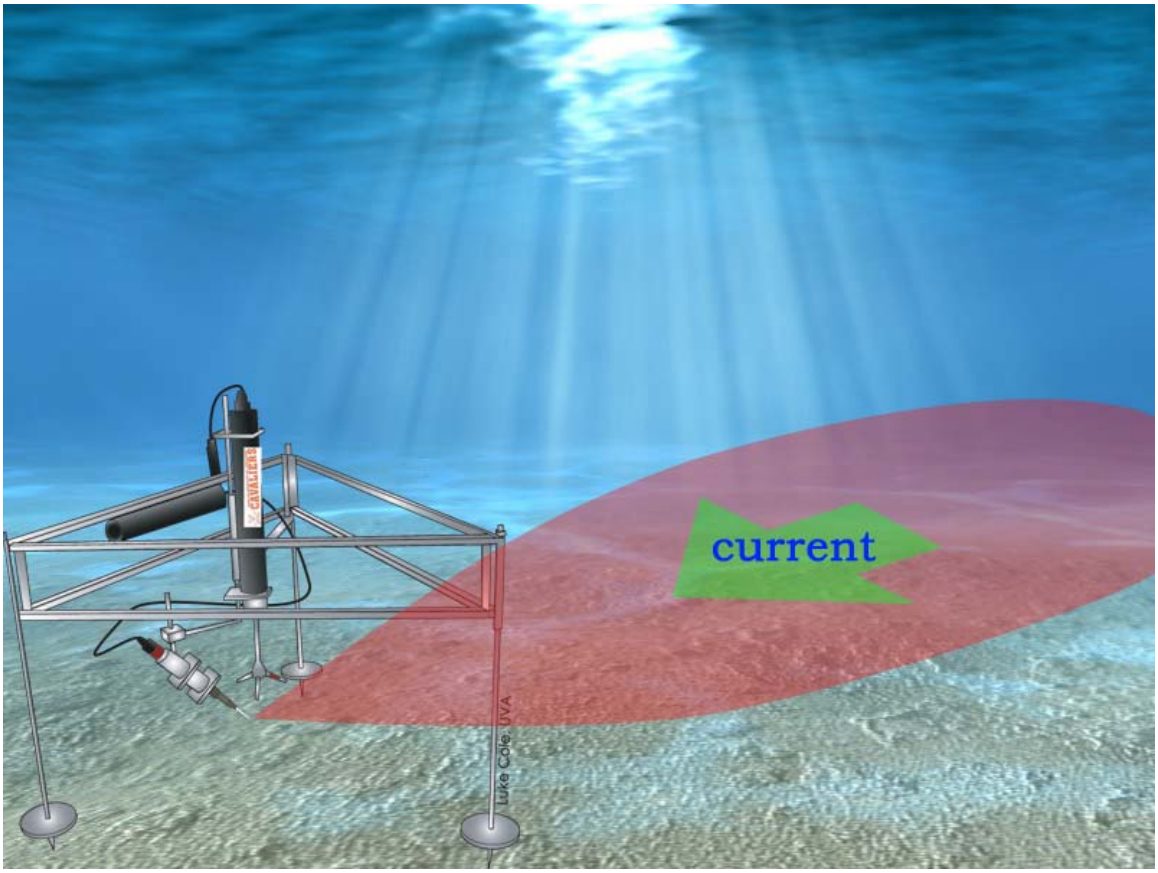

Figure 24: Schematic of eddy correlation footprint upstream of eddy correlation system.

Eddy correlation DO fluxes: This study is the first of its kind to show high-temporal resolution DO fluxes for a seagrass-dominated ecosystem under true environmental conditions. Because of the eddy correlation technique's non-invasive sampling, variations of the DO flux can be incorporated into ecosystem metabolism calculations more accurately than other methods. This makes quantifying ecosystem metabolism rates in dynamic environments like South Bay possible, where physical factors such as currents, temperature and light influence metabolism rates on time scales of minutes to seasons. The hourly DO fluxes calculated with the eddy correlation technique highlight this variability temporally over a diurnal cycle and from day to day, and spatially between sites (Figures 18a&b).

DO flux observations from the two sites show a similar response to diurnal changes to light. It is interesting to note that bare sediment deployment 3 occurred under the lowest mean daily PAR (possibly due to overcast skies) and also did not have any positive DO fluxes and significantly lower negative DO fluxes than the other bare sediment deployments. Anomalous hourly DO fluxes were observed in several of the eddy correlation deployments for this study. Anomalies included positive DO fluxes during dark periods and negative DO fluxes during light periods. Several other studies have made similar observations (Kemp and Boynton 1980 and references within). This study also observed a large increase in hourly DO fluxes during and for several hours following sunset over the vegetated site, which has previously not been reported. Similar observations have been made with the eddy correlation technique over bare sediments in other marine environments (Peter Berg, personal communication), and the possible reasons for this pattern is explored in further detail in the Appendix. In all, individual

eddy correlation deployments showed consistent patterns of hourly DO fluxes variability over a diurnal cycle. However, DO flux variability was high among consecutive hours.

DO flux variability: Results from the stepwise multiple linear regressions suggest that several environmental variables account for some of the variation of hourly DO fluxes from all deployments in the vegetated and bare sediment sites (Table 3). It should be noted that a strict entry and remove criterion of 0.05 was used for all stepwise multiple liner regressions in this study. More liberal values have been used in other studies (e.g. Hovel et al. 2002, Caffrey 2004) and would likely cause more variables to be included in the models and slightly increase the model R^2.

It was not surprising that PAR was the most important predictor of DO flux variation (Figure 15). PAR has previously been shown to be an important predictor ecosystem metabolism in other coastal systems during the summer (D'Avanzo et al. 1996, Ziegler & Benner 1998). Results from the linear regressions show that the eddy correlation technique is capable of capturing the response of seagrasses to short-term variations in light availability, on the order of minutes to hours, such as local turbidity events or variations in incident light (e.g., passing clouds). Seagrasses were also observed responding to short-term variations in current flow within the coastal bay, likely onset by surface wind and tides. The regression models also show that variability in ambient water column DO concentrations influences DO fluxes at both sites (Figure 16).

This study is the first to report a significant relationship between DO fluxes and significant wave height for a seagrass-dominated community. The relationship between significant wave height and DO fluxes was positive for the vegetated site, but negative

for the bare sediment site (for the running average DO flux only) (Figure 17). The negative relationship may be the result of increased R associated with increased pumping of DO rich water into oxygen-starved sediments. Studies have shown that DO penetrates farther into permeable sediments with increased hydrodynamics (Prech and Huettel 2003, Prech and Huettel 2004, Prech et al. 2004). The positive relationship between DO fluxes and significant wave height may be due to increasing hydrodynamics reducing leaf self-shading and the thickness of the diffusion boundary layer at the leaf surface, enhancing photosynthesis (i.e. Fonseca & Kenworthy 1987, Gambi et al. 1990, Koch 1994, Koch 1999).

The relationship between DO fluxes and wave-induced vertical velocities was been observed by Kuwae et al. (2006) over bare sediment using the eddy correlation technique. This relationship highlights the advantage of the eddy correlation technique's ability to measure DO fluxes both *in situ* and non-intrusively. Despite the scarcity of evidence showing this relationship over different substrates, it is not unexpected when using the eddy correlation technique. This is because the vertical velocity used by the eddy correlation technique to calculate fluxes can be influenced by wave orbitals. This relationship can clearly be seen in Figure 25, where the period of the vertical velocity (red) is synchronized with the oscillations in water depth (blue) caused by surface waves from vegetated deployment 5.

Water depth can be considered influential to DO fluxes in several ways. First, water depth can serve as a proxy for tidal stage. From this perspective water depth may be autocorrelated to current speed and direction due to magnitude and direction of ebbing and flooding tides on a semi-diurnal tidal cycle. While the models for vegetated

deployments 4, 5 and 6 do not include current speed, vegetated deployments 5 and 6 do include current direction as significant variable. However variance inflation factors of current direction were well below 10 in either case. Water depth can also influence seagrass production due to light attenuation in the water column and light availability at the leaf surface.

It is interesting that water temperature was not included in any of the models as a significant parameter. Significant relationships between ecosystem metabolism and water temperature seasonally have been observed in similar studies (Moriarty et al. 1990, Ziegler & Benner 1998, Caffrey 2004). The variation in water temperature during this study was low (Figures 7b - 14b). It is likely that increased air temperatures and solar radiation during June and July stunted pronounced diurnal variations of water temperature and its influence on metabolic activity.

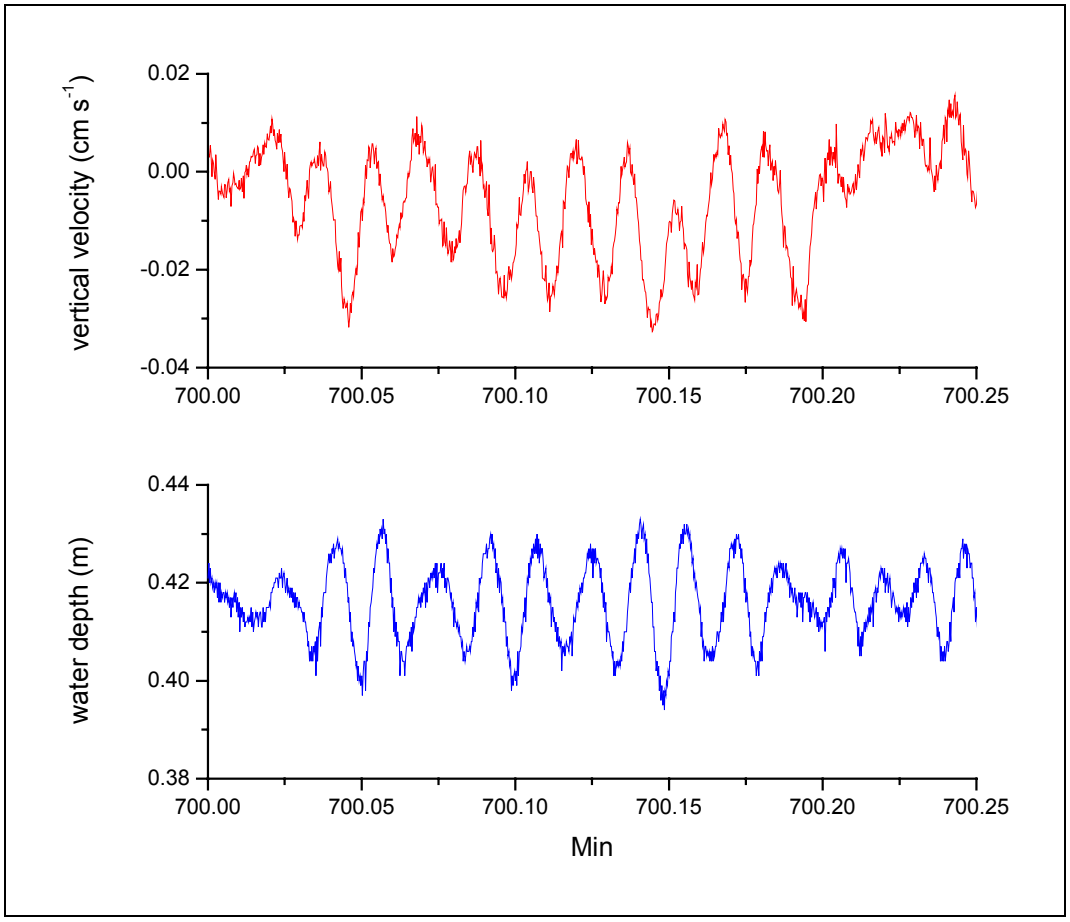

Figure 25. Relationship between vertical velocity (red) and water depth (blue) from 700.0 to 700.25 min into vegetated deployment 5.

Seagrass community metabolism: The vegetated site was observed to have rates of R and GPP nearly twice that of the bare sediment site (Figure 19). These results are in agreement with Linedeboom and deBree (1982), who found both GPP and R to be significantly greater in *Z. marina* beds than in nearby bare sediment areas. Erftemeijer et al. (1993) found tropical meadows of seagrasses also to be more productive than the nearby bare sediment. However, Barron et al. (2004) observed rates of R and GPP to decrease over time as bare sediment was recolonized with seagrasses.

Even though a mean autotrophic state was calculated for all vegetated eddy correlation deployments, the variation in trophic state for individual eddy correlation deployments suggests a near metabolic balance is probably a more correct picture of the average trophic state. The bare sediment site was predicted to be net heterotrophic during this study. Benthic summer heterotrophy has also been observed within seagrass-dominated ecosystems in a Danish estuary (Gazeau et al 2005), the Netherlands (Lindeboom and DeBree 1982), and the Chesapeake Bay (Murray and Wetzel 1987). In contrast, net autotrophic conditions have been observed for benthic microalgal-dominated environments over the spring and summer in Hog Island Bay, switching to net heterotrophy in the fall as a result of lower benthic autotrophy and high pelagic heterotrophy (McGlathery et al 2001).

Of the metabolism studies performed in *Z. marina*-dominated ecosystems, rates of GPP were similar to rates from this study (Table 7). Rates of R from this study were slightly higher than other published results. This caused rates of NEM from this study to be lower than previous studies. This can likely be attributed to seasonal variations in metabolism and the young age of the recolonized seagrass communities in South Bay.

The age of a seagrasses meadow is known to influence community metabolism. Barron et al. (2004) observed a switch from net autotrophic conditions to heterotrophic conditions as seagrasses recolonized a coastal lagoon in Spain. The authors observed *C. nodosa* younger than 2 yr to have a net uptake of dissolved organic carbon (DOC) while older growth had a net release. The authors attribute the switch in trophic state to several factors including the increase in old growth *C. nodosa* biomass shading itself and the photosynthetically active benthos beneath it, the support of more diverse micro and macrofaunal communities in more established beds, and the import of organic matter. The South Bay sites in this study were initially seeded in 2001, and although they were approximately the same age as the *C. nodosa* meadows, sediment organic matter in the South Bay seagrass meadows was relatively low (Table 1). It is possible that as the restored South Bay meadows continue to mature and accumulate organic matter, NEM will change, and the sites may become heterotrophic. It is also important to note that the ratio of below-to- aboveground biomass is higher in the *C. nodosa* seagrass than *Z. marina* meadows, and so respiration is likely higher in the *C. nodosa* meadows.

Seasonality is also known to influence community metabolism in temperate coastal environments. Table 7 shows a range of seasonal and annual averages of NEM from *Z. marina* communities. Martin et al (2005) observed considerably high rates of NEM during the spring in France. Murray and Wetzel (1987) found a notable decline in P and R during June and July in a seagrass community in the Chesapeake Bay near South Bay. Lindeboom and DeBree (1982) observed a near balance of NEM from spring through late summer measurements in the Netherlands. Nixon and Oviatt (1972) predicted a slightly heterotrophic *Z. marina* community from midsummer measurements

in a coastal pond in Rhode Island, USA. Based on these published studies, rates of NEM appear to be highest in the spring and decrease into late summer and fall, probably due to the increased production of the macrophytes in the spring and decrease in the late summer and fall. High temperatures typically lead to a disproportionate increase in respiration relative to production, and seagrasses in the Virginia region slough leaves in late summer. In the fall, lower temperatures and lower incident light levels lead to lower areal production rates. Based on these observed trends, the June and July measurements from this study likely coincided with the transition from the increased early summer production to the late summer decline.

The idea of a transition in the vegetated site's trophic state may be supported by the fact that three out of our five eddy correlation deployments from the vegetated site were net heterotrophic, suggesting that a near metabolic balance may be a more accurate characterization of the vegetated site during this study. Several studies have observed near ecosystem metabolic balances during the summer in seagrass communities, including Santos et al. (2004) for *Z. noltii* and *C. nodosa* communities in southern Portugal, D'Avanzo et al. (1996) for a *Z. marina*-dominated estuary annually in Massachusetts, USA, Ziegler and Benner (1998) for a *Z. marina* community in Texas, USA, and Lindeboom and deBree (1982) for a *Z. marina* community in the Netherlands. Lindeboom and Sandee (1989) and Erftemeijer et al. (1993) also have observed metabolic balances in tropical seagrass communities.

Assuming water column metabolism is negligible in South Bay (McGlathery et al. 2001) coupled with the observation of low densities of drift macroalgae in the footprint of our measurements, the difference in metabolism rates of the bare sediment site from the

vegetated site can provide an estimate of metabolism of the seagrass and epiphyte component of the vegetated ecosystem (Murray and Wetzel 1987, Hansen 2000). Seagrass and epiphyte R was -72.3 mmol O_2 m^{-2} d^{-1}, P (calculated as [vegetated GPP - bare sediment GPP] - seagrass and epiphyte R) was 81.4 mmol O_2 m^{-2} d^{-1}. It should be noted that water column metabolism rates increased slightly in a nearby coastal bay following a mid-summer decline in macroalgal biomass (McGlathery et al. 2001), so these calculations are only a first-order estimate. However, these estimates are similar to summer measurements of *Z. marina* and epiphytes from a nearby community reported by Murray and Wetzel (1987), where water column and sediment components of a seagrass-dominated ecosystem were measured individually. This suggests that water column metabolism may not have been a significant source of ecosystem metabolism during this study. Routine monitoring through the VCR/LTER program have shown water column dissolved nutrient and chlorophyll concentrations to be low in these coastal bays (http://www.vcrlter.virginia.edu/data/eml2/datamap.html).

Location	Species	Time of Year	GPP	R	Method	Source
Coastal Pond, RI, USA	*Z. marina*	August	141	191	Open-water	Nixon & Oviatt (1972)
Brackish Lake, Netherlands	*Z. marina*	March - October	16 - 94	4 - 31	Benthic chamber	Lindeboom and DeBree (1982)
Shallow Estuary, MA, USA	*Z. marina*	Annual Average	257	125 - 156	Open-water	D'Avanzo et al (1996)
Coastal Bay, France	*Z. marina*	March - April	156	53.8	Benthic chamber	Martin et al (2005)
Chesapeake Bay, VA, USA	*Z. marina*	Annual Average	132	82	Benthic chamber	Murray and Wetzel (1987)
Coastal Bay, VA, USA	*Z. marina*	June and July	143	120	Eddy correlation	This study

Table 7. Comparison of respiration (R) and gross primary production (GPP) of this study with published results over *Z. marina*-dominated environments. Units in mmol C m^{-2} d^{-1} using a PQ = 1.19 and RQ = 1.0. *Table adapted from Ziegler and Benner (1998).*

Implications for seagrass restoration: The results from this study provide valuable information about seagrass-dominated environments in the context of recolonization and ecosystem function. One aspect of ecosystem function that is of great interest in coastal communities is the role of seagrasses as coastal filters of nutrients (Bricker and Stevenson 1996, D'Avanzo et al. 1996, Welsh et al. 2000, Kemp et al. 2005). This is especially important in temperate environments that experience eutrophication from anthropogenic inputs as they are reported to cause a shift from seagrass-dominated to macroalgal-dominated ecosystems under increased loading (Hauxwell et al. 2003, Lee et al. 2004). The increase in anthropogenic development of coastal landscapes worldwide has led to a greater need to understand these processes in order to conserve coastal environments and their inhabitants.

NEM was converted to units of carbon (mmol of C) using an empirically derived community photosynthetic quotient (PQ) of 1.19 calculated specifically for a *Z. marina* community (Martin et al. 2005) for the vegetated site and a PQ of 1.25 (Murray and Wetzel 1987) for the bare sediment site. NEM was estimated to be 19.2 mmol of C m^{-2} d^{-1} for the vegetated site (Table 8). NEM was estimated to be -81.6 mmol of C m^{-2} d^{-1} for the bare sediment site.

The autotrophic state of the vegetated site suggests that it is a sink of C during the summer growing season. In contrast, the heterotrophic state of the bare sediment site suggests that it acts as a source of C. Because of the similar benthic composition of the bare sediment site and the vegetated site, the case could be made that the bare sediment within the vegetated site is also heterotrophic and a source of C to the seagrasses. If this were the case, then the internal cycling C from the bare sediment to the seagrasses would

suggest that South Bay is generally autochthonous. Barron et al. (2004) found that as seagrasses recolonized bare sediment substrates the system move from autochthonous to allochthonous. The authors suggested that the transition was due to the increased benthic decomposition as a result of increased OM in the sediment that had settled out of the water column due to increased seagrass canopy biomass.

Nitrogen assimilation was predicted using the molar ratio of carbon to nitrogen (C:N) within the tissue of the *Z. marina* at the vegetated site (e.g. McGlathery et al 2001, Hauxwell et al. 2003). Because the percent total biomass of the other primary producers within the vegetated site was not quantified, these calculations are only a first order estimate. The C:N molar ratio of seagrasses varies considerably both within the plant (Touchette et al 2003) and spatial and temporally within a meadow (Fourqurean et al 1997, Lee et al. 2004, Papadimitriou et al. 2005, Hasegawa et al. 2007). A C:N ratio of 19.9 for *Z. marina* new growth during the summer (Fourqurean et al. 1997) was used for this study because metabolism was measured over the summer growing season. N assimilation was estimated to be 1.0 mmol of N m^{-2} d^{-1} for the vegetated site (Table 8). These low rates are similar to rates reported by Hauxwell et al. (2003) specifically for *Z. marina* communities under low N loading in a New England estuary. The low rate of N assimilation for vegetated site suggests it is a marginal sink of N during the summer growing season.

		mmol O_2 m^{-2} d^{-1} NEM	mmol C m^{-2} d^{-1} NEM	mmol N m^{-2} d^{-1} N assimilation
Vegetated (*Zostera marina*)				
	RA	23.2	27.6	1.4
	LD	16.1	19.2	1.0
Bare sediment (benthic microalgae)				
	RA	-39.2	-49.0	
	LD	-65.3	-81.6	

Table 8. Vegetated site NEM in units of mmol O_2 m^{-2} d^{-1} and mmol C m^{-2} d^{-1} using a PQ of 1.19. N assimilation calculated with a C:N ration of 19.9. Calculations performed with running average (RA) and linear detrend (LD) DO fluxes.

Comparison with open-water datasonde method: The use of DO change from open-water measurements for calculating rates of metabolism generally make the following assumptions: (1) the water column is well mixed; (2) R is constant over the diurnal cycle; (3) the horizontal flux of DO is zero (Seeley 1969). Like benthic chambers, these assumptions may be sources of significant error in coastal highly dynamic environments. As the eddy correlation DO fluxes show (Figure 6a&b), rates of R are highly variable over diurnal cycles. Kemp and Boynton (1980) observed that open-water measurements are strongly influenced by horizontal DO fluxes in shallow estuaries. In addition open-water methods must be corrected for air-water exchange (Seeley 1969, Nixon and Oviatt 1972, Kemp and Boynton 1980, Marino and Howarth 1993, D'avanzo et al. 1996, Ziegler and Benner 1998, Caffrey 2004) requiring local wind speed data to be known. Air-water exchange in this study was seen to be nearly an order of magnitude larger than the DO change calculated by the datasonde and had a significant influence on calculating ecosystem metabolism (Figure 20).

Rates of R are estimated based on mean differences in consecutive dark rates of DO change and rates of P are estimated by mean differences in consecutive light rates of DO change. Multiple sources of error can result from this simple calculation depending on the temporal frequency of the DO measurements. Typical open water measurements are based on a sampling frequency of 1 hour or longer (e.g. D'Avanzo et al. 1996, Caffrey et al. 2004). 15-min averages of DO fluxes from the eddy correlation technique can be highly variable. Single measurements at lower temporal frequencies will certainly overlook this variability. Because it is difficult to obtain rates of R during light hours and typically a mean value of R from dark measurements is used to represent rates of R for

light hours (e.g. Lindeboom and Sandee 1989), variation of R during light hours is ignored and the assumption that R is equal in both the dark and light must be made. Variations of R during the dark are known to be influenced by environmental variables such as water temperature, wave action and current flow (Malan and McLachlan 1991, Plus et al. 2001, Huettel et al. 2003). Since these environmental variables vary during dark and light periods of the day, so should R. By ignoring variation in the rates of R during light hours may be another source of error in open-water metabolism calculations.

The discrepancy in datasonde and eddy correlation DO fluxes (Figure 20) and metabolism calculations (Figure 22) suggest that eddy correlation measurements are more accurate in coastal environments. Because *in situ* benthic chambers are less accurate than open-water measurements due to the exclusion of environmental variables (Kemp and Boynton 1980, Ziegler and Benner 1998) and laboratory core incubations provide even less accurate measurements than *in situ* benthic chamber due to complete removal from environment, the eddy correlation technique is the most accurate measurements of community scale DO fluxes and metabolism to date. Rates of DO change measured with open-water techniques observe changes in mean DO concentrations and are not true fluxes, but rather DO change. As a result, the open-water method is prone to influences of horizontal and air-water DO fluxes corrupting measured rates of DO change. As this study shows, these influences can be large and may result in inaccurate estimates of DO fluxes and community metabolism.

Other DO flux method considerations: It should be noted that using DO fluxes to calculate ecosystem metabolic over vegetated substrates is not without criticism. The majority of these criticisms center around missing terms of the DO flux mass balance. For example, in seagrass-dominated environments the storage of DO within seagrass lacunae could lead to an underestimation of seagrass P. Lindeboom and deBree (1982) observed rapid linear response of *Z. marina* P and R rates in light and dark incubations and a high correlation of above-ground biomass of different lacunal storage volumes and consumption rates. They concluded that over a diurnal cycle, lacunal DO storage within *Z. marina* were not believed to have a significant influence on the rates of either P or R. DO is known to be released from the tips of *Z. marina* rhizomes and is likely consumed in the rhizosphere and never reported in seagrass-dominated ecosystem rates of P and R. Frederiksen and Glud (2006) have suggested that about 12% of the diffusive DO uptake is meet by this mechanism and concluded that is an insignificant component of benthic R. R may also be underestimated due to oxidation of compounds such as sulfate and iron but is also assumed to be negligible when calculating ecosystem-scale processes like community metabolism. Community based DO fluxes are also not entirely understood. Several studies, including this one, have observed anomalous diurnal DO patterns (see Appendix).

Benthic microcosm method considerations: To use DO change from benthic microcosms: for calculating rates of metabolism the following assumptions are generally made: (1) steady state solute exchange conditions exist during the incubation; (2) hydrodynamic influences are negligible; (3) sampled area is representative of ecosystem (Viollier et al. 2003). However one or more of these assumptions may lead to significant

sources of error in dynamic environments like coastal bays. Attempts have been made to account for wave action (Malan and McLachlan 1991), turbulence intensities (Oldham et al. 2004), and hydrodynamic properties (Tengberg et al. 2004 and references within), including modified stirring techniques like Savonius rotors (e.g. Tengberg 1995, Ziegler and Benner 1998). At best benthic chambers may mimic local light and some hydrodynamic conditions, but usually ignore them altogether (Barron et al. 2004). Under certain conditions chambers are also known to develop gas bubbles, resulting in an underestimation of P (Revsbech et al. 1981, Lindeboom and DeBree 1982). Benthic chambers are also notoriously difficult to deploy on biogenic structures such as oysters, corals, and seagrasses. Despite the wide use of benthic chambers over seagrass, the mere presence of the chamber has a significant influence on the local hydrodynamics within the canopy (e.g. Lindeboom and DeBree 1982, Ziegler and Benner 1998, Hansen et al. 2000, Plus et al. 2001, Martin et al. 2005, Thouzeau 2007). These problems can be compounded by issues of scaling (Fonseca 1996, Bostrom et al. 2006). Micro-environments within seagrass communities are known to be extremely heterogeneous in flora and fauna type and density (Mattila et al. 1999, Turner et al. 1999, Bostrom et al. 2006) which can influence ecosystem function (Hebert et al. 2007) and hydrodynamics (Koch et al. 2006). Benthic chambers are not well suited for seagrass-dominated ecosystems due to the exclusion of physical forcing and the problems associated with scaling.

Conclusions:

The high temporal resolution of the eddy correlation technique provides a better understanding of DO flux variability, and allows more accurate calculations of ecosystem metabolism. Furthermore, the eddy correlation technique's non-invasive nature provided new insight into diurnal DO flux variation and relationship with environmental variables. This included, until now, the previously unreported relationship between DO flux variability and significant wave height over vegetated substrates. Concurrent open-water datasonde DO change show marginal agreement with the eddy correlation technique. Differences in DO flux estimates and ecosystem metabolism between the two approaches highlight the problems associated with the current methods used to calculate DO fluxes and ecosystem metabolism. South Bay metabolism was in near metabolic balance during the June and July sampling period, with the vegetated substrate being net autotrophic and the bare sediment substrate net heterotrophic. Estimates of C cycling suggest that the bare sediment is a net source of C while the vegetated substrate was a net sink. N assimilation calculations indicate an increased assimilation and temporary retention of N in the benthic community as it shifts from bare to algal-dominated and ultimately seagrass-dominated substrate with the successful seagrass restoration efforts. This study highlights the importance of seagrasses in coastal bays and the necessity to understand ecosystem metabolism as it relates to ecosystem function and overall health.

Literature Cited:

6-Series Multiparameter Water Quality Sondes User Manual. YSI, Inc USA. October 2006 (Revision D).

Abdelrhman, M. 2007. Modeling coupling between eelgrass *Zostera marina* and water flow. *Marine Ecology Progress Series*. 338: 81 – 96.

Ackerman, J., Okubo, A. 1993. Reduce mixing in a Marine Macrophyte Canopy. *Functional Ecology*. 7(3): 305 – 309.

Agawin, N., Duarte, C. 2002. Evidence of direct particle trapping by a tropical seagrass meadow. *Estuaries*. 25(6A): 1205 – 1209.

Arnold, G, Luckenbach, M, Unger, M. 2004. Runoff from tomato cultivation in the estuarine environment: biological effect of farm management practices. *Journal of Experimental Marine Biology and Ecology*. 298: 323 – 346.

Barron, C., Marba, N., Terrados, J., Kennedy, H., Duarte, C. 2004. Community metabolism and carbon budget along a gradient of seagrass (*Cymodocea nodosa*) colonization. *Limnology and Oceanography*. 49(5): 1642 – 1651.

Berg, P, Roy, H, Janssen, F, Meyer, V, Jorgensen, B, Huttel, M, de Beer, D. 2003. Oxygen uptake by aquatic sediments measured with a novel non-invasive eddy-correlation technique. *Marine Ecology Progress Series*. 261: 75–83.

Berg, P., Rysqaard, S., Funch, P., Sejr, M. 2001. Effects of bioturbation on solutes and solids in marine sediments. *Aquatic Microbial Ecology*. 26(1): 81 – 94.

Berg, P, Roy, H, Wiberg, P. 2007. Eddy correlation flux measurements: The sediment surface area that contributes to the flux. *Limnology and Oceanography*. 52(4): 1672–1684.

Berninger, U., Huettel, M. 1997. Impact of flow on oxygen dynamics in photosynthetically active sediments. *Marine Ecology Progress Series*. 12: 291 – 302.

Binzer, T., Borum, J., Pedersen, O. 2005. Flow velocity affects internal oxygen conditions in the seagrass *Cymodocea nodosa*. *Aquatic Botany*. 83: 239 – 247.

Borum, J. 1996. Shallow waters and land/sea boundaries. In: Jorgensen, B., Richardson, K. (eds). Eutrophication in coastal marine ecosystems. Coastal and Estuarine Studies. Vol. 52. *American Geophysical Union*. Washington, D.C. 179 – 203.

Bostrom, C., Bonsdorff, E., Kangas, P., Norkko, A. 2002. Long-term changes of a brackish-water eelgrass (Zostera marina L.) community indicate effects of coastal eutrophication. *Estuarine, Coastal and Shelf Science*. 55: 795 – 804.

Bostrom, C., Jackson, E., Simenstad, C. 2006. Seagrass landscapes and their effects on associated fauna: A review. *Estuarine, Coastal and Shelf Science*. 68: 383 – 403.

Bricker, S., Stevenson, J. 1996. Nutrients in coastal waters: a chronology and synopsis of research. *Estuaries*. 19: 337 – 341.

Caffery, J. 2004. Factors controlling net ecosystem metabolism in U.S. estuaries. *Estuaries*. 27(1): 90 – 101.

Charpy-Roubaud, C., Sournia, A. 1990. The comparative estimation of photoplanktonic and microphytobenthic production in the oceans. *Marine Microbial Food Webs*. 4: 31 – 57.

Cody, R., Smith, J. 2006. Applied statistics and the SAS programming language. 5th edition. Pearson Education, Inc. Pearson Prentice Hall. New Jersey, USA.

D'Avanzo, C., Kremer, J., Wainright, S. 1996. Ecosystem production and respiration in response to eutrophication in shallow temperate estuaries. *Marine Ecology Progress Series*. 141: 263 – 274.

Ehrenhauss, S., Huettel, M. 2004. Advective transport and decomposition of chain-forming planktonic diatoms in permeable sands. *Journal of Sea Research*. 52: 179 – 197.

Erftemeijer, P., Osinga, R., Mars, A. 1993. Primary production of seagrass beds in South Sulawesi (Indonesia): a comparison of habitats, methods and species. *Aquatic Botany*. 46: 67 – 90.

Fenchel, T., Glud, R. 2000. Benthic primary production and O_2-CO_2 dynamics in a shallow-water sediment: spatial and temporal heterogeneity. *Ophelia*. 53(3): 159 – 171.

Fonseca, M, Fisher, J, Zieman, J, Thayer, G. 1982. Influence of the seagrass, *Zostera marina* L., on current flow. *Estuarine, Coastal and Shelf Science*. 14(4): 351 – 358.

Fonseca, M., Kenworthy, W. 1987. Effects of current on photosynthesis and distribution of seagrasses. *Aquatic Botany*. 27: 59 – 78.

Fonseca, M. 1989. Sediment stabilization by *Halophila decipiens* in comparison to other seagrasses. *Estuaries, Coastal and Shelf Science*. 29: 501 – 507.

Fonseca, M., Cahalan, J. 1992. A preliminary evaluation of wave attenuation by four species of seagrass. *Estuarine, Coastal and Shelf Science*. 35: 565 – 576.

Fonseca, M. 1996. Scale dependence in the study of seagrass systems. *Seagrass Biology: Proceedings of an international workshop*. Rottnest Island, Australia. January 25 – 29, 1996. 95 – 104.

Forster, S, Huettel, M, Ziebis, W. 1996. Impact of boundary layer flow velocity on oxygen utilization in coastal sediments. *Marine Ecology Progress Series*. 143: 173 – 185.

Fourqurean, J., Moore, T., Fry, B., Hollibaugh, J. 1997. Spatial and temporal variation in C:N:P ratios, δ15N, and δ13C of eelgrass *Zostera marina* as indicators of ecosystem processes, Tomales Bay, California, USA. *Marine Ecology Progress Series*. 157: 147 – 157.

Franke, U, Polerecky, L, Precht, E, Huettel, M. 2006. Wave tank study of particulate organic matter degradation in permeable sediments. *Limnology and Oceanography*. 51(2): 1084 – 1096.

Frederiksen, M., Glud, R. 2006. Oxygen dynamics in the rhizosphere of *Zostera marina*: a two-dimensional planar optode study. *Limnology and Oceanography*. 51(2): 1072 – 1083.

Gambi, C. M, Nowell, A, Jumars, P. 1990. Flume observations on flow dynamics in *Zostera marina* (eelgrass) beds. *Marine Ecology Progress Series*. 61: 159 – 169.

Gazeau, F., Vieira Borges, A., Barron, C., Duarte, C., Iversen, N., Middelburg, J., Delille, B., Pizay, M., Frankignoulle, M., Gattuso, J. 2005. Net ecosystem metabolism in micro-tidal estuary (Randers Fjord, Denmark): evaluation of methods. *Marine Ecology Progress Series*. 301: 23 – 41.

Ghisalberti M., Nepf H. 2002. Mixing layers and coherent structures in vegetated aquatic flows . *Journal of Geophysical Research*. 107(C2): 1 –11.

Glud, R., Gundersen, J., Holby, O. 1999. Benthic *in situ* respiration in the upwelling area off central Chile. *Marine Ecology Progress Series*. 186: 9 – 18.

Grizzle, R., Short, F., Newell, C., Hoven, H., Kindblom, L. 1996. Hydrodynamically induced synchronous waving of seagrasses: 'monami' and its possible effects on larval mussel settlement. *Journal of Experimental Marine Biology and Ecology*. 206: 165 – 177.

Hansen, JW, Pedersen, A, Berntsen, J, Ronbog, I, Hansen, L, Lomstein, B. 2000. Photosynthesis, respiration, and nitrogen uptake by different compartments of a *Zostera marina* community. *Aquatic Botany*. 66: 281 – 295.

Hasegawa, N., Hori, M., Mukai, H. 2007. Seasonal shifts in seagrass bed primary producers in a cold-temperate estuary: Dynamics of eelgrass *Zostera marina* and associated epiphytic algae. *Aquatic Botany*. 86: 337 – 345.

Hauxwell, J., Cebrian, J., Valiela, I. 2003. Eelgrass *Zostera marina* loss in temperate estuaries: relationship to land-derived nitrogen loads and effect of light limitation imposed by algae. *Marine Ecology Progress Series*. 247: 59 – 73.

Hebert, A., Morse, J., Eldridge, P. 2007. Small-scale heterogeneity in the geochemisty of seagrass vegetated and non-vegetaed estuarine sediments: causes and consequences. *Aquatic Geochemisty*. 13: 19 – 39.

Hovel, K, Fonseca, M, Myer, D, Kenworthy, W, Whitfield, P. 2002. Effects of seagrass landscape structure, structural complexity and hydrodynamic regime on macrofaunal densities in North Carolina seagrass beds. *Marine Ecology Progress Series*. 243: 11 – 24.

Hovel, K. 2003. Habitat fragmentation in marine landscapes: relative effects of habitat cover and configuration on juvenile crab survival in California and North Carolina seagrass beds. *Biological Conservation*. 110: 401 – 412.

Huettel, M, Gust, G. 1992. Impact of bioroughness on intertidal solute exchange in permeable sediments. *Marine Ecology Progress Series*. 89: 253 – 267.

Huettel, M., Rusch, A. 2000. Transport and degradation of phytoplankton in permeable sediment. *Limnology and Oceanography*. 45(3): 534 – 549.

Huettel, M., Roy, H., Precht, E., Ehrenhauss, S. 2003. Hydrodynamical impact on biogeochemical processes in aquatic sediments. *Hydrobiologia*. 494: 231 – 236.

Jahnke, R., Christiansen, M. 1989. A free-vehicle benthic chamber instrument for sea floor studies. *Deep Sea Research*. 36: 625–637.

Jorgensen, B., Revsbech, N. 1985. Diffusive boundary layers and the oxygen uptake of sediments and detritus. *Limnology and Oceanography*. 30(1): 111 – 122.

Kaldy, J., Onuf, C., Eldridge, P., Cifuentes, L. 2002. Carbon budget for a subtropical seagrass dominated coastal lagoon: How important are seagrasses to total ecosystem net primary production? *Estuaries*. 24(4A): 528 – 539.

Kemp, W., Boynton, W. 1980. Influence of biological and physical processes on DO dynamics in an estuarine system: Implications for measurements of community metabolism. *Estuarine, Coastal and Marine Science*. 11: 407 – 431.

Kemp, W., Smith, E., Marvin-DiPasquale, M., Boynton, W. 1997. Organic carbon balance and net ecosystem metabolism in Chesapeake Bay. *Marine Ecology Progress Series*. 150: 229 – 248.

Kemp, W., Boynton W., Adolf J., Boesch D., Boicourt W., Brush G., Cornwell J., Fisher T., Glibert P., Hagy J., Harding L., Houde E., Kimmel D., Miller W., Newell R., Roman

M., Smith E., Stevenson J. 2005. Eutrophication of Chesapeake Bay: historical trends and ecological interactions. *Marine Ecology Progress Series*. 303: 1 – 29.

Koch, E. W. 1994. Hydrodynamics, diffusion-boundary layers and photosynthesis of the seagrass *Thalassia testudinum* and *Cymodocea nodosa*. *Marine Biology*. 118: 767 – 776.

Koch, E, Gust, G. 1999. Water flow in tide- and wave-dominated beds of the seagrass *Thalassia testudinum*. *Marine Ecology Progress Series*. 184: 63 – 72.

Koch, E. 2001. Beyond light: physical, geological, and geochemical parameters as possible submersed aquatic vegetation habitat requirements. *Estuaries*. 24(1): 1 – 17.

Koch, E., Ackerman, J., Verduin, J., van Keulen, M. In: Larkum, A. Orth, R., Duarte, C. 2006. Seagrasses: Biology, Ecology and Conservation. Springer. Dordrecht, The Netherlands.

Kraemer, G., Alberte, R. 1993. Age-related patterns of metabolism and biomass in subterranean tissues of *Zostera marina* (eelgrass). *Marine Ecology Progress Series*. 95: 193 – 203.

Kuwae, T., Kamio, K., Inoue, T., Miyoshi, E., Uchiyama, Y. 2006. Oxygen exchange flux between sediment and water in an intertidal sandflat, measured *in situ* by the eddy-correlation method. *Marine Ecology Progress Series*. 307: 59 – 68.

Larkum, A. Orth, R., Duarte, C. 2006. Seagrasses: Biology, Ecology and Conservation. Springer. Dordrecht, The Netherlands.

Lee, K., Short, F., Burdick, D. 2004. Development of a nutrient pollution indicator using the seagrass, *Zostera marina*, along nutrient gradients in three New England estuaries. *Aquatic Botany*. 78: 197 – 216.

Lindeboom, H., deBree, B. 1982. Daily production and consumption in an eelgrass (*Zostera marina*) community in saline Lake Grevelingen: Discrepancies between the O_2 and 14C method. *Netherlands Journal of Sea Research*. 16: 362 – 379.

Lindeboom, H., Sandee, A. 1989. Production and consumption of tropical seagrass fields in eastern Indonesia measured with bell jars and microelectrodes. *Neatherlands Journal of Sea Research*. 23: 181 – 190.

Liss, P.S., Slater, P.G. 1974. Flux of gases across the air-sea interface. *Nature*. 247: 181 – 184.

Madsen, J., Chambers, P., James, W., Koch, E., Westlake, D. 2001. The interaction between water movement, sediment dynamics and submersed macrophytes. *Hydrobiologia*. 444: 71 – 84.

Malan, D, McLachlan, A. 1991. *In situ* oxygen fluxes in a nearshore coastal marine system: a new approach to quantify the effect of wave action. *Marine Ecology Progress Series*. 73: 69 – 81.

Marino, R., Howarth, R. 1993. Atmospheric oxygen exchange in the Hudson River: dome measurements and comparison with other natural waters. *Estuaries*. 16(3A): 433 – 445.

Martin, S., Clavier, J., Guarini, J., Chauvaud, L., Hily, C., Gral, J., Thouzeau, G., Jean, F., Richard, J. 2005. Comparison of *Zostera marina* and maerl community metabolism. *Aquatic Botany*. 83: 161 – 174.

Mattila, J., Chaplin, G., Eilers, M., Heck Jr., K., O'Neal, J., Valentine, J. 1999. Spatial and diurnal distribution of invertebrate and fish fauna of a *Zostera marina* bed and nearby unvegetated sediments in Damariscotta River, Maine (USA). *Journal of Sea Research*. 41: 321 – 332.

McGlathery, K, Anderson, I, Tyler, C. 2001. Magnitude and variability of benthic and pelagic metabolism in a temperate coastal lagoon. *Marine Ecology Progress Series*. 216:1 – 15.

Meysman, F, Galaktionov, O., Middelburg, J. 2005. Irrigation patterns in permeable sediments induced by burrow ventilation: a case study of *Arenicola marina*. *Marine Ecology Progress Series*. 303: 195 – 212.

Moncreiff, C., Sullivan, M., Daehnick, A. 1992. Primary production dynamics in seagrass beds of Mississippi Sound: the contributions of seagrass, epiphytic algae, sanda microflora, and phytoplankton. *Marine Ecology Progress Series*. 87: 161 – 171.

Moore, K, Neckles, H, Orth, R. 1996. *Zostera marina* (eelgrass) growth and survival along a gradient of nutrients and turbidity in the lower Chesapeake Bay. *Marine Ecology Progress Series.* 142: 247 – 259.

Moriarty, D., Roberts, D., Pollard, P. 1990. Primary and bacterial productivity of tropical seagrass communities in the Gulf of Carpentaria, Australia. *Marine Ecology Progress Series*. 61: 145 – 157.

Murray, L, Wetzel, R. 1987. Oxygen production and consumption associated with the major autotrophic components in two temperate seagrass communities. *Marine Ecology Progress Series*. 38: 231 – 239.

Nagel, J. 2007. Plant-sediment interactions and biogeochemical cycling for seagrass communities in Chesapeake Bay and Florida Bay" Ph.D. Dissertation. University of Maryland – Center for Environmental Science.

Nelson, T., Waaland, R. 1997. Seasonality of eelgrass, epiphyte, and grazer biomass and productivity in subtidal eelgrass meadows subjected to moderate tidal amplitude. *Aquatic Botany*. 56: 51 – 74.

Nepf, H. 1999. Drag, turbulence, and diffusion in flow through emergent vegetation. *Water Resources Research*. 35(2): 479-489.

Nepf, H., Vivoni, E. 2000. Flow structure in depth-limited, vegetated flow. *Journal of Geophysical Research*. 105(C12): 28,547 – 28,557.

Nixon, S, Oviatt, C. 1972. Preliminary measurements of midsummer metabolism in beds of Eelgrass, *Zostera marina*. *Ecology*. 53(1): 150 – 153.

Odum, H. 1956. Primary production in flowing waters. *Limnology and Oceanography*. 1(2): 102 – 117.

Odum, H. 1957. Trophic structure and productivity of Silver Spring, Florida. *Ecological Monographs*. 27: 55–112.

Oldham, C., Ivey, G., Pullin, C. 2004. Estimation of a characteristic friction velocity in stirred benthic chambers. *Marine Ecology Progress Series*. 279: 291 – 295.

Orth, R., Moore, K. 1983. Chesapeake Bay: and unprecedented decline in submerged aquatic vegetation. *Science*. 222: 51 – 53.

Orth, R, Fishman, J, Harwell, M, Marion, S. 2003. Seed-density effects on germination and initial seedling establishment in eelgrass *Zostera marina* in the Chesapeake Bay region. *Marine Ecology Progress Series*. 250: 71 – 79.

Orth, R, Luckenbach, M, Marion, S, Moore, K, Wilcox, D. 2006. Seagrass recovery in the Delmarva Coastal Bays, USA. *Aquatic Botany*. 84: 26 – 36.

Pamatmat, M., Fenton, D. 1968. An instrument for measuring subtidal benthic metabolism *in situ*. *Limnology and Oceanography*. 13: 537–540.

Papadimitriou, S., Kennedy, H., Kennedy, D., Borum, J. 2005. Seasonal and spatial variation in the organic carbon and nitrogen concentration and their stable isotopic composition in *Zostera marina* (Denmark). *Limnology and Oceanography*. 50(4): 1084 – 1095.

Pinckney, J., Zingmark, R. 1991. Effects of tidal stage and sun angles on intertidal benthic microalgal productivity. *Marine Ecology Progress Series*. 76: 81 – 89.

Plus, M., Deslous-Paoli, J., Auby, I., Dagault, F. 2001. Factors influencing primary production of seagrass beds (*Zostera noltii* Hornem.) in the Thau lagoon (French Mediterranean coast). *Experimental Marine Biology and Ecology*. 259: 63 – 84.

Precht, E, Huettel, M. 2003. Advective pore-water exchange driven by surface gravity waves and its ecological implications. *Limnology and Oceanography*. 48(4): 1647 – 1684.

Precht, E., Franke, U., Polerecky, L., Huettel, M. 2004. Oxygen dynamics in permeable sediments with wave-driven pore water exchange. *Limnology and Oceanography*. 49(3) 693 – 705.

Revsbech, N., Jorgensen, B., Brix, O. 1981. Primary production of microalgae in sediments measured by oxygen microprofile, $H_{14}CO_3$ - fixation and oxygen exchange methods. *Limnology and Oceanography*. 26(4): 717 – 730.

Revsbech, N. P. 1989. An oxygen microelectrode with a guard cathode. *Limnology and Oceanography*. 34: 474-478.

Røy, H., Markus, H., Jørgensen., B. 2002. Transmission of oxygen concentration fluctuations through the diffusive boundary layer overlying aquatic sediments. *Limnology and Oceanography*. 49(3) 686 – 692.

Røy, H., Markus, H., Jørgensen., B. 2005. The influence of topography on the functional exchange surface of soft sediments, assessed from sediment topography measured *in situ*. *Limnology and Oceanography*. 50(1) 106 – 112.

Santos, R., Silva, J., Alexandre, A., Navarro, N., Barron, C., Duarte, C. 2004. Ecosystem metabolism and carbon fluxes of a tidally-dominated coastal lagoon. *Estuaries*. 27(6): 977 – 985.

Seeley, C. 1969. The diurnal curve in estimates of primary productivity. *Chesapeake Science*. 10(3&4): 322 – 326.

Short, F., Burdick, D., Kaldy III, J. 1995. Mesocosm experiments quantify the effects of eutrophication on eelgrass, *Zostera marina*. *Limnology and Oceanography*. 40: 740 – 749.

Stull, R. 1988. An introduction to boundary layer meteorology. Kluwer Academic Publishers. Dordrecht, The Netherlands. 51 – 56 , 427 – 428.

Stutes, A., Cebrian, J., Corcoran, A. 2006. Effects of nutrient enrichment and shading on sediment primary production and metabolism in eutrophic estuaries. *Marine Ecology Progress Series*. 312: 29 – 43.

Sundback, K., Miles, A., Goransson, E. 2000. Nitrogen fluxes, denitrification and the role of microphytobenthos in microtidal shallow-water sediments: an annual study. *Marine Ecology Progress Series*. 200: 59 – 76.

Tengberg, A., De Bovee, F., Hall, P., Berelson, W., Chadwick, D., Ciceri, G., Crassous, P., Devol, A., Emerson, S., Gage, J., Glud, R., Graziottini, F., Gundersen, J., Hammond, D., Helder, W., Hinga, K., Holby,O., Jahnke, R., Khripounoff, A., Lieberman, S., Nuppenau, V., Pfannkuche, O., Reimers, C., Rowe, G., Sahami, A., Sayles, F., Schurter, M., Smallman, D., Wehrli, B., De Wilde, P. 1995. Benthic chamber and profiling landers in oceanography – a review of design, technical solutions and functioning. *Progress in Oceanography*. 35: 253 – 294.

Tengberg, A., Stahl, H., Gust, G., Muller, V., Arning, U., Andersson, H., Hall, P. 2004. Intercalibration of benthic flux chambers I. Accuracy of flux measurements and influence of chamber hydrodynamics. *Progress in Oceanography*. 60: 1 – 28.

Thomsen, M, McGlathery, K, Tyler, C. 2006. Macroalgal distribution in a shallow, soft-bottom lagoon, with emphasis on the nonnative *Gracilaria vermiculophylla* and *Codium fragile*. *Estuaries and Coasts*. 29: 465 – 473.

Thouzeau, G., Grall, J., Clavier, J., Chauvaud, L., Jean, F., Leynaert, A., ni Longphuirt, S., Amice, E., Amouroux, D. 2007. Spatial and temporal variability of benthic

biogeochemical fluxes associated with macrophytic and macrofaunal distributions in the Thau lagoon (France). *Estuarine, Coastal and Shelf Science*. 72: 432 – 446.

Touchette, B., Burkholder, J. 2000. Review of nitrogen and phosphorus metabolism in seagrass. *Journal of Experimental Marine Biology and Ecology*. 250: 133 – 167.

Touchette, B., Burkholder, J., Glasgow, H. 2003. Variations in eelgrass (*Zostera marina* L.) morphology and internal nutrient composition as influenced by increased temperate and water column nitrate. *Estuaries*. 23(1): 142 – 155.

Turner, S., Hewitt, J., Wilkinson, M., Morrisey, D., Thrush, S., Cummings, V., Funnell, G. 1999. Seagrass patches and landscapes: The influence of wind-wave dynamics and hierarchical arrangements of spatial structure on macrofaunal seagrass communities. *Estuaries*. 22(4): 1016 – 1032.

Tyler, A., McGlathery, K., Anderson, I. 2001. Macroalgal mediation of dissolved organic nitrogen fluxes in a temperate coastal lagoon. *Estuarine, Coastal and Shelf Science*. 53: 155 – 168.

Vector Current Meter User Manual. Nortek AS, Norway. August 2005.

Viollier, E., Rabouille, C., Apitz, S., Breuer, E., Chaillou, G., Dedieu, K., Furukawa, Y., Grenz, C., Hall, P., Janssen, F., Morford, J., Poggiale, J., Roberts, S., Shimmield, T.,

Taillefert, M., Tengberg, A., Wenzhofer, F., Witte, U. 2003. Benthic biogeochemistry: state of the art technologies and guidelines for the future of *in situ* survey. *Journal of Experimental Marine Biology and Ecology*. 285 – 286: 5 – 31.

Wanninkhof, R. 1992. Relationship between wind speed and gas exchange over the ocean. *Journal of Geophysical Research*. 97(C5): 7373 – 7382.

Welsh, D., Bartoli, M., Nizzoli, D., Castaldelli, G., Riou, S., Viaroli, P. 2000. Denitrification, nitrogen fixation, community primary productivity and inorganic-N and oxygen fluxes in an intertidal *Zostera noltii* meadow. *Marine Ecology Progress Series*. 208: 65 - 77.

Wenzhofer, F., Glud, R. 2004. Small-scale spatial and temporal variability in coastal benthic O_2 dynamics: Effects of fauna activity. *Limnology and Oceanography*. 49(5): 1471 – 1481.

Wyngaard, J. 1989. Scalar fluxes in the planetary boundary layer – theory, modeling and measurement. *Boundary Layer Meteorology*. 50: 49 – 75.

Ziebis, W., Huttel, M., Forster, S. 1996. Impact of biogenic sediment topography on oxygen fluxes in permeable seabeds. *Marine Ecology Progress Series*. 140: 227 – 237.

Ziegler S, Benner R. 1998. Ecosystem metabolism in a subtropical, seagrass-dominated lagoon. *Marine Ecology Progress Series*. 173: 1-12.

Appendix:

Anomalous DO flux: An example of the anomalous natural variation observed due to the high-resolution DO flux measurements is highlighted by a phenomenon observed in vegetated deployments 3 and 5 (Figure A1). During both deployments, an abnormally large DO flux was observed after sunset. A close analysis of the data shows that this unexpected result is real. It is hypothesized is that this sudden increase in DO fluxes is caused by gaseous oxygen under supersaturated conditions dissolving into the water column as a result of cooling water temperature (Figures 8b and 10b) with the decrease in solar radiation. Evidence to support this hypothesis can be seen by the coincidence of the measured DO concentration (red closed circles) approaching the DO saturation concentration (blue closed circles) during the pulse (around minute 300 – 400 in the top figure and 400 – 600 in the bottom figure of Figure A1). This abiotic process has not been directly addressed in other studies but may have been observed in two time series reported by Nixon and Oviatt (1972). Several other studies have observed anomalous diurnal patterns in DO, including increases at night, in hydrodynamically active estuarine environments (Kemp and Boynton 1980 and references within). This phenomenon is likely overlooked in most studies because of the low temporal-frequency measurements used in highly dynamic environments.

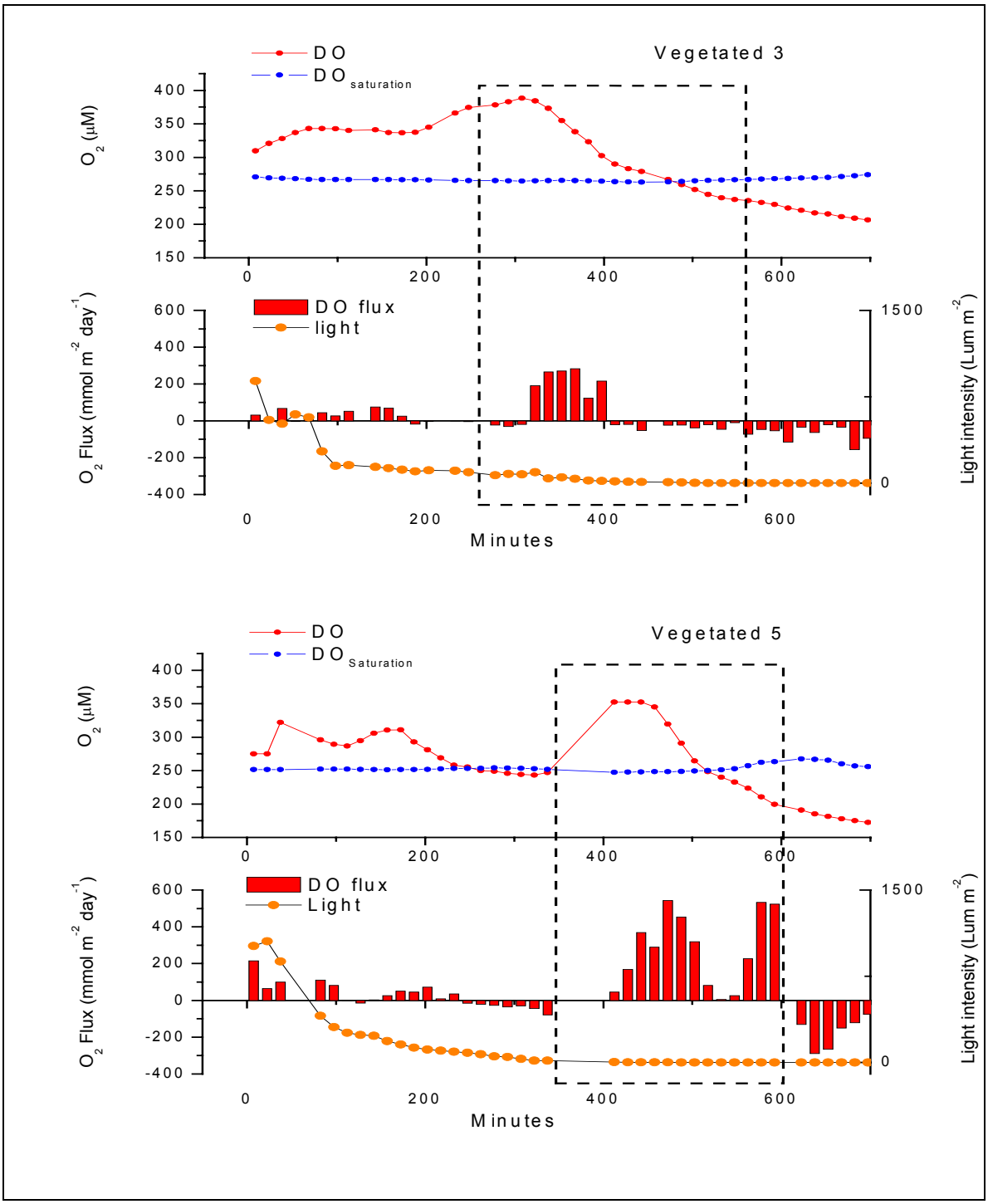

Figure A1. Sunset anomalous DO fluxes identified by the black checker box for deployments 3 (top figure) and 5 (bottom figure). Within each figure the upper graph is the 15-min mean DO concentration (red circles) and DO saturation concentration (blue circles) and the lower graph is the 15-min mean running average fluxes (red bars) from start of deployment with light on the left-axis (orange circles).

Sample frequency	[Hz]	Sampling rate of the Vector
Burst interval	[s]	Duration of sampling time
Number of samples per burst		Number of sample in a burst interval
O_2 concentration flag		Calculates O_2 concentration based on the flag. A flag of 0 calculates the O_2 concentration from the ALL components. A flag of 1 calculates the O_2 concentration from the AC and ALL components. A flag of 2 calculates the O_2 concentration from the AC component and a ambient field O_2 concentration.
O_2 mean concentration	[μM]	Only used if flag 2 (above) for calculating the O_2 concentration from the AC component and the ambient field O_2 concentration.
Number of data points to skip for auto adjustment		Used to ignore data points at beginning of a time series, where picoammeter is initializing.
Microelectrode null current	[pA]	The current measured by the microelectrode in anoxic conditions
Microelectrode current at known O_2 concentration	[pA]	The current measured by the microelectrode at a known concentration of O_2.
O_2 concentration of known microelectrode current	[μM]	The O_2 concentration for the known current of the microelectrode above.
Output time preference		Controls how time data is expressed. Flag 0 for seconds, flag 1 for minutes, and flag 2 for hours.

Table A1. ExtractNortek Version 1.2 parameters for calculating the oxygen concentration.

Rotation of coordinates		Rotates coordinate system so there is no mean transverse flow for time series (flag 1 = yes, flag 2 = no)
Ambient dissolved oxygen flux		Accounts for ambient changes in DO over time series (flag 1 = yes, flag 2 = no)
Measuring height	[cm]	The height of the measuring volume from the measuring surface.
Data sample frequency	[Hz]	Frequency at which input file data is sampled
Time window for averaging data	[s]	Number of seconds used to calculate eddy flux with mean removal method.
Number of data points in running average		Number of data points used to calculate the eddy flux with the running average method.
Number of data points to skip between discrete time series.		Number of data points skipped, generally during picoammeter auto-adjusting, before calculating the eddy flux for each method.

Table A2. EddyFlux Version 1.2 parameters for calculating the eddy correlation DO flux.

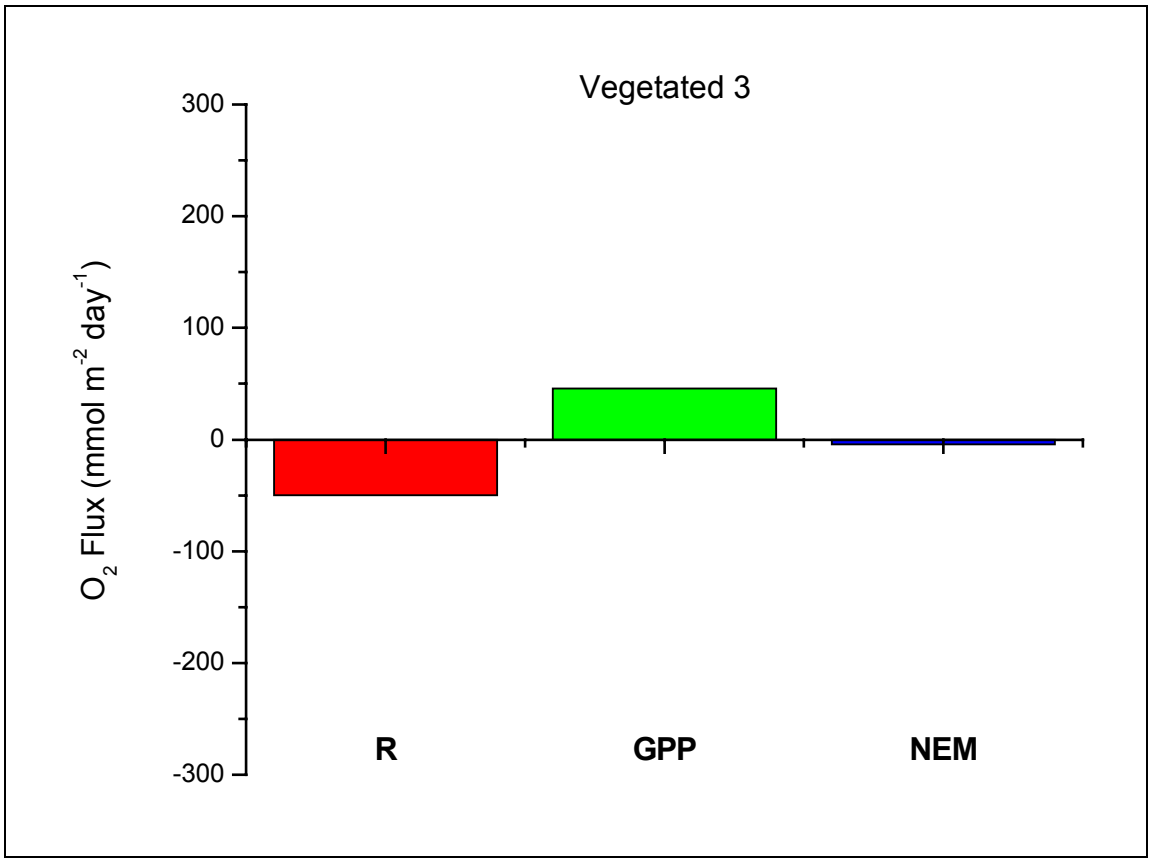

Figure A2a. Vegetated 3 ecosystem metabolism parameters from left to right: respiration, R (red), gross primary production, GPP (green), and net ecosystem metabolism, NEM (blue) in mmol O_2 m^{-2} day^{-1}.

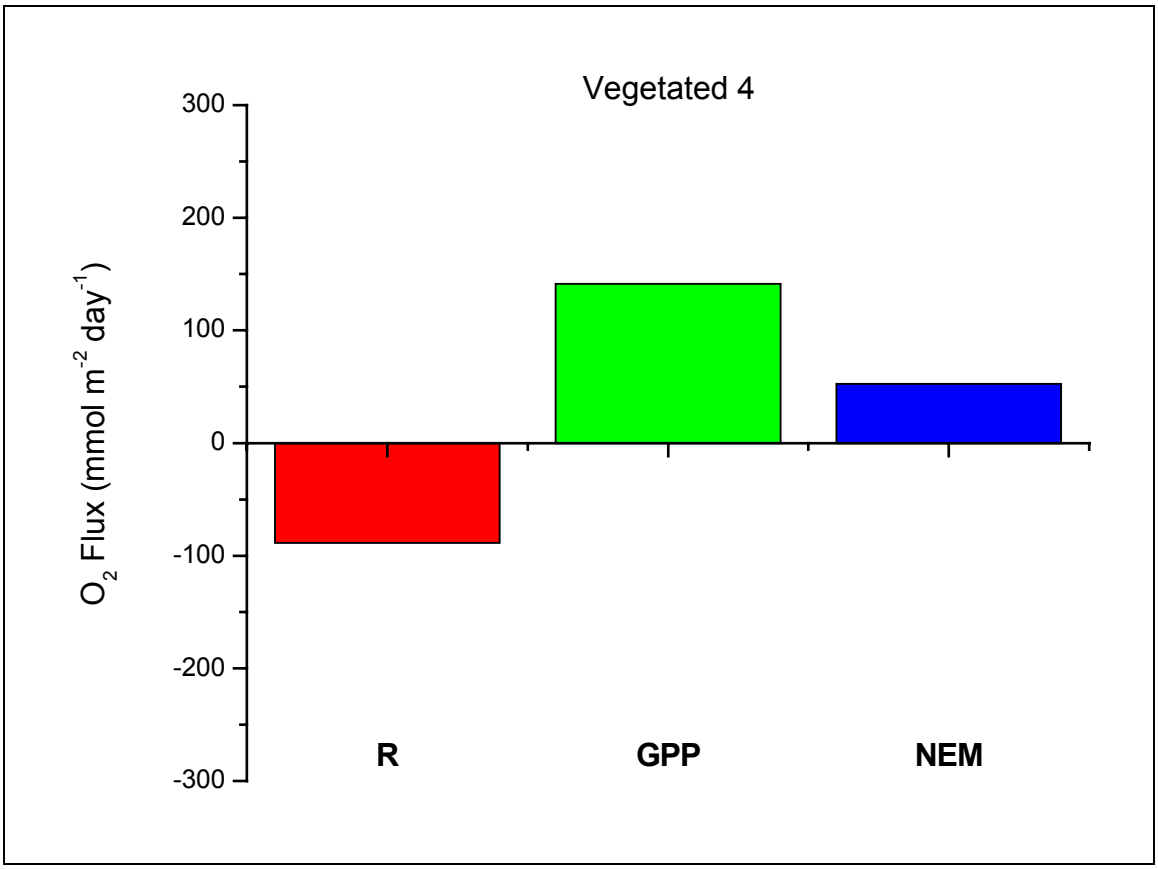

Figure A2b. Vegetated 4 ecosystem metabolism parameters from left to right: respiration, R (red), gross primary production, GPP (green), and net ecosystem metabolism, NEM (blue) in mmol O_2 m^{-2} day^{-1}.

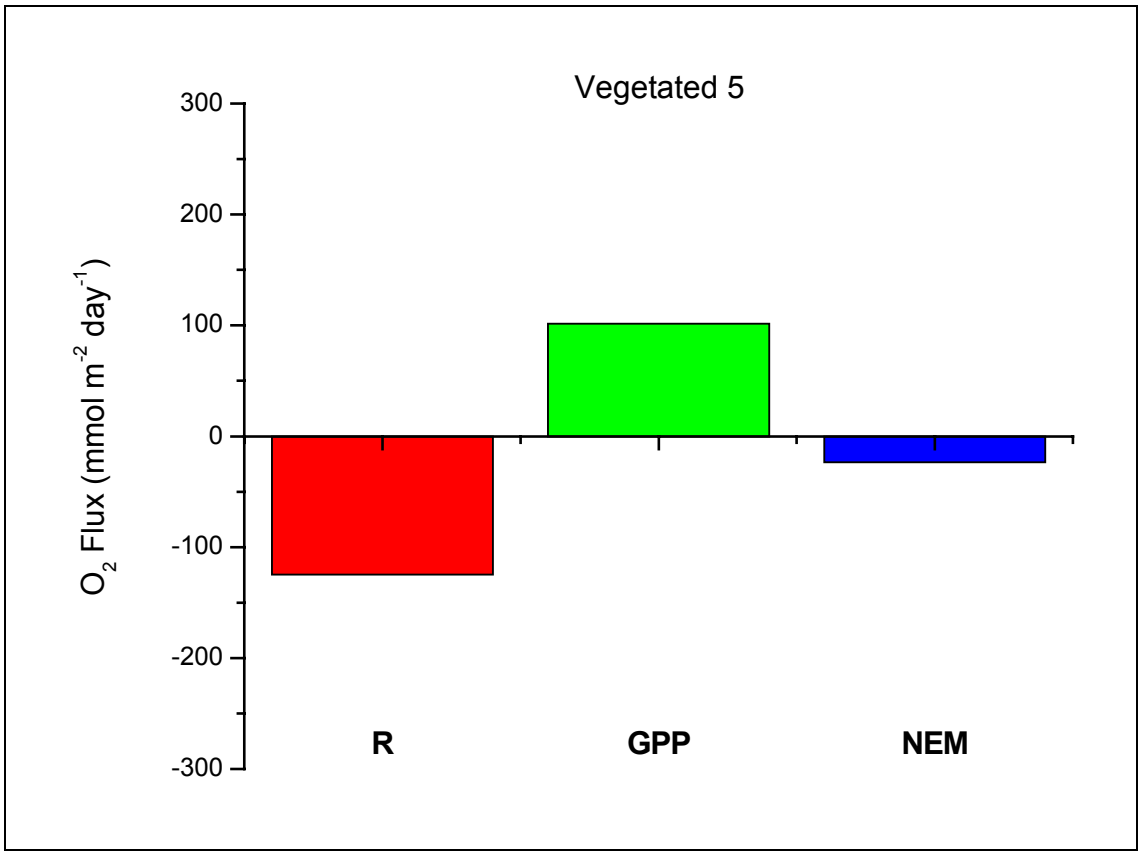

Figure A2c. Vegetated 5 ecosystem metabolism parameters from left to right: respiration, R (red), gross primary production, GPP (green), and net ecosystem metabolism, NEM (blue) in mmol O_2 m^{-2} day^{-1}.

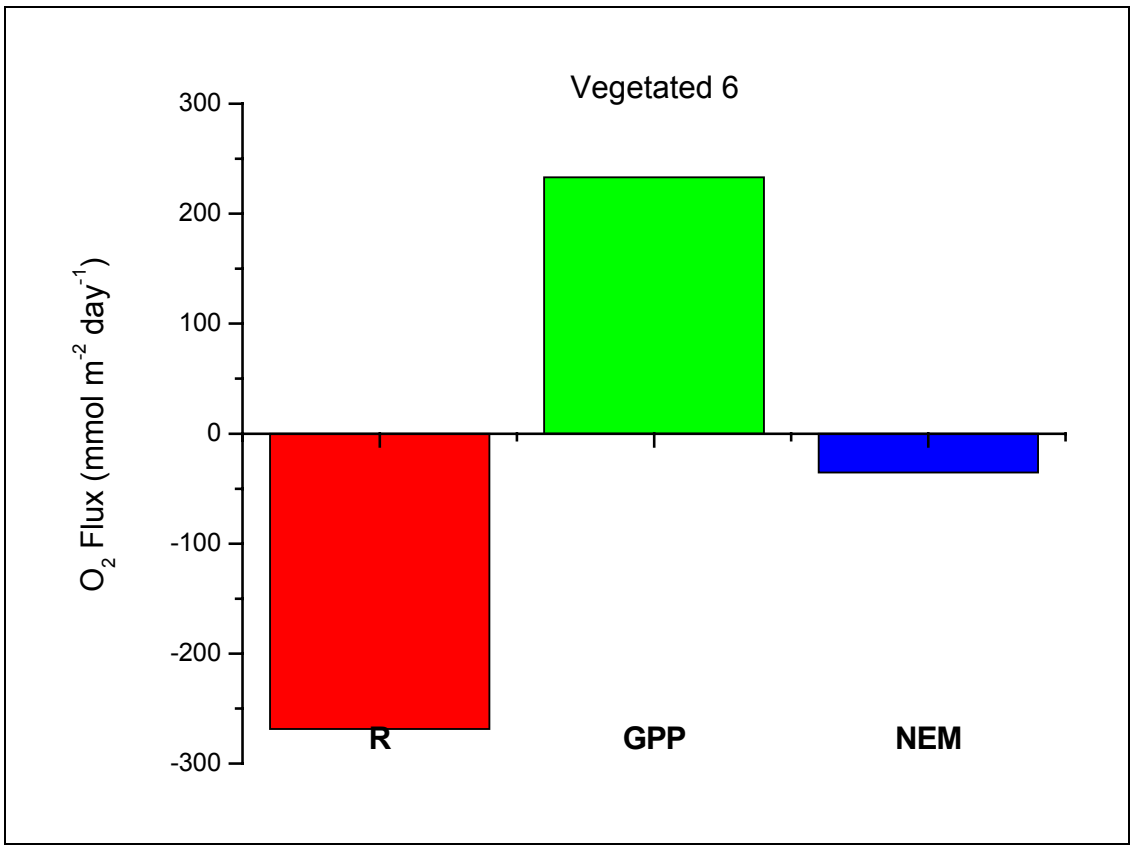

Figure A2d. Vegetated 6 ecosystem metabolism parameters from left to right: respiration, R (red), gross primary production, GPP (green), and net ecosystem metabolism, NEM (blue) in mmol O_2 m^{-2} day^{-1}.

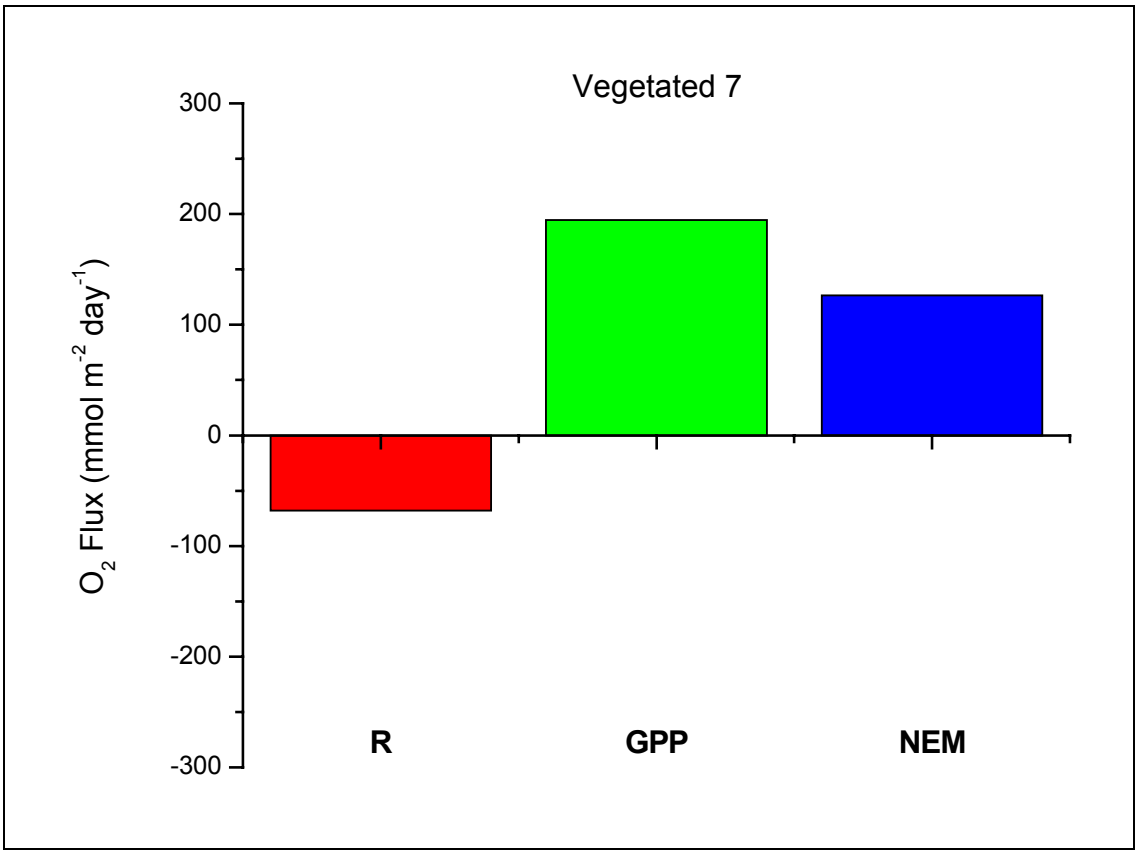

Figure A2e. Vegetated 7 ecosystem metabolism parameters from left to right: respiration, R (red), gross primary production, GPP (green), and net ecosystem metabolism, NEM (blue) in mmol O_2 m^{-2} day^{-1}.

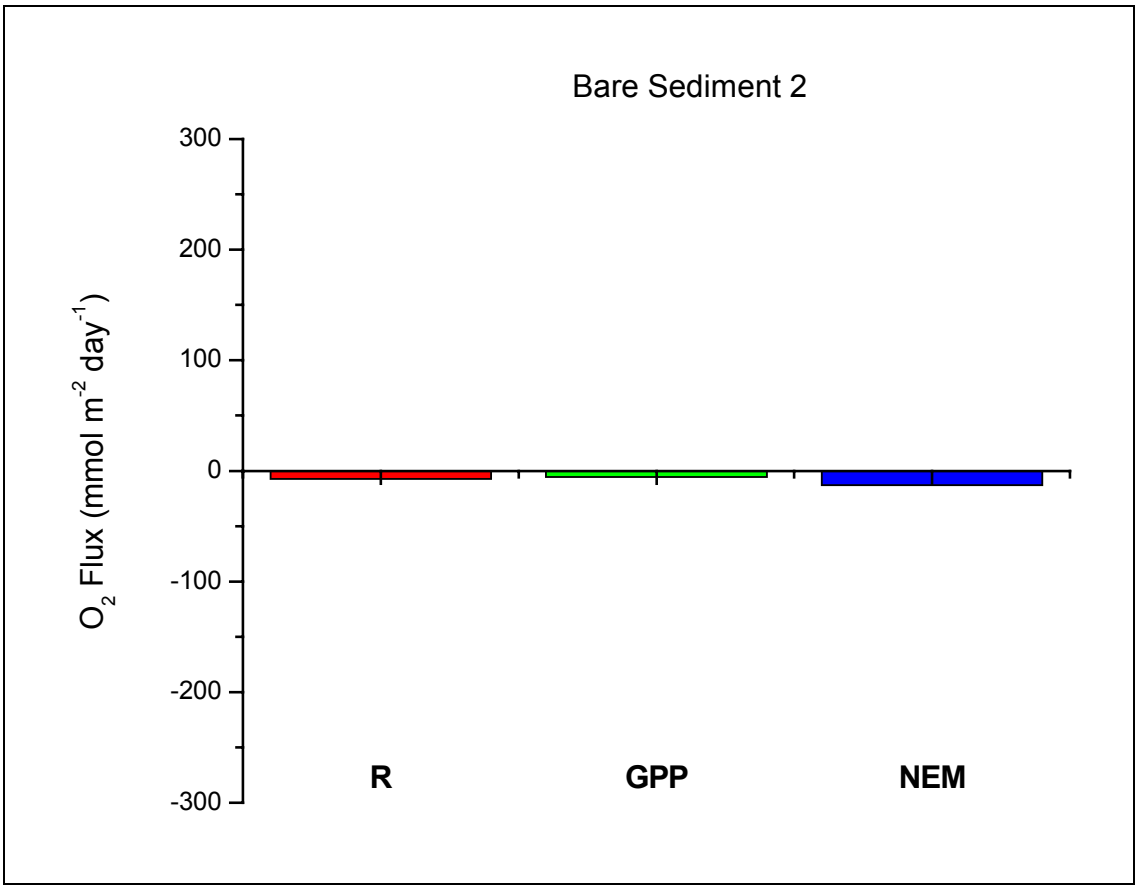

Figure A2f. Bare sediment 2 ecosystem metabolism parameters from left to right: respiration, R (red), gross primary production, GPP (green), and net ecosystem metabolism, NEM (blue) in mmol O_2 m^{-2} day^{-1}.

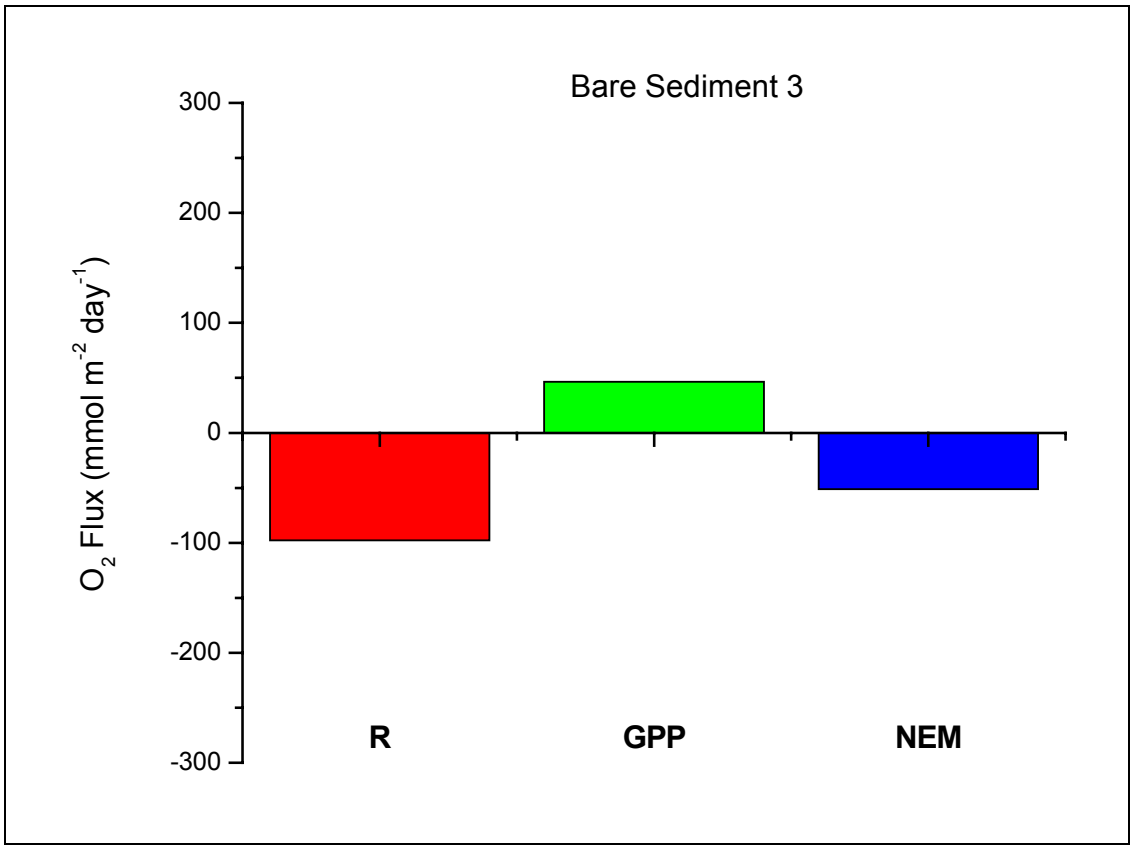

Figure A2g. Bare sediment 3 ecosystem metabolism parameters from left to right: respiration, R (red), gross primary production, GPP (green), and net ecosystem metabolism, NEM (blue) in mmol O_2 m^{-2} day^{-1}.

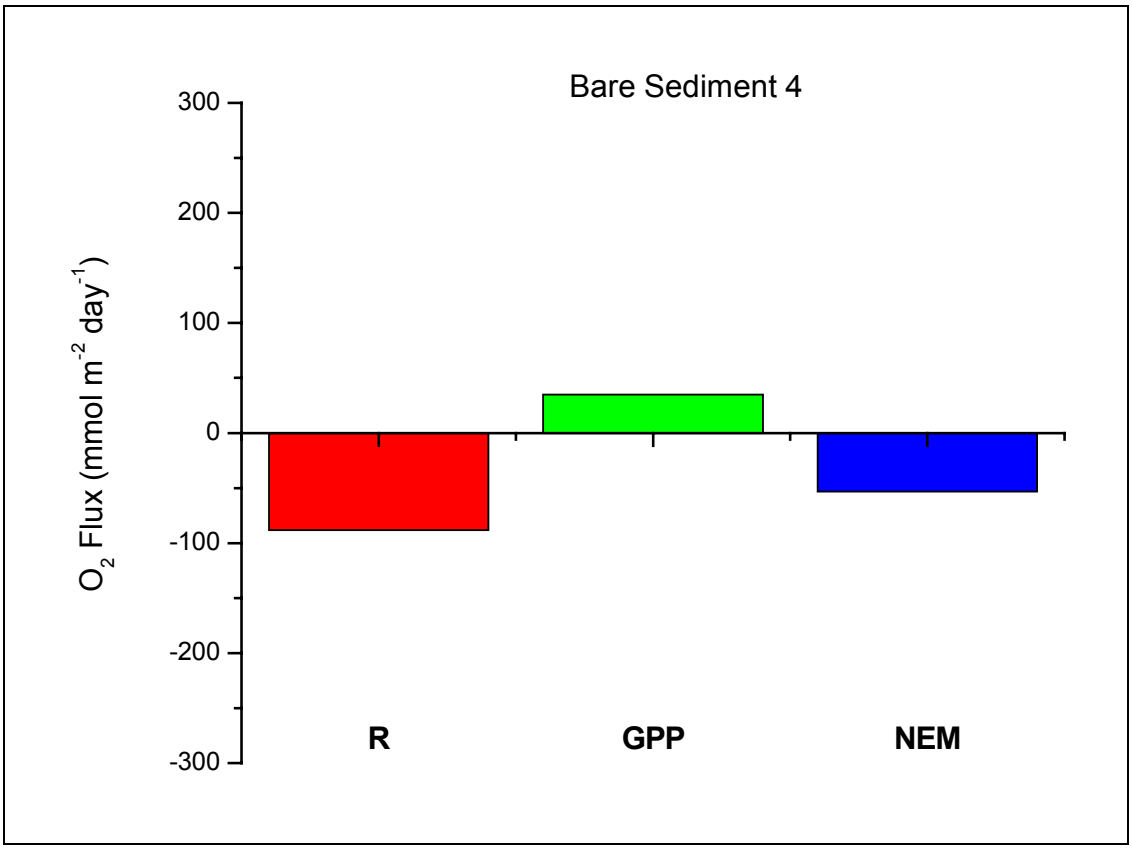

Figure A2h. Bare sediment 4 ecosystem metabolism parameters from left to right: respiration, R (red), gross primary production, GPP (green), and net ecosystem metabolism, NEM (blue) in mmol O_2 m^{-2} day^{-1}.

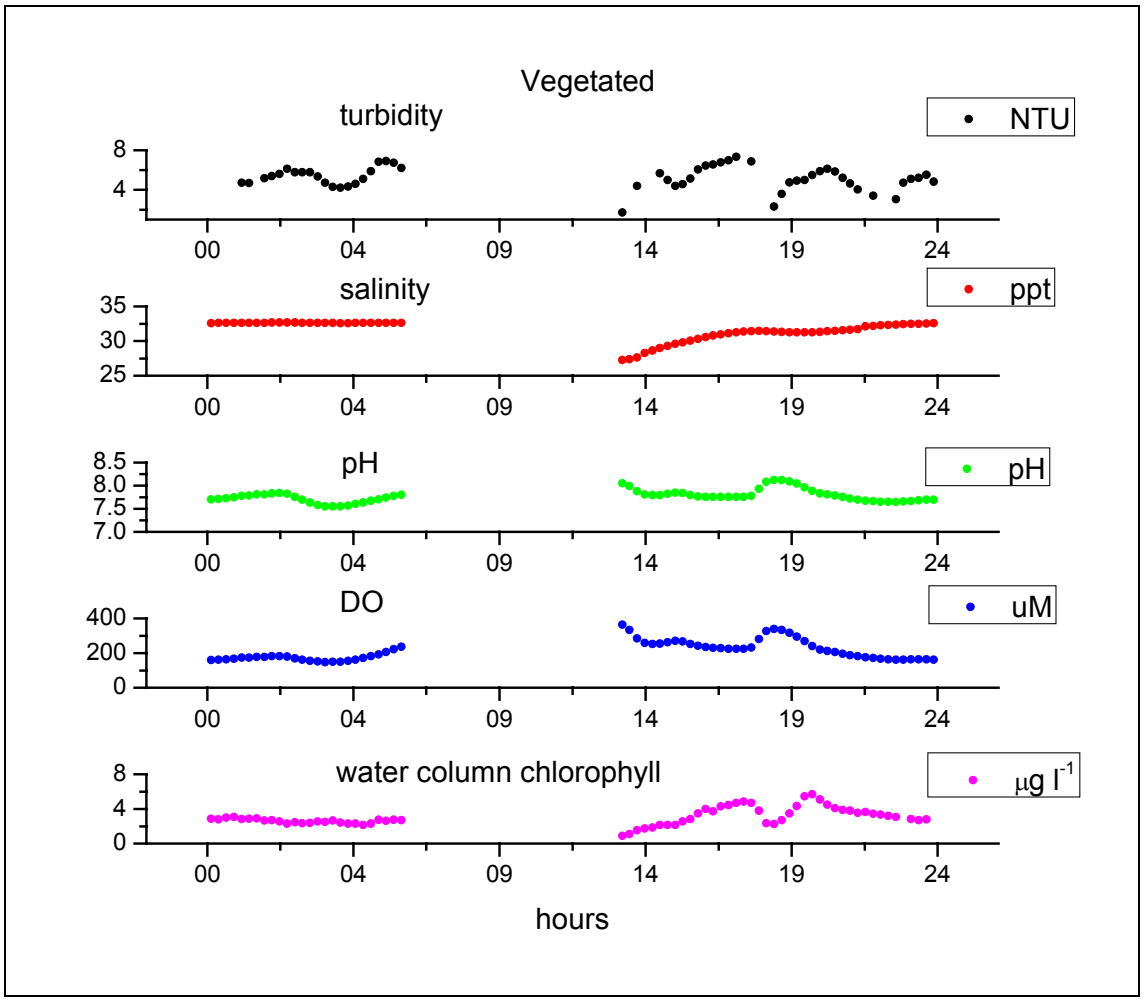

Figure A3a. Water quality parameters from the vegetated datasonde deployment (July 10, 2007). From top to bottom: Turbidity, salinity, pH, DO, and water column chlorophyll.

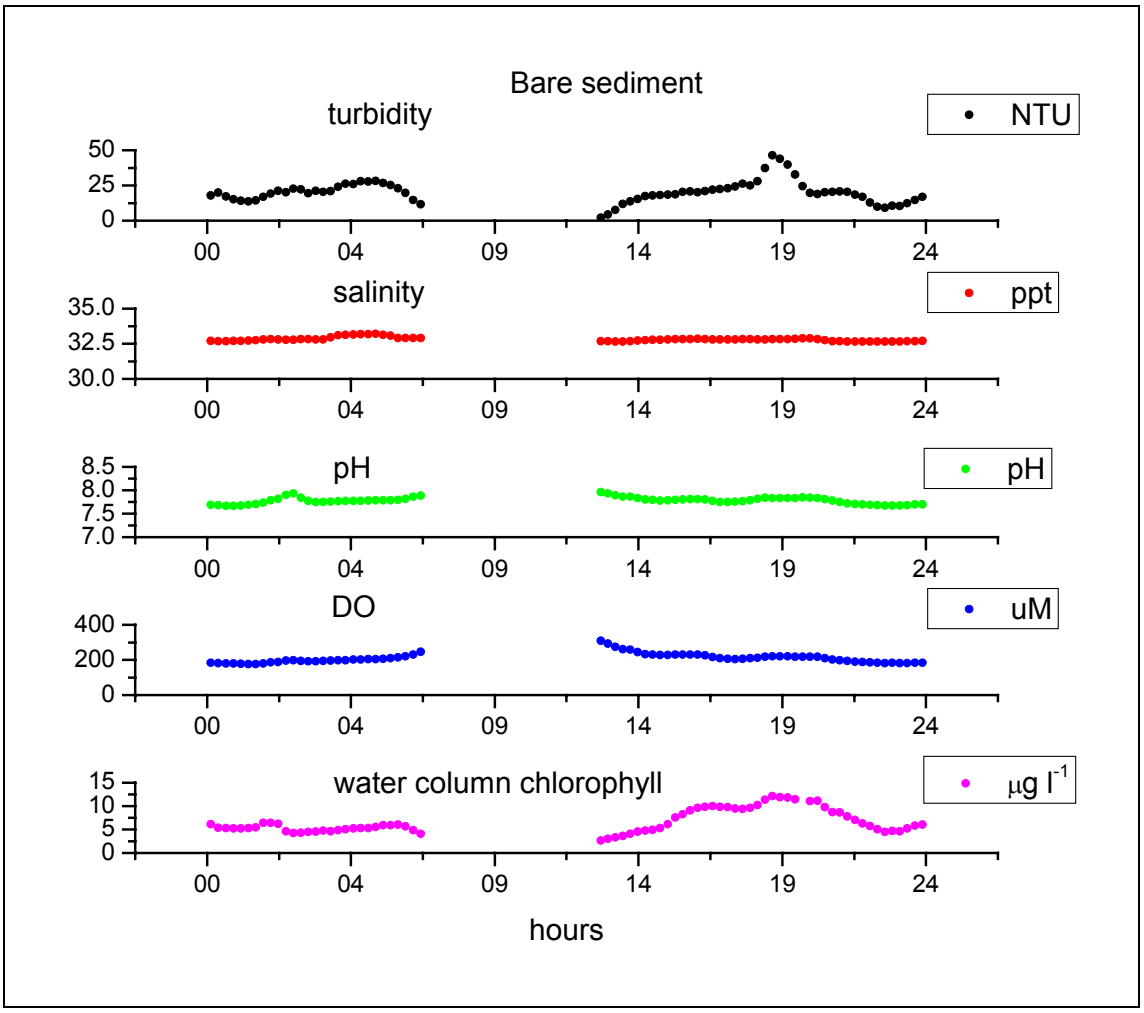

Figure A11b. Water quality parameters from the bare sediment datasonde deployment (July 11, 2007). From top to bottom: Turbidity, salinity, pH, DO, and water column chlorophyll.

Table A3a. 15-min average data eddy correlation deployment bare sediment site – deployment 2 – June 20 – 21, 2007

Real Time	Time	U	Ux	Uy	Uz	O2	LD DO Flux	RA DO Flux	Depth	CurDir	ZeroPd	Hs	Temp	O2 Sat	Light Intensity
	min	cm s-1	cm s-1	cm s-1	cm s-1	uM	mmol O2 m-2 d-1	mmol O2 m-2 d-1	m	degrees	s	m	C	uM	lum m-2
9:07:30	7.50	4.18	-2.39	-3.43	-0.18	221.46	-0.11	-8.11	0.75	125.30	1.33	0.10	25.95	264.39	530.87
9:22:30	22.50	3.89	-2.30	-3.13	-0.21	222.36	-57.75	-38.46	0.82	189.20	1.40	0.08	25.96	264.33	627.66
9:52:30	52.50	4.64	-2.39	-3.97	-0.23	228.95	-17.24	-2.24	0.96	185.10	1.41	0.10	25.93	264.47	347.26
10:07:30	67.50	4.72	-2.47	-4.02	-0.23	228.99	-32.52	-19.53	1.03	184.70	1.48	0.12	25.91	264.57	298.81
10:22:30	82.50	4.38	-3.03	-3.15	-0.15	226.03	9.10	-13.00	1.09	196.70	1.59	0.13	25.89	264.67	257.17
10:37:30	97.50	4.41	-2.60	-3.56	-0.13	222.71	-18.20	-17.20	1.16	189.50	1.59	0.12	25.90	264.61	218.94
10:52:30	112.50	4.04	-2.93	-2.77	-0.17	221.10	-10.83	-17.85	1.24	199.40	1.65	0.11	25.92	264.53	195.03
11:07:30	127.50	5.13	-3.38	-3.85	-0.25	222.84	-22.31	-18.67	1.30	194.90	1.68	0.12	25.93	264.46	183.92
11:22:30	142.50	3.93	-2.86	-2.69	-0.22	223.07	-34.61	-15.91	1.36	199.40	1.68	0.13	25.97	264.31	181.83
11:37:30	157.50	3.87	-2.96	-2.48	-0.25	221.96	-31.35	-21.53	1.42	203.60	1.73	0.12	26.00	264.17	167.45
11:52:30	172.50	3.97	-2.41	-3.15	-0.28	223.33	-32.29	-17.44	1.46	190.80	1.75	0.12	26.02	264.08	157.16
12:07:30	187.50	3.15	-2.50	-1.91	-0.14	223.91	-54.75	-17.16	1.52	205.20	1.83	0.13	26.04	264.01	151.43
12:22:30	202.50	4.98	-3.70	-3.32	-0.32	223.82	-67.43	-36.08	1.56	201.30	1.82	0.13	26.03	264.02	143.79
12:37:30	217.50	4.17	-2.96	-2.92	-0.23	225.15	-63.80	-22.15	1.60	199.20	1.91	0.14	26.03	264.05	135.17
12:52:30	232.50	3.51	-2.29	-2.66	-0.15	229.00	-62.75	-11.00	1.63	194.90	1.95	0.14	26.03	264.06	128.98
13:07:30	247.50	3.02	-1.59	-2.56	-0.21	231.82	-54.06	-21.75	1.64	185.70	1.90	0.14	25.98	264.28	125.14
13:22:30	262.50	3.35	-0.96	-3.20	-0.25	232.74	-31.76	-15.40	1.64	171.20	1.93	0.15	25.86	264.80	118.52
13:37:30	277.50	2.27	0.55	-2.18	-0.29	236.71	-49.35	-18.57	1.62	140.00	1.93	0.15	25.53	266.27	102.39
13:52:30	292.50	2.31	-1.04	-2.06	-0.12	243.36	-76.37	-20.77	1.60	179.80	1.97	0.17	25.34	267.15	96.89
14:07:30	307.50	2.61	0.25	-2.58	-0.22	247.52	-44.60	-22.22	1.57	148.50	2.06	0.13	25.28	267.41	95.33
14:22:30	322.50	1.69	1.09	-1.28	-0.16	248.10	-63.64	-30.82	1.53	114.50	2.03	0.12	25.20	267.76	102.51
14:37:30	337.50	2.05	1.54	-1.35	-0.19	247.99	-23.62	-9.41	1.49	105.40	1.93	0.12	25.10	268.26	100.34
14:52:30	352.50	2.44	1.94	-1.46	-0.23	249.54	-72.99	-21.78	1.46	100.00	1.96	0.12	24.89	269.21	98.61
15:07:30	367.50	2.67	2.56	-0.68	-0.30	253.57	-50.48	-23.12	1.41	78.50	1.89	0.12	24.93	269.01	98.26
15:22:30	382.50	3.18	3.16	0.20	-0.26	255.25	-40.46	-27.91	1.35	59.90	1.93	0.14	24.99	268.76	96.71
15:37:30	397.50	3.70	3.33	1.58	-0.28	256.99	-27.24	-23.47	1.29	38.00	1.88	0.14	25.13	268.10	97.73
15:52:30	412.50	4.37	3.52	2.59	-0.20	257.51	-18.68	-24.07	1.24	27.10	1.86	0.14	25.19	267.83	96.70
16:07:30	427.50	4.09	3.56	2.01	-0.22	258.16	-56.84	-45.35	1.19	34.00	1.82	0.13	25.21	267.72	84.73
16:22:30	442.50	3.78	3.17	2.05	-0.23	259.89	-58.43	-46.16	1.15	30.00	1.80	0.13	25.24	267.59	82.60

16:37:30	457.50	5.91	4.37	3.97	-0.27	262.70	-41.56	-47.84	1.09	20.90	1.76	0.10	25.26	267.50	83.62
16:52:30	472.50	5.68	4.28	3.72	-0.32	266.57	-23.84	-26.56	1.03	22.10	1.67	0.09	25.30	267.34	83.96
17:07:30	487.50	6.04	4.71	3.77	-0.31	270.21	-19.39	-18.55	0.97	24.30	1.64	0.09	25.32	267.21	82.97
17:22:30	502.50	7.10	5.08	4.95	-0.34	274.82	-1.90	-0.42	0.91	18.70	1.61	0.07	25.39	266.90	78.51
17:37:30	517.50	6.05	4.28	4.27	-0.31	280.76	-23.97	-8.74	0.85	18.40	1.45	0.06	25.45	266.65	74.64
17:52:30	532.50	6.51	4.32	4.85	-0.40	285.77	-10.82	-2.35	0.80	14.30	1.44	0.05	25.50	266.42	68.18
18:22:30	562.50	4.28	2.40	3.53	-0.35	295.40	-15.17	-12.36	0.72	7.50	1.48	0.03	25.54	266.23	51.37
18:37:30	577.50	4.46	2.35	3.79	-0.28	298.13	10.69	0.10	0.69	5.00	1.45	0.03	25.55	266.20	52.40
18:52:30	592.50	2.25	1.46	1.71	-0.17	303.99	-39.33	-46.59	0.66	12.60	1.44	0.02	25.57	266.11	51.41
19:07:30	607.50	1.55	0.76	1.35	-0.07	310.36	-22.95	-13.65	0.65	4.20	1.44	0.03	25.59	266.02	41.69
19:22:30	622.50	0.65	-0.16	0.63	0.00	310.36	-18.63	-3.57	0.64	320.80	1.41	0.03	25.60	265.96	44.03
19:37:30	637.50	0.78	-0.77	0.14	-0.03	309.87	-19.70	-11.98	0.66	253.70	1.44	0.03	25.63	265.83	32.08
19:52:30	652.50	0.80	-0.80	0.06	-0.05	310.21	-8.48	-7.81	0.67	248.80	1.52	0.03	25.63	265.81	23.49
20:07:30	667.50	0.35	-0.30	-0.18	-0.03	307.81	-7.60	-2.50	0.68	225.20	1.41	0.03	25.59	265.99	19.14
20:22:30	682.50	0.49	-0.09	-0.48	-0.04	304.96	-8.42	-3.82	0.72	163.10	1.49	0.02	25.55	266.17	8.32
20:52:30	712.50	1.17	-0.70	-0.93	-0.11	293.96	-11.95	-7.52	0.82	190.50	2.01	0.02	25.40	266.86	0.06
21:07:30	727.50	0.94	-0.57	-0.74	-0.08	292.17	-16.27	-1.91	0.86	192.80	2.33	0.02	25.32	267.24	0.00
21:22:30	742.50	0.93	-0.55	-0.75	-0.07	290.90	-13.43	-5.31	0.91	189.20	2.36	0.02	25.31	267.28	0.00
21:37:30	757.50	1.52	-1.03	-1.11	-0.12	289.17	1.24	-2.57	0.98	197.60	2.71	0.02	25.29	267.35	0.00
21:52:30	772.50	2.50	-1.53	-1.97	-0.07	276.96	-16.66	-0.63	1.06	190.80	2.94	0.02	25.24	267.61	0.00
22:22:30	802.50	2.08	-1.14	-1.74	-0.06	268.17	3.84	-1.10	1.19	185.60	3.53	0.02	25.13	268.12	0.00
22:37:30	817.50	1.03	-0.71	-0.75	0.01	263.95	-11.27	-3.64	1.25	198.10	3.42	0.03	25.08	268.34	0.00
22:52:30	832.50	1.28	-0.48	-1.18	-0.06	261.74	-6.43	-2.73	1.29	175.70	3.68	0.03	25.04	268.54	0.00
23:07:30	847.50	0.95	-0.77	-0.55	-0.02	260.43	-14.33	-10.67	1.36	205.90	3.74	0.03	25.00	268.71	0.00
23:22:30	862.50	1.27	-0.80	-0.98	-0.12	257.80	-22.58	-28.70	1.43	193.60	4.27	0.03	24.97	268.86	0.00
23:37:30	877.50	1.20	-0.82	-0.88	-0.02	254.09	-12.77	-4.11	1.49	196.40	4.07	0.03	24.95	268.97	0.00
23:52:30	892.50	0.95	-0.76	-0.58	-0.03	250.85	-36.83	-18.76	1.54	205.20	4.05	0.03	24.91	269.11	0.00
0:07:30	907.50	0.86	-0.25	-0.82	-0.05	248.60	-15.05	-7.99	1.57	173.00	3.56	0.03	24.89	269.21	0.00
0:22:30	922.50	0.56	-0.36	-0.43	-0.02	245.49	-23.57	-8.49	1.59	190.00	3.43	0.03	24.87	269.33	0.00
0:52:30	952.50	1.15	-0.65	-0.95	-0.10	240.81	-11.63	-6.46	1.66	188.40	4.01	0.03	24.78	269.74	0.00
1:07:30	967.50	0.86	-0.13	-0.85	-0.07	237.12	-19.07	-6.15	1.69	162.50	3.97	0.03	24.74	269.94	0.00
1:22:30	982.50	0.99	-0.40	-0.91	-0.08	234.77	-7.03	-3.13	1.71	179.40	4.43	0.03	24.67	270.26	0.00

1:37:30	997.50	1.14	0.16	-1.12	-0.11	232.83	-8.88	-5.10	1.72	145.80	4.56	0.04	24.56	270.77	0.00
1:52:30	1012.50	1.59	1.04	-1.18	-0.18	231.18	-10.33	-5.12	1.70	113.20	4.60	0.03	24.46	271.26	0.00
2:07:30	1027.50	2.47	2.10	-1.29	-0.21	232.35	-14.15	-1.53	1.68	94.20	4.09	0.03	24.43	271.40	0.00
2:22:30	1042.50	2.53	2.00	-1.54	-0.16	231.44	-20.82	-10.78	1.65	101.40	4.32	0.03	24.40	271.57	0.00
2:37:30	1057.50	3.32	2.92	-1.57	-0.14	230.16	-13.89	-7.13	1.61	90.90	3.55	0.02	24.36	271.75	0.00
2:52:30	1072.50	2.58	2.42	-0.85	-0.20	230.94	-39.09	-1.88	1.56	83.80	3.42	0.02	24.33	271.90	0.00
3:07:30	1087.50	2.54	2.53	-0.21	-0.18	230.46	-13.74	-8.68	1.51	68.80	3.52	0.02	24.31	272.00	0.00
3:22:30	1102.50	2.68	2.67	0.27	-0.13	227.82	-13.88	-12.69	1.46	57.80	2.62	0.02	24.32	271.96	0.00
3:52:30	1132.50	3.10	2.62	1.64	-0.22	227.28	-14.84	-14.88	1.34	31.70	1.61	0.04	24.34	271.86	0.00
4:07:30	1147.50	3.82	3.09	2.21	-0.32	226.81	-17.45	-5.54	1.27	27.00	1.65	0.07	24.33	271.89	0.00
4:22:30	1162.50	5.06	3.85	3.27	-0.28	225.37	-13.59	-1.86	1.20	22.90	1.71	0.07	24.34	271.85	0.00
4:37:30	1177.50	5.64	4.21	3.74	-0.23	225.00	-4.14	-3.65	1.14	21.30	1.54	0.08	24.33	271.88	0.00
4:52:30	1192.50	5.37	3.97	3.61	-0.23	223.45	16.12	-8.43	1.08	21.00	1.60	0.09	24.30	272.03	0.00
5:07:30	1207.50	5.47	4.05	3.67	-0.19	222.16	-18.59	-17.05	1.02	21.10	1.56	0.09	24.24	272.32	0.00
5:22:30	1222.50	6.23	4.63	4.16	-0.28	221.94	-37.70	-13.91	0.96	21.40	1.73	0.06	24.17	272.66	0.00
5:37:30	1237.50	5.34	3.73	3.81	-0.30	221.54	-29.47	-11.23	0.91	17.40	1.47	0.09	24.10	273.01	0.16
5:52:30	1252.50	5.09	3.31	3.85	-0.31	220.31	-14.45	-9.83	0.86	13.80	1.49	0.10	24.04	273.33	1.53

Table A3b. 15-min average data eddy correlation deployment bare sediment site – deployment 3 – July 9 - 10, 2007

Real Time	Time	U	Ux	Uy	Uz	O2	LD DO Flux	RA DO Flux	Depth	CurDir	ZeroPd	Hs	Temp	O2 Sat	Light Intensity
	min	cm s-1	cm s-1	cm s-1	cm s-1	uM	mmol O2 m-2 d-1	mmol O2 m-2 d-1	m	degrees	s	m	C	uM	lum m-2
11:07:30	7.5	5.861	3.728	4.516	-0.237	486.04	-2251.4	144.41	0.41	310.8	1.4	0.03	28.5	254.15	1253.84
11:22:30	22.5	7.866	4.606	6.365	-0.377	461.27	68.994	105.59	0.46	196.5	1.38	0.03	27.908	256.21	1038.69
11:37:30	37.5	8.724	5.868	6.437	-0.488	429.18	95.027	48.962	0.53	203	1.37	0.03	27.863	256.38	649.49
11:52:30	52.5	10.1	7.263	6.998	-0.536	401.18	-233.11	4.202	0.6	206.4	1.42	0.03	27.887	256.29	448.15
12:22:30	82.5	10.927	8.478	6.879	-0.45	358.08	142.21	136.96	0.76	211.3	1.39	0.08	28.118	255.39	300.53
12:37:30	97.5	9.943	8.146	5.69	-0.359	362.21	169.38	161.39	0.85	215.5	1.43	0.08	28.198	255.08	199.21
12:52:30	112.5	9.22	7.311	5.607	-0.342	371.59	156.03	52.669	0.94	212.9	1.47	0.11	28.264	254.82	176.34
13:07:30	127.5	7.729	6.335	4.419	-0.273	347.16	31.573	42.472	1.03	215.5	1.5	0.11	28.348	254.5	156.13
13:22:30	142.5	6.754	5.138	4.377	-0.244	327.56	18.888	24.593	1.12	210	1.52	0.11	28.452	254.1	134.94
13:52:30	172.5	5.008	4.371	2.443	-0.096	299.69	212.06	68.459	1.28	221.4	1.52	0.12	28.579	253.63	95.14
14:07:30	187.5	4.306	3.936	1.743	-0.077	301.66	-43.602	-4.725	1.36	227	1.6	0.12	28.633	253.42	78.70
14:22:30	202.5	3.843	3.61	1.312	-0.114	299.48	-78.981	-4.378	1.43	229.9	1.6	0.13	28.691	253.21	66.47
14:52:30	232.5	1.803	1.722	0.53	-0.077	311.37	10.282	-68.728	1.54	234.4	1.67	0.14	28.888	252.48	54.08
15:07:30	247.5	1.117	1.053	0.369	-0.053	330.11	-602.11	-215.81	1.58	232.5	1.69	0.15	29.012	252.02	50.40
15:22:30	262.5	0.628	0.343	0.513	-0.117	349.6	-224.53	-116.86	1.62	194.8	1.73	0.15	29.093	251.73	46.57
15:37:30	277.5	0.779	0.692	0.34	-0.113	359.73	-250.1	-107.08	1.67	222.6	1.74	0.16	29.151	251.51	40.94
15:52:30	292.5	0.645	0.177	0.608	-0.121	374.66	-641.55	-42.553	1.7	178.5	1.73	0.15	29.205	251.32	35.44
16:07:30	307.5	1.183	-1.165	0.034	-0.204	388.31	-204.81	-120.42	1.72	72.7	1.75	0.15	29.267	251.1	30.64
16:22:30	322.5	3.354	-3.085	-1.274	-0.32	405.04	-582.06	-247.22	1.72	48.2	1.79	0.15	29.334	250.86	30.73
16:37:30	337.5	3.288	-3.133	-0.952	-0.291	420.34	-816.93	-523.78	1.73	54.7	1.76	0.16	29.509	250.24	31.68
16:52:30	352.5	5.52	-5.286	-1.49	-0.556	458.51	-978.6	-555.02	1.72	55	1.78	0.17	29.759	249.36	34.75
17:22:30	382.5	7.857	-7.399	-2.566	-0.631	517.06	-83.32	-81.537	1.66	51.6	1.74	0.18	29.885	248.93	27.08
18:07:30	427.5	8.728	-7.857	-3.747	-0.63	371.81	-96.263	-41.763	1.5	45.2	1.55	0.19	30.218	247.8	10.84
18:22:30	442.5	11.086	-9.957	-4.809	-0.801	354.85	-155.52	-22.909	1.44	43.6	1.62	0.17	29.405	250.61	9.52
18:37:30	457.5	12.447	-9.99	-7.4	-0.595	328.23	-41.607	-48.177	1.37	34.6	1.56	0.18	28.767	252.93	8.73
18:52:30	472.5	9.815	-8.388	-5.067	-0.551	313.12	-15.202	-79.905	1.3	38.7	1.54	0.18	28.029	255.74	7.22
19:07:30	487.5	14.263	-10.73	-9.347	-0.942	304.09	-72.532	-60.352	1.23	29.5	1.52	0.19	27.517	257.76	5.87
19:22:30	502.5	13.285	-10.8	-7.698	-0.788	297.57	-84.785	-41.05	1.16	34.9	1.46	0.19	27.21	259.01	4.47
19:52:30	532.5	15.066	-11.03	-10.22	-0.96	316.94	-227.99	-136.9	1.02	27.3	1.39	0.2	27.067	259.6	2.62

20:22:30	562.5	16.664	-11.42	-12.1	-1.008	309.91	-187	-70.147	0.87	23.2	1.33	0.18	27.028	259.77	0.46
20:37:30	577.5	16.419	-11.39	-11.79	-0.906	306.49	-106.25	-32.569	0.8	25	1.49	0.09	26.844	260.53	0.04
21:22:30	622.5	17.266	-10.81	-13.42	-1.123	279.85	-136.25	-43.759	0.6	18.7	1.38	0.07	26.435	262.27	0.00
21:52:30	652.5	13.215	-7.976	-10.52	-0.562	273.1	-558.06	-362.9	0.49	17.1	1.34	0.06	26.308	262.82	0.00
22:07:30	667.5	12.704	-7.835	-9.988	-0.483	267.94	-649.5	-445.9	0.45	18.4	1.37	0.04	26.247	263.09	0.00
22:22:30	682.5	10.311	-6.029	-8.364	-0.092	265.16	-402.04	-422.09	0.42	16.4	1.34	0.04	26.186	263.35	0.00
22:52:30	712.5	5.847	-3.55	-4.644	-0.15	265.42	-72.881	-175.31	0.38	17.6	1.35	0.04	26.076	263.83	0.00
23:07:30	727.5	4.376	-2.401	-3.656	-0.124	261.83	-196.44	-314.54	0.38	14.4	1.35	0.04	26.055	263.93	0.00
23:22:30	742.5	1.906	-1.446	-1.242	-0.038	258.12	-191.52	-311.36	0.38	29.6	1.33	0.04	26.031	264.03	0.00
23:37:30	757.5	2.316	0.628	2.229	0.016	257.26	-90.232	-92.692	0.41	175.9	1.31	0.04	25.997	264.18	0.00
23:52:30	772.5	2.799	2.031	1.909	-0.259	255.51	-30.774	-12.989	0.43	206.3	1.35	0.03	25.957	264.36	0.00
0:07:30	787.5	4.1	2.144	3.49	-0.187	244.15	19.626	33.996	0.46	192.9	1.34	0.03	25.93	264.48	0.00
0:22:30	802.5	4.695	2.944	3.654	-0.149	247.28	282.93	28.75	0.5	198.8	1.37	0.03	25.918	264.53	0.00
0:37:30	817.5	6.374	4.119	4.863	-0.125	248.95	8.2	15.595	0.55	200.7	1.37	0.04	25.961	264.34	0.00
1:07:30	847.5	8.346	6.258	5.513	-0.302	256.82	85.29	88.565	0.68	208.8	1.41	0.05	26.024	264.06	0.00
1:22:30	862.5	7.301	5.361	4.949	-0.256	258.86	95.889	108.37	0.74	207.6	1.36	0.11	26.062	263.89	0.00
1:37:30	877.5	6.788	5.097	4.481	-0.137	258.94	22.307	40.22	0.8	209	1.35	0.11	26.108	263.7	0.00
1:52:30	892.5	6.246	4.935	3.824	-0.194	257.83	-26.401	-16.919	0.86	212.7	1.46	0.1	26.132	263.59	0.00
2:07:30	907.5	4.674	3.385	3.219	-0.173	256.17	-12.63	-14.707	0.92	207.3	1.44	0.12	26.133	263.58	0.00
2:22:30	922.5	4.85	3.521	3.333	-0.149	254.88	-32.831	-12.495	0.98	207.1	1.45	0.12	26.12	263.64	0.00
2:37:30	937.5	4.897	4.098	2.676	-0.157	252.48	-65.613	-71.047	1.04	217.1	1.53	0.11	26.111	263.68	0.00
2:52:30	952.5	3.723	2.564	2.69	-0.233	252.19	-48.846	-46.709	1.1	204	1.52	0.12	26.103	263.71	0.00
3:07:30	967.5	4	3.031	2.605	-0.168	252.43	-68.539	-63.394	1.16	209.9	1.53	0.13	26.104	263.71	0.00
3:22:30	982.5	3.14	2.635	1.705	-0.106	252.34	-161.02	-126.28	1.21	217	1.58	0.13	26.1	263.73	0.00
3:37:30	997.5	2.35	1.89	1.391	-0.13	252.62	-176.27	-154.16	1.26	213.8	1.61	0.13	26.095	263.75	0.00
3:52:30	1012.5	0.974	0.552	0.802	-0.006	254.01	-171.04	-129.84	1.29	196.7	1.56	0.12	26.087	263.79	0.00
4:07:30	1027.5	0.517	-0.006	0.507	-0.102	254.12	-191.66	-74.037	1.32	159.6	1.5	0.12	26.095	263.75	0.00
4:22:30	1042.5	0.769	0.038	0.766	-0.058	257.77	-118.19	-83.331	1.35	161.1	1.76	0.06	26.153	263.5	0.00
4:37:30	1057.5	0.269	-0.14	0.224	-0.048	249.13	-344.42	-46.375	1.37	127.9	1.74	0.07	26.142	263.54	0.00
5:22:30	1102.5	4.709	-4.681	-0.375	-0.353	247.29	-126.94	-71.941	1.35	66.3	1.74	0.05	26.024	264.06	0.00
5:37:30	1117.5	5.165	-5.149	-0.241	-0.332	250.09	-55.418	-51.53	1.32	67.9	1.89	0.04	25.971	264.29	0.00
5:52:30	1132.5	4.878	-4.859	-0.283	-0.33	252.55	-11.721	-24.122	1.29	67.4	1.67	0.05	25.867	264.76	0.07

6:07:30	1147.5	5.723	-5.494	-1.554	-0.392	251.81	-31.585	-17.421	1.24	55	1.69	0.04	25.788	265.11	0.71
6:22:30	1162.5	6.351	-5.826	-2.507	-0.322	248.37	-7.981	-12.8	1.19	47.3	1.58	0.04	25.959	264.35	2.06
6:37:30	1177.5	7.921	-6.664	-4.241	-0.585	245.12	-32.937	-30.558	1.12	38.3	1.57	0.04	26.12	263.64	4.09
6:52:30	1192.5	8.398	-6.723	-5.003	-0.548	245.15	7.837	-18.826	1.06	33.6	1.53	0.05	26.241	263.11	7.76
7:07:30	1207.5	7.412	-5.7	-4.723	-0.379	243.22	-10.461	-20.061	1.01	30.9	1.51	0.03	26.344	262.66	11.92
7:22:30	1222.5	7.961	-5.75	-5.493	-0.367	240.84	46.999	26.058	0.95	26.5	1.53	0.03	26.42	262.34	18.14
7:37:30	1237.5	9.145	-6.526	-6.377	-0.612	237.66	70.205	25.292	0.89	25.8	1.48	0.03	26.491	262.03	27.52
7:52:30	1252.5	9.243	-6.395	-6.651	-0.536	236.63	80.683	60.894	0.82	23.8	1.47	0.03	26.571	261.69	38.79
8:07:30	1267.5	10.27	-6.701	-7.761	-0.593	236.1	135.72	121.74	0.77	21.1	1.49	0.02	26.586	261.63	44.41
8:22:30	1282.5	10.563	-6.618	-8.206	-0.655	239.12	203.01	162.87	0.7	19.8	1.44	0.02	26.606	261.54	79.26
8:37:30	1297.5	11.784	-7.372	-9.175	-0.563	252.1	245.49	296.06	0.64	19.1	1.37	0.03	26.679	261.23	104.36
8:52:30	1312.5	12.355	-7.54	-9.766	-0.647	266.7	6.121	20.737	0.58	18.1	1.37	0.03	26.805	260.7	149.12
9:07:30	1327.5	10.747	-6.497	-8.548	-0.457	278.4	83.804	68.396	0.53	17.7	1.38	0.02	26.977	259.98	189.00
9:22:30	1342.5	11.266	-6.344	-9.297	-0.496	288.69	50.41	30.057	0.48	14.9	1.41	0.02	27.021	259.79	329.72

Table A3c. 15-min average data eddy correlation deployment bare sediment site – deployment 4 – July 11- 12, 2007

Real Time	Time	U	Ux	Uy	Uz	O2	LD DO Flux	RA DO Flux	Depth	CurDir	ZeroPd	Hs	Temp	O2 Sat	Light Intensity
	min	cm s-1	cm s-1	cm s-1	cm s-1	uM	mmol O2 m-2 d-1	mmol O2 m-2 d-1	m	degrees	s	m	C	uM	lum m-2
13:07:30	7.50	5.22	-2.94	4.29	-0.34	290.35	339.67	211.51	0.39	235.70	1.29	0.09	29.31	250.94	4530.02
13:22:30	22.50	7.24	-1.02	7.16	-0.34	289.67	26.23	29.39	0.46	199.80	1.32	0.09	29.42	250.56	4720.06
13:37:30	37.50	8.44	0.28	8.44	-0.20	272.69	121.47	108.29	0.52	211.00	1.27	0.14	29.47	250.37	4127.33
13:52:30	52.50	9.02	1.31	8.91	-0.42	256.52	190.60	144.23	0.59	217.90	1.35	0.12	29.37	250.71	3704.25
14:07:30	67.50	10.49	2.05	10.27	-0.63	250.74	55.69	40.41	0.68	220.50	1.42	0.12	29.41	250.57	3545.38
14:22:30	82.50	9.84	1.68	9.68	-0.57	248.60	112.92	47.10	0.77	218.90	1.48	0.13	29.58	249.98	2524.71
14:37:30	97.50	9.23	1.77	9.05	-0.50	236.90	120.36	64.13	0.87	220.70	1.53	0.13	29.67	249.67	1670.62
14:52:30	112.50	9.16	2.79	8.71	-0.53	227.43	249.20	139.22	0.97	227.00	1.63	0.14	29.71	249.52	1125.63
15:07:30	127.50	7.07	2.29	6.68	-0.46	227.68	120.61	104.60	1.05	228.50	1.70	0.14	29.79	249.26	858.53
15:22:30	142.50	6.17	1.47	5.98	-0.40	221.36	64.48	63.03	1.13	222.80	1.72	0.13	29.85	249.06	603.50
15:37:30	157.50	5.33	1.70	5.04	-0.29	219.32	47.83	21.42	1.21	228.10	1.69	0.14	29.90	248.87	469.12
15:52:30	172.50	4.62	1.87	4.23	-0.22	218.94	98.29	90.88	1.30	232.70	1.75	0.14	29.93	248.76	298.25
16:07:30	187.50	3.75	1.44	3.45	-0.25	220.14	-108.48	-77.00	1.38	231.60	1.80	0.14	29.92	248.82	86.05
16:22:30	202.50	2.22	0.35	2.18	-0.20	220.09	-79.70	-51.11	1.45	219.10	1.80	0.17	29.90	248.89	98.85
16:37:30	217.50	2.66	1.12	2.41	-0.13	219.86	-66.61	-20.33	1.52	234.30	1.80	0.15	29.91	248.83	126.27
16:52:30	232.50	3.28	1.21	3.04	-0.16	221.47	-133.63	-23.23	1.58	231.40	1.87	0.14	29.90	248.86	96.31
17:07:30	247.50	3.33	0.95	3.18	-0.21	220.63	-101.76	-61.21	1.64	225.90	1.98	0.16	29.87	248.98	68.20
17:22:30	262.50	3.78	0.94	3.66	-0.09	216.72	-22.11	-46.03	1.69	224.30	1.92	0.15	29.78	249.29	44.47
17:37:30	277.50	2.96	0.01	2.95	-0.21	209.87	-55.06	-20.11	1.74	210.00	1.98	0.15	29.68	249.64	41.41
17:52:30	292.50	2.36	-1.34	1.93	-0.25	201.62	-53.63	-30.78	1.78	174.70	1.93	0.14	29.59	249.94	32.35
18:07:30	307.50	1.73	-1.65	-0.50	-0.18	196.04	-148.16	-126.46	1.80	103.60	1.93	0.16	29.55	250.09	22.99
18:22:30	322.50	2.41	-2.36	0.19	-0.43	193.41	-184.46	-88.57	1.82	122.70	1.89	0.14	29.52	250.19	15.50
18:37:30	337.50	3.48	-3.45	-0.30	-0.35	191.30	-90.95	-79.59	1.81	115.20	1.88	0.12	29.44	250.49	12.36
18:52:30	352.50	6.24	-6.06	-1.42	-0.56	189.14	-177.47	-118.72	1.78	106.20	1.72	0.15	29.19	251.37	5.12
19:07:30	367.50	7.06	-6.31	-3.12	-0.50	193.10	-110.19	-85.45	1.75	93.20	1.92	0.19	29.19	251.37	0.04
19:22:30	382.50	6.80	-5.77	-3.55	-0.68	195.13	-99.84	-81.95	1.70	87.70	2.02	0.16	29.30	250.99	0.00
19:37:30	397.50	6.77	-5.17	-4.33	-0.55	196.16	-348.95	-163.24	1.66	79.40	1.83	0.19	29.35	250.81	0.00
19:52:30	412.50	9.01	-6.98	-5.66	-0.62	203.64	-268.15	-294.27	1.62	80.10	2.09	0.36	29.32	250.90	0.00
20:07:30	427.50	7.47	-3.18	-6.75	-0.35	206.41	-216.39	-193.94	1.54	55.00	2.19	0.30	29.28	251.05	0.00
20:22:30	442.50	8.97	-4.78	-7.57	-0.57	205.30	-110.45	-100.59	1.45	60.60	2.02	0.22	29.27	251.10	0.00
20:37:30	457.50	10.61	-4.96	-9.36	-0.59	205.87	-100.60	-117.34	1.38	57.80	1.79	0.20	29.26	251.14	0.00
20:52:30	472.50	11.81	-4.39	-10.94	-0.71	205.45	-124.14	-95.40	1.31	50.90	1.69	0.16	29.25	251.15	0.00
21:07:30	487.50	11.75	-3.39	-11.23	-0.61	203.87	-57.19	-86.42	1.24	45.60	1.60	0.15	29.32	250.92	0.00

21:22:30	502.50	13.43	-3.40	-12.98	-0.61	205.30	-120.52	-90.55	1.18	43.80	1.70	0.07	29.38	250.69	0.00
21:37:30	517.50	14.48	-2.76	-14.20	-0.72	205.30	-110.58	-69.70	1.12	40.00	1.78	0.04	29.44	250.46	0.00
21:52:30	532.50	15.44	-3.50	-15.01	-0.83	206.25	-120.63	-75.02	1.05	42.30	1.67	0.03	29.52	250.20	0.00
22:07:30	547.50	18.20	-2.78	-17.97	-0.83	205.66	-110.94	-61.76	0.97	37.60	1.44	0.16	29.35	250.79	0.00
22:22:30	562.50	18.92	-2.17	-18.78	-0.80	197.81	-24.37	-32.21	0.87	36.00	1.49	0.16	28.96	252.20	0.00
22:37:30	577.50	19.14	-2.46	-18.95	-1.02	187.68	-14.04	-14.23	0.80	36.20	1.53	0.15	28.64	253.40	0.00
22:52:30	592.50	17.17	-1.41	-17.09	-0.89	180.75	13.38	-17.86	0.73	33.70	1.47	0.16	28.34	254.53	0.00
23:07:30	607.50	17.24	-1.20	-17.17	-0.96	176.17	-62.02	-34.09	0.66	31.90	1.55	0.13	28.09	255.50	0.00
23:52:30	652.50	15.87	0.64	-15.84	-0.80	162.20	1.62	-1.65	0.44	26.90	1.37	0.12	27.53	257.71	0.00
0:07:30	667.50	16.07	1.28	-16.00	-0.81	158.86	-45.71	-7.58	0.37	24.50	1.30	0.11	27.11	259.45	0.00
0:22:30	682.50	14.65	1.52	-14.56	-0.60	156.10	-94.38	-66.33	0.32	22.90	1.30	0.07	25.88	264.74	0.00
0:37:30	697.50	14.27	1.50	-14.18	-0.57	153.17	-69.79	-63.82	0.30	23.00	1.57	0.01	26.26	263.07	0.00
0:52:30	712.50	8.94	-0.21	-8.93	-0.38	149.60	-285.52	-213.93	0.30	29.60	1.57	0.01	27.00	259.89	0.00
1:07:30	727.50	3.51	-3.48	0.38	-0.30	150.12	-226.11	-166.62	0.31	123.90	1.32	0.05	27.01	259.83	0.00
1:22:30	742.50	3.46	-1.28	3.20	-0.24	146.24	-6.33	-8.89	0.34	185.60	1.25	0.09	26.98	259.97	0.00
1:37:30	757.50	3.74	-2.03	3.12	-0.28	146.90	-175.24	-159.42	0.37	177.80	1.26	0.08	26.94	260.12	0.00
1:52:30	772.50	5.15	-1.52	4.91	-0.29	147.64	-140.45	-140.64	0.41	190.80	1.29	0.08	26.95	260.07	0.00
2:07:30	787.50	3.32	-0.76	3.23	-0.23	149.40	-245.73	-210.07	0.45	196.60	1.33	0.09	26.98	259.95	0.00
2:22:30	802.50	4.78	-2.01	4.34	-0.16	152.23	-121.43	-93.17	0.50	182.90	1.37	0.09	26.99	259.91	0.00
2:37:30	817.50	5.80	0.87	5.73	-0.17	150.13	-86.71	-73.85	0.55	217.80	1.41	0.09	27.00	259.88	0.00
2:52:30	832.50	7.07	-1.27	6.95	-0.35	149.45	-54.87	-36.99	0.61	198.80	1.30	0.14	27.06	259.65	0.00
3:07:30	847.50	10.74	0.86	10.69	-0.49	149.47	-56.89	-62.11	0.69	213.70	1.34	0.13	27.19	259.10	0.00
3:22:30	862.50	10.80	2.43	10.51	-0.54	147.88	-51.03	-47.01	0.79	222.10	1.35	0.14	27.27	258.78	0.00
3:37:30	877.50	11.24	2.52	10.94	-0.56	147.41	-34.31	-30.20	0.89	222.00	1.56	0.08	27.33	258.53	0.00
3:52:30	892.50	7.89	2.28	7.55	-0.39	145.62	-67.92	-51.24	0.94	226.10	1.44	0.15	27.40	258.25	0.00
4:07:30	907.50	4.83	0.82	4.75	-0.29	146.68	-261.20	-205.33	0.98	219.10	1.49	0.14	27.49	257.87	0.00
4:22:30	922.50	5.74	2.27	5.26	-0.30	146.62	-180.88	-157.18	1.04	231.90	1.56	0.15	27.59	257.46	0.00
4:37:30	937.50	7.45	1.85	7.20	-0.41	147.46	-140.58	-144.52	1.11	223.90	1.53	0.16	27.63	257.30	0.00
4:52:30	952.50	7.05	0.82	7.00	-0.40	149.63	-60.93	-81.14	1.16	215.50	1.63	0.18	27.64	257.29	0.00
5:07:30	967.50	7.77	0.56	7.74	-0.38	154.24	-82.45	-67.37	1.22	213.50	1.67	0.17	27.61	257.39	0.00
5:22:30	982.50	8.77	1.79	8.57	-0.49	159.57	-161.12	-141.33	1.28	221.10	1.72	0.17	27.62	257.35	0.00
5:37:30	997.50	8.49	1.30	8.38	-0.35	162.03	-166.42	-131.37	1.34	217.40	1.69	0.19	27.63	257.30	0.00
5:52:30	1012.50	6.86	1.75	6.63	-0.31	167.03	-275.95	-136.98	1.38	224.00	1.73	0.17	27.43	258.13	0.05
6:07:30	1027.50	5.15	-0.45	5.13	-0.15	171.50	-188.10	-210.11	1.40	205.10	1.80	0.17	26.96	260.04	2.28
6:22:30	1042.50	5.12	-2.41	4.51	-0.22	169.89	-135.88	-138.63	1.40	181.00	1.77	0.16	26.71	261.09	5.01
6:37:30	1057.50	6.24	-1.22	6.10	-0.40	164.74	-53.57	-67.53	1.41	197.30	1.81	0.16	26.50	262.01	11.72

6:52:30	1072.50	6.15	-1.87	5.84	-0.36	161.59	-108.48	-103.76	1.42	191.00	1.78	0.16	26.35	262.64	13.98
7:07:30	1087.50	5.83	-1.07	5.72	-0.35	159.93	-30.72	-38.00	1.43	198.50	1.67	0.15	26.30	262.84	14.88
7:22:30	1102.50	4.62	0.17	4.60	-0.31	160.40	-99.95	-85.63	1.42	211.70	1.71	0.15	26.28	262.94	38.63
7:37:30	1117.50	2.72	-0.30	2.69	-0.28	161.04	-58.77	-35.92	1.42	203.10	1.69	0.16	26.30	262.87	52.53
7:52:30	1132.50	1.70	-1.50	0.67	-0.41	162.67	-107.84	-59.07	1.38	144.90	1.70	0.16	26.32	262.78	72.40
8:07:30	1147.50	3.83	-3.21	-2.05	-0.43	165.41	-124.02	-92.87	1.33	87.90	1.66	0.17	26.18	263.39	83.87
8:22:30	1162.50	4.98	-2.76	-4.12	-0.41	166.56	-107.30	-95.74	1.28	63.40	1.73	0.17	26.33	262.74	100.12
8:37:30	1177.50	6.64	-3.38	-5.71	-0.28	168.40	-23.96	-45.21	1.21	59.90	1.72	0.16	26.34	262.70	128.44
8:52:30	1192.50	8.12	-2.57	-7.69	-0.53	171.06	-91.45	-83.32	1.15	47.80	1.71	0.17	26.46	262.17	199.94
9:07:30	1207.50	8.50	-2.58	-8.08	-0.54	171.33	-48.57	-26.46	1.08	46.80	1.71	0.17	26.67	261.28	253.41
9:22:30	1222.50	9.69	-1.72	-9.51	-0.71	174.14	-97.97	-100.08	1.02	38.80	1.65	0.15	26.75	260.93	353.63
9:37:30	1237.50	10.33	-1.72	-10.17	-0.64	175.50	-84.31	-75.17	0.95	38.30	1.52	0.14	26.84	260.56	493.33
9:52:30	1252.50	10.45	-1.01	-10.37	-0.71	175.99	-42.87	-37.31	0.88	34.20	1.50	0.13	26.98	259.95	691.48
10:07:30	1267.50	10.07	-0.61	-10.03	-0.60	178.54	-61.31	-56.24	0.82	32.90	1.47	0.12	27.18	259.15	979.67
10:22:30	1282.50	11.12	-0.02	-11.10	-0.69	181.97	-75.65	-72.88	0.75	29.20	1.40	0.12	27.41	258.18	1449.07

Table A3d. 15-min average data eddy correlation deployment vegetated site – deployment 3 – June 25- 26, 2007

Real Time	Time	U	Ux	Uy	Uz	O2	LD DO Flux	RA DO Flux	Depth	CurDir	ZeroPd	Hs	Temp	O2 Sat	Light Intensity
	min	cm s-1	cm s-1	cm s-1	cm s-1	uM	mmol O2 m-2 d-1	mmol O2 m-2 d-1	m	degrees	s	m	C	uM	lum m-2
12:07:30	7.50	1.68	1.63	0.31	-0.27	309.82	8.75	32.18	0.46	227.80	1.37	0.05	24.61	270.53	886.29
12:22:30	22.50	1.81	1.77	0.11	-0.38	320.74	75.16	8.99	0.49	180.30	1.31	0.07	24.84	269.47	548.24
12:37:30	37.50	1.29	1.24	-0.31	-0.19	328.22	101.28	68.04	0.54	198.00	1.33	0.07	24.98	268.82	515.57
12:52:30	52.50	1.02	1.01	-0.08	-0.12	336.89	34.21	-2.07	0.59	185.80	1.34	0.09	25.14	268.07	596.76
13:07:30	67.50	1.03	0.98	-0.31	-0.12	343.20	125.67	15.25	0.64	204.50	1.37	0.10	25.32	267.24	570.73
13:22:30	82.50	0.91	0.91	-0.02	-0.08	343.09	54.98	44.74	0.70	185.40	1.37	0.13	25.42	266.79	275.39
13:37:30	97.50	0.63	0.61	-0.12	-0.01	342.62	51.34	27.53	0.75	198.00	1.41	0.12	25.42	266.79	148.86
13:52:30	112.50	1.29	1.28	-0.14	-0.01	340.28	92.79	52.51	0.81	193.90	1.32	0.16	25.39	266.89	154.72
14:22:30	142.50	1.48	1.47	-0.15	0.01	341.31	108.51	75.28	0.94	189.90	1.43	0.14	25.42	266.79	139.66
14:37:30	157.50	1.26	1.26	-0.11	-0.01	337.13	91.33	69.98	1.00	189.10	1.45	0.15	25.42	266.77	128.33
14:52:30	172.50	0.87	0.84	-0.23	-0.08	336.59	104.80	26.03	1.07	200.20	1.48	0.15	25.44	266.68	115.50
15:07:30	187.50	0.69	0.68	-0.03	-0.12	337.29	72.80	-18.08	1.12	184.60	1.52	0.15	25.47	266.56	100.55
15:22:30	202.50	0.30	-0.03	0.16	-0.25	345.02	-35.84	-2.20	1.17	93.20	1.45	0.17	25.52	266.30	110.42
15:52:30	232.50	1.15	-1.00	0.38	-0.42	366.19	64.93	-0.56	1.25	27.40	1.58	0.14	25.68	265.58	106.30
16:07:30	247.50	0.29	-0.13	-0.06	-0.25	374.63	3.17	-3.76	1.31	330.80	1.56	0.14	25.74	265.34	94.56
16:37:30	277.50	0.31	0.06	0.00	-0.31	378.36	-81.99	-22.81	1.39	243.90	1.67	0.07	25.78	265.15	68.34
16:52:30	292.50	0.88	-0.84	0.03	-0.29	383.05	-98.62	-30.57	1.42	5.70	1.68	0.07	25.82	264.97	79.53
17:07:30	307.50	1.38	-1.20	0.53	-0.44	388.61	-11.05	-19.33	1.44	26.80	1.52	0.15	25.86	264.78	75.30
17:22:30	322.50	2.18	-1.92	0.79	-0.65	384.32	284.85	190.90	1.44	24.90	1.59	0.15	25.82	264.95	94.60
17:37:30	337.50	3.09	-2.68	1.32	-0.78	373.26	328.04	266.21	1.43	30.70	1.57	0.16	25.74	265.33	41.26
17:52:30	352.50	2.86	-2.30	1.44	-0.89	354.75	432.02	271.32	1.42	37.60	1.54	0.16	25.70	265.52	50.53
18:07:30	367.50	2.95	-2.61	1.09	-0.84	338.39	459.91	283.25	1.41	26.60	1.56	0.17	25.75	265.27	37.63
18:22:30	382.50	3.53	-2.99	1.66	-0.88	323.37	258.32	124.69	1.39	34.20	1.59	0.17	25.85	264.83	21.80
18:37:30	397.50	4.28	-3.85	1.59	-0.97	302.58	233.75	216.26	1.36	27.80	1.56	0.17	25.96	264.36	17.90
18:52:30	412.50	5.42	-4.91	1.89	-1.31	289.90	22.46	-19.59	1.32	26.10	1.51	0.19	26.09	263.80	13.87
19:07:30	427.50	6.34	-5.89	1.98	-1.25	282.97	-23.81	-18.37	1.27	23.60	1.55	0.17	26.19	263.35	11.50
19:22:30	442.50	5.41	-4.91	1.87	-1.28	278.81	-121.80	-52.11	1.23	26.50	1.49	0.17	26.22	263.20	9.81
19:52:30	472.50	6.01	-5.66	1.65	-1.15	266.72	-15.63	-24.02	1.12	21.30	1.45	0.19	26.16	263.46	7.22
20:07:30	487.50	7.88	-7.45	2.11	-1.49	259.33	-16.03	-22.76	1.05	20.30	1.57	0.11	26.01	264.13	4.71
20:22:30	502.50	9.11	-8.80	1.37	-1.91	251.83	-29.96	-37.34	0.99	13.40	1.56	0.10	25.82	264.97	1.11
20:37:30	517.50	9.35	-9.12	0.88	-1.85	244.61	-7.42	-19.70	0.92	9.90	1.52	0.09	25.65	265.73	0.16
20:52:30	532.50	8.86	-8.59	1.23	-1.77	239.44	-58.01	-45.91	0.85	13.20	1.49	0.10	25.53	266.28	0.00
21:07:30	547.50	9.35	-9.09	0.84	-2.05	237.05	-65.47	-9.89	0.79	9.70	1.43	0.10	25.46	266.58	0.00

21:22:30	562.50	9.02	-8.80	0.51	-1.92	235.30	-94.89	-72.63	0.73	8.50	1.43	0.09	25.40	266.86	0.00
21:37:30	577.50	8.82	-8.64	0.22	-1.77	232.62	-9.60	-46.69	0.68	6.30	1.39	0.09	25.26	267.52	0.00
21:52:30	592.50	8.55	-8.35	0.42	-1.78	229.64	-64.91	-53.23	0.63	7.80	1.37	0.07	25.12	268.14	0.00
22:07:30	607.50	8.14	-7.97	-0.17	-1.66	224.15	-129.43	-114.34	0.58	4.30	1.36	0.07	25.03	268.55	0.00
22:22:30	622.50	8.96	-8.80	-0.01	-1.69	220.67	-80.39	-33.94	0.53	4.30	1.36	0.06	24.94	269.00	0.00
22:37:30	637.50	7.99	-7.84	0.00	-1.52	217.07	-60.17	-62.44	0.50	4.50	1.32	0.07	24.83	269.51	0.00
22:52:30	652.50	7.96	-7.83	-0.38	-1.40	215.50	-36.49	-21.14	0.47	2.10	1.36	0.05	24.69	270.15	0.00
23:07:30	667.50	6.51	-6.39	0.33	-1.21	211.41	-47.25	-33.62	0.46	7.20	1.45	0.04	24.48	271.18	0.00
23:22:30	682.50	5.15	-5.02	-0.60	-0.97	209.18	-186.44	-155.98	0.45	358.60	1.54	0.02	24.20	272.53	0.00
23:37:30	697.50	5.19	-5.04	-0.62	-1.05	206.67	-125.24	-94.36	0.44	357.40	1.69	0.01	23.89	274.05	0.00
23:52:30	712.50	4.87	-4.69	-0.73	-1.06	203.63	-104.93	-87.22	0.44	355.80	1.66	0.01	23.73	274.83	0.00
0:07:30	727.50	4.04	-3.86	-0.60	-1.04	200.52	-207.67	-182.93	0.44	354.40	1.64	0.01	23.75	274.73	0.00
0:22:30	742.50	2.81	-2.62	-0.41	-0.92	197.66	-50.33	-33.98	0.44	357.40	1.54	0.01	24.03	273.33	0.00
0:52:30	772.50	1.11	0.91	0.63	0.17	192.85	5.55	-1.63	0.45	150.70	1.67	0.02	24.49	271.13	0.00
1:07:30	787.50	2.29	1.88	1.28	0.33	192.05	-22.83	-12.21	0.46	147.80	1.38	0.04	24.48	271.15	0.00
1:22:30	802.50	2.58	2.22	1.32	0.11	190.91	-2.52	-8.88	0.49	153.60	1.31	0.04	24.47	271.23	0.00
1:37:30	817.50	1.70	1.61	0.51	-0.15	188.15	-85.11	-58.26	0.53	168.00	1.34	0.04	24.45	271.30	0.00
2:07:30	847.50	2.11	1.78	1.09	-0.26	186.29	-70.79	-16.61	0.60	153.00	1.35	0.05	24.43	271.41	0.00
2:37:30	877.50	1.69	1.29	1.04	-0.30	187.28	-192.16	-57.70	0.68	144.90	1.37	0.09	24.41	271.51	0.00
2:52:30	892.50	2.14	2.08	0.46	-0.18	188.76	-41.11	-15.37	0.73	171.50	1.41	0.08	24.39	271.61	0.00
3:22:30	922.50	2.26	2.07	0.80	-0.45	187.80	-52.86	-30.60	0.83	162.30	1.48	0.10	24.38	271.65	0.00
3:52:30	952.50	1.65	1.54	0.54	-0.25	187.83	-106.35	-53.37	0.93	164.30	1.50	0.09	24.37	271.71	0.00
4:07:30	967.50	0.94	0.92	0.15	-0.16	187.76	-127.48	-35.28	0.98	175.90	1.53	0.08	24.36	271.76	0.00
4:22:30	982.50	0.68	0.30	0.52	-0.30	187.07	-144.81	-15.12	1.02	124.50	1.55	0.07	24.34	271.86	0.00
4:37:30	997.50	0.63	0.39	0.44	-0.23	187.16	-202.84	-67.55	1.06	136.40	1.41	0.14	24.31	272.00	0.00
4:52:30	1012.50	1.31	-0.98	0.83	-0.29	186.56	-184.96	-56.34	1.09	46.20	1.49	0.13	24.28	272.15	0.00
5:07:30	1027.50	2.16	-1.34	1.58	-0.60	187.18	-190.37	-34.37	1.12	54.60	1.39	0.16	24.24	272.35	0.00
5:22:30	1042.50	2.49	-2.07	1.25	-0.60	187.50	-197.80	-117.40	1.14	34.80	1.48	0.15	24.21	272.49	0.00
5:37:30	1057.50	3.79	-3.04	2.10	-0.84	186.18	-175.35	-107.46	1.15	38.30	1.48	0.18	24.20	272.52	0.08
5:52:30	1072.50	3.94	-3.34	1.91	-0.86	183.49	-61.07	-24.42	1.15	34.90	1.51	0.19	24.20	272.50	1.00
6:22:30	1102.50	4.30	-3.94	1.34	-1.08	176.69	-26.98	-36.48	1.12	24.20	1.50	0.16	24.23	272.36	7.22
6:37:30	1117.50	3.91	-3.56	1.35	-0.90	178.06	-125.04	-42.90	1.10	25.70	1.44	0.18	24.25	272.27	13.58
6:52:30	1132.50	3.22	-2.93	1.08	-0.76	180.44	-85.79	-23.38	1.07	25.30	1.51	0.13	24.27	272.16	23.31
7:07:30	1147.50	4.31	-3.89	1.54	-1.02	183.92	-71.09	-29.57	1.03	26.00	1.51	0.11	24.30	272.05	31.16
7:22:30	1162.50	4.57	-4.04	1.81	-1.14	186.63	-81.15	-27.39	1.00	28.90	1.41	0.15	24.31	271.99	34.30
7:37:30	1177.50	5.50	-5.09	1.68	-1.26	190.52	-33.04	-12.01	0.95	22.70	1.50	0.12	24.33	271.90	40.56

7:52:30	1192.50	4.91	-4.65	1.15	-1.09	192.61	-36.49	-34.27	0.90	18.20	1.48	0.11	24.39	271.59	39.16
8:07:30	1207.50	5.05	-4.83	0.96	-1.14	194.71	-9.54	-0.03	0.85	15.90	1.48	0.09	24.47	271.20	44.92
8:37:30	1237.50	6.80	-6.61	0.77	-1.38	--	0.45	0.56	0.75	11.20	1.44	0.06	24.60	270.62	142.80
8:52:30	1252.50	7.29	-7.12	0.48	-1.48	--	0.01	-0.01	0.70	8.60	1.38	0.08	24.69	270.16	119.25
9:07:30	1267.50	6.47	-6.31	0.42	-1.35	--	-0.48	-0.51	0.66	7.80	1.37	0.06	24.81	269.60	134.91
9:22:30	1282.50	6.23	-6.10	0.38	-1.21	--	0.32	0.31	0.62	8.60	1.37	0.05	24.94	268.97	168.88

Table A3e. 15-min average data eddy correlation deployment vegetated site – deployment 4 – June 26- 27, 2007

Real Time	Time	U	Ux	Uy	Uz	O2	LD DO Flux	RA DO Flux	Depth	CurDir	ZeroPd	Hs	Temp	O2 Sat	Light Intensity
	min	cm s-1	cm s-1	cm s-1	cm s-1	uM	mmol O2 m-2 d-1	mmol O2 m-2 d-1	m	degrees	s	m	C	uM	lum m-2
13:37:30	7.50	1.91	1.82	-0.53	-0.25	297.27	223.47	151.88	0.53	202.10	1.33	0.06	28.10	255.44	0.00
13:52:30	22.50	3.33	3.11	-1.16	-0.25	294.28	321.01	231.53	0.61	190.60	1.34	0.08	28.21	255.05	0.00
14:07:30	37.50	3.32	2.91	-1.59	-0.30	294.19	352.77	330.43	0.67	198.30	1.32	0.11	28.27	254.79	0.00
14:22:30	52.50	3.70	3.25	-1.72	-0.38	290.08	239.91	211.82	0.74	197.80	1.40	0.09	28.25	254.88	0.00
14:37:30	67.50	3.19	2.85	-1.40	-0.24	291.74	352.11	319.30	0.81	197.10	1.38	0.14	28.25	254.89	0.00
14:52:30	82.50	2.67	2.17	-1.53	-0.22	289.67	397.65	350.12	0.88	204.50	1.39	0.15	28.20	255.08	0.00
15:07:30	97.50	2.12	1.92	-0.87	-0.23	287.63	340.57	218.35	0.95	194.80	1.40	0.16	28.20	255.07	0.00
15:22:30	112.50	1.10	0.96	-0.52	-0.16	284.95	235.99	159.19	1.01	199.70	1.43	0.16	28.25	254.89	0.00
15:37:30	127.50	0.62	-0.36	0.40	-0.31	286.25	-235.92	-63.30	1.06	42.10	1.47	0.16	28.35	254.49	0.00
15:52:30	142.50	0.41	0.02	0.21	-0.35	291.67	-32.42	-55.85	1.12	65.10	1.48	0.16	28.49	253.95	0.00
16:07:30	157.50	0.52	-0.45	-0.07	-0.25	296.50	41.14	-46.50	1.17	344.20	1.53	0.16	28.62	253.47	0.00
16:22:30	172.50	0.59	-0.29	0.27	-0.44	300.98	13.71	-22.48	1.24	35.40	1.52	0.18	28.76	252.96	0.00
16:52:30	202.50	2.11	-1.55	1.35	-0.50	308.84	-41.36	-59.75	1.34	32.50	1.64	0.19	29.09	251.72	0.00
17:07:30	217.50	2.12	-1.70	1.06	-0.68	314.06	-216.81	-187.70	1.37	24.00	1.56	0.18	29.18	251.41	0.00
17:22:30	232.50	0.63	-0.34	0.44	-0.29	314.80	-47.21	-51.39	1.40	41.80	1.59	0.15	29.18	251.42	0.00
18:37:30	307.50	2.41	-1.69	1.58	-0.68	295.48	234.84	117.75	1.46	33.00	1.64	0.17	28.50	253.93	0.00
18:52:30	322.50	4.07	-3.27	2.26	-0.87	284.03	286.15	188.58	1.43	24.80	1.58	0.17	28.34	254.52	0.00
19:07:30	337.50	3.54	-2.76	2.13	-0.61	263.58	768.76	555.47	1.41	27.90	1.56	0.16	28.39	254.34	0.00
19:22:30	352.50	3.46	-2.46	2.34	-0.67	240.89	402.41	311.68	1.37	34.10	1.49	0.15	28.54	253.78	0.00
19:37:30	367.50	3.85	-2.89	2.44	-0.68	229.55	93.47	53.37	1.32	30.70	1.60	0.07	28.76	252.93	0.00
19:52:30	382.50	4.97	-3.82	3.02	-0.98	224.98	3.58	-25.12	1.27	29.00	1.47	0.17	28.99	252.09	0.00
20:07:30	397.50	5.33	-4.32	2.96	-0.97	221.06	-69.18	-76.37	1.22	24.80	1.56	0.13	29.10	251.71	0.00
20:22:30	412.50	6.33	-5.45	3.02	-1.15	215.42	-117.22	-116.14	1.17	19.30	1.43	0.19	29.21	251.31	0.00
20:37:30	427.50	7.54	-6.73	3.16	-1.26	213.76	-367.05	-321.40	1.12	15.70	1.49	0.17	29.22	251.28	0.00
20:52:30	442.50	7.31	-6.50	3.13	-1.15	208.40	-92.90	-63.20	1.05	16.50	1.51	0.13	28.84	252.65	0.00
21:37:30	487.50	9.49	-8.56	3.78	-1.59	180.31	-0.54	-22.16	0.85	14.30	1.45	0.12	27.61	257.41	0.00
21:52:30	502.50	9.76	-8.81	3.83	-1.71	176.83	-83.09	-67.01	0.79	13.90	1.45	0.09	27.50	257.84	0.00
22:07:30	517.50	9.74	-9.16	2.85	-1.69	175.15	-123.83	-101.08	0.73	7.50	1.42	0.09	27.39	258.28	0.00
22:22:30	532.50	9.75	-9.10	2.94	-1.91	172.54	-104.63	-110.01	0.67	8.50	1.40	0.09	27.21	259.00	0.00
22:52:30	562.50	9.02	-8.31	3.12	-1.57	166.86	-176.50	-117.62	0.56	11.80	1.36	0.07	26.86	260.46	0.00
23:07:30	577.50	9.49	-8.81	3.13	-1.66	165.84	-137.76	-131.52	0.50	9.50	1.38	0.06	26.54	261.83	0.00
23:22:30	592.50	9.14	-8.52	2.92	-1.55	162.99	-115.76	-110.80	0.46	9.10	1.37	0.06	25.80	265.06	0.00
23:37:30	607.50	8.81	-8.34	2.46	-1.42	160.51	-122.73	-103.33	0.45	7.10	1.69	0.02	25.00	268.71	0.00

23:52:30	622.50	6.44	-6.13	1.76	-0.86	157.67	-121.36	-104.71	0.44	5.50	1.62	0.01	24.84	269.44	0.00
0:07:30	637.50	5.94	-5.68	1.51	-0.80	154.90	-93.65	-96.47	0.44	5.10	1.60	0.01	24.92	269.10	0.00
0:22:30	652.50	4.92	-4.74	1.19	-0.53	153.79	-197.17	-244.24	0.44	4.60	1.68	0.01	25.01	268.68	0.00
0:37:30	667.50	3.57	-3.44	0.83	-0.46	152.77	-218.88	-201.66	0.44	2.80	1.57	0.01	25.08	268.33	0.00
0:52:30	682.50	3.09	-2.89	1.02	-0.40	150.44	-216.55	-158.41	0.44	7.90	1.63	0.01	25.19	267.85	0.00
1:07:30	697.50	2.19	-1.89	1.04	-0.38	148.29	-87.20	-66.65	0.44	17.60	1.60	0.01	25.20	267.78	0.00
1:22:30	712.50	1.14	0.68	0.89	-0.23	146.46	-65.90	-59.97	0.43	115.80	1.57	0.01	24.77	269.77	0.00
1:37:30	727.50	1.29	0.97	0.77	-0.34	146.04	-51.23	-28.13	0.43	129.80	1.61	0.01	24.88	269.29	0.00
1:52:30	742.50	1.09	-0.27	1.03	-0.26	144.62	-4.17	-31.34	0.43	64.50	1.52	0.01	25.55	266.16	0.00
2:07:30	757.50	2.51	1.94	1.59	-0.10	144.06	-79.76	-76.80	0.43	129.40	1.65	0.02	25.71	265.48	0.00
2:22:30	772.50	3.06	2.94	0.74	-0.45	143.42	-44.55	-37.71	0.45	155.30	1.39	0.04	25.71	265.45	0.00
2:37:30	787.50	3.69	3.64	0.31	-0.49	141.93	-31.46	-36.81	0.48	164.00	1.31	0.06	25.73	265.38	0.00
2:52:30	802.50	3.14	3.10	-0.45	-0.27	141.37	-73.49	-78.58	0.53	177.50	1.32	0.06	25.75	265.30	0.00
3:07:30	817.50	3.35	3.32	-0.27	-0.33	142.31	-31.85	-34.02	0.59	174.70	1.35	0.08	25.75	265.28	0.00
3:37:30	847.50	2.39	2.37	0.00	-0.27	143.43	-106.50	-76.04	0.69	170.40	1.42	0.07	25.71	265.45	0.00
3:52:30	862.50	2.25	2.23	0.09	-0.32	143.39	-98.41	-56.55	0.75	167.50	1.33	0.18	25.66	265.68	0.00
4:07:30	877.50	1.16	0.73	0.89	-0.17	143.34	-92.23	-65.16	0.79	118.70	1.36	0.16	25.58	266.04	0.00
4:22:30	892.50	2.26	-0.47	2.16	-0.47	143.57	-123.11	-81.91	0.83	68.00	1.49	0.11	25.52	266.33	0.00
4:37:30	907.50	2.58	-0.94	2.29	-0.73	143.23	-189.26	-139.16	0.87	56.60	1.51	0.12	25.46	266.57	0.00
4:52:30	922.50	2.51	-1.07	2.17	-0.68	142.99	-97.74	-77.32	0.91	53.20	1.43	0.17	25.43	266.74	0.00
5:07:30	937.50	2.15	-0.35	2.09	-0.38	142.76	-112.17	-75.82	0.95	70.50	1.59	0.11	25.39	266.91	0.00
5:22:30	952.50	1.06	-0.25	0.93	-0.44	142.12	-1.85	-3.82	0.99	66.00	1.42	0.16	25.36	267.04	0.00
5:37:30	967.50	1.48	-0.42	1.33	-0.50	141.34	-92.87	-82.70	1.03	62.40	1.46	0.17	25.34	267.15	0.00
5:52:30	982.50	1.51	-0.56	1.35	-0.39	140.48	-86.77	-38.88	1.07	57.70	1.43	0.17	25.34	267.14	0.00
6:07:30	997.50	2.60	-1.83	1.75	-0.58	139.08	-114.81	-97.53	1.08	33.00	1.44	0.19	25.36	267.04	0.00
6:22:30	1012.50	3.86	-2.92	2.41	-0.80	137.39	-110.29	-76.64	1.09	28.90	1.54	0.15	25.38	266.97	0.00
6:37:30	1027.50	4.95	-3.89	2.95	-0.86	135.55	-81.87	-71.94	1.09	27.10	1.48	0.18	25.37	267.00	0.00
6:52:30	1042.50	4.29	-3.33	2.55	-0.91	135.70	-163.35	-136.88	1.08	27.60	1.45	0.18	25.37	267.00	0.00
7:07:30	1057.50	5.23	-3.78	3.44	-1.10	137.44	-127.15	-87.37	1.08	32.50	1.47	0.18	25.38	266.97	0.00
7:22:30	1072.50	4.25	-3.01	2.86	-0.93	138.63	-76.94	-49.49	1.06	34.20	1.47	0.18	25.38	266.97	0.00
7:37:30	1087.50	3.93	-3.13	2.25	-0.78	139.62	-31.35	-22.92	1.03	25.60	1.42	0.18	25.40	266.87	0.00
7:52:30	1102.50	5.12	-4.29	2.57	-1.08	140.06	-54.85	-44.66	1.00	21.10	1.57	0.13	25.42	266.76	0.00
8:07:30	1117.50	5.02	-4.34	2.32	-0.99	141.35	-5.50	-9.47	0.95	18.80	1.60	0.11	25.46	266.59	0.00
8:22:30	1132.50	6.24	-5.54	2.60	-1.21	143.93	2.17	8.80	0.90	15.30	1.52	0.11	25.49	266.44	0.00
8:37:30	1147.50	7.38	-6.69	2.84	-1.32	147.46	113.23	81.54	0.84	13.00	1.49	0.11	25.51	266.35	0.00
8:52:30	1162.50	7.65	-7.04	2.64	-1.40	151.15	177.06	154.21	0.79	10.60	1.49	0.09	25.55	266.20	0.00

9:07:30	1177.50	8.81	-8.07	3.12	-1.67	153.61	321.88	173.93	0.73	11.30	1.45	0.09	25.59	265.99	0.00

Table A3f. 15-min average data eddy correlation deployment vegetated site – deployment 5 – July 10- 11, 2007

Real Time	Time	U	Ux	Uy	Uz	O2	LD DO Flux	RA DO Flux	Depth	CurDir	ZeroPd	Hs	Temp	O2 Sat	Light Intensity
	min	cm s-1	cm s-1	cm s-1	cm s-1	uM	mmol O2 m-2 d-1	mmol O2 m-2 d-1	m	degrees	s	m	C	uM	lum m-2
13:37:30	7.5	3.117	-3.001	0.766	-0.35	274.97	297.89	215.29	0.7	104.9	1.38	0.06	29.087	251.75	1013.80
13:52:30	22.5	3.009	-2.925	0.6	-0.371	275.2	66.718	64.35	0.78	204.8	1.35	0.11	29.134	251.58	1055.21
14:07:30	37.5	3.319	-3.131	0.997	-0.464	322.23	-673.34	99.615	0.88	211.3	1.4	0.12	29.113	251.65	879.61
14:52:30	82.5	1.878	-1.676	0.764	-0.369	295.95	415.76	110.41	1.17	217.6	1.47	0.14	28.918	252.37	406.55
15:07:30	97.5	1.31	-0.991	0.793	-0.322	289.34	303.46	81.053	1.25	230.1	1.63	0.06	28.923	252.35	308.33
15:22:30	112.5	0.813	-0.063	0.747	-0.316	286.93	104.74	0.109	1.32	274.9	1.72	0.04	28.959	252.22	257.99
15:37:30	127.5	0.738	0.275	0.648	-0.223	294.78	143.36	-14.135	1.39	306.3	1.87	0.04	29.051	251.88	240.60
15:52:30	142.5	0.426	-0.362	0.167	-0.148	305.83	40.917	3.329	1.45	225.1	1.74	0.05	29.138	251.56	232.03
16:07:30	157.5	1.127	-0.939	0.553	-0.285	310.64	118.35	26.547	1.51	224	2.03	0.04	29.183	251.4	186.72
16:22:30	172.5	1.095	-1	0.408	-0.183	310.96	326.75	50.778	1.56	216.3	2.25	0.03	29.152	251.51	157.13
16:37:30	187.5	1.256	-1.078	0.59	-0.259	292.79	328.49	46.287	1.6	222.1	2.47	0.03	29.084	251.76	128.74
16:52:30	202.5	1.744	-1.656	0.445	-0.316	281.01	289.25	72.165	1.63	208.5	2.56	0.04	29.005	252.05	112.08
17:07:30	217.5	1.173	-1.082	-0.207	-0.405	269.14	91.707	9.033	1.65	184.9	2.38	0.03	28.887	252.48	102.76
17:22:30	232.5	1.503	-1.444	-0.091	-0.405	258.37	15.257	35.71	1.65	189.9	2.74	0.03	28.729	253.06	94.86
17:37:30	247.5	1.464	-0.69	-1.274	-0.211	255.46	-59.841	-16.013	1.63	131.7	3.03	0.02	28.658	253.33	83.88
17:52:30	262.5	1.365	-1.051	-0.788	-0.373	249.91	-76.898	-21.132	1.61	156.4	3.1	0.03	28.572	253.65	71.76
18:07:30	277.5	2.004	-1.69	-0.994	-0.416	248.92	-82.731	-26.611	1.59	163.1	3.43	0.02	28.467	254.05	54.21
18:22:30	292.5	1.908	-0.063	-1.869	-0.376	245.82	-96.094	-35.309	1.55	107.6	2.88	0.02	28.548	253.74	47.62
18:37:30	307.5	1.257	-0.468	-1.154	-0.167	244.21	-56.668	-29.348	1.5	125.1	2.35	0.02	28.63	253.43	30.54
18:52:30	322.5	1.659	0.054	-1.628	-0.315	243.29	-148.28	-44.452	1.46	102.1	2.43	0.02	28.818	252.73	15.91
19:07:30	337.5	1.906	0.955	-1.646	-0.09	247.1	-163.96	-78.841	1.41	73.9	2.34	0.02	29.074	251.79	16.93
20:22:30	412.5	7.995	7.647	-2.21	-0.75	352.53	107.02	45.151	1.04	29.3	1.58	0.02	30.29	247.56	3.04
20:37:30	427.5	8.127	7.774	-2.285	-0.626	352.47	255.62	168.29	0.96	30	1.51	0.03	30.211	247.82	2.10
20:52:30	442.5	8.417	8.15	-1.998	-0.658	352.45	344.15	369.38	0.89	26.5	1.45	0.04	30.116	248.14	1.58
21:07:30	457.5	6.93	6.77	-1.373	-0.55	345.42	366.27	289.19	0.81	24.4	1.44	0.03	30.058	248.34	1.15
21:22:30	472.5	7.372	7.233	-1.339	-0.484	319.55	584.79	543.77	0.74	23.8	1.47	0.02	30.041	248.39	0.71
21:37:30	487.5	9.195	9.044	-1.481	-0.745	290.86	421.52	453.78	0.66	22.5	1.47	0.02	29.95	248.7	0.35
21:52:30	502.5	8.594	8.512	-1.106	-0.409	264.64	342.19	319.82	0.59	21.2	1.45	0.01	29.754	249.38	0.07
22:07:30	517.5	10.636	10.519	-1.338	-0.834	248.54	63.11	81.168	0.53	20.4	1.4	0.02	29.49	250.3	0.00
22:22:30	532.5	9.386	9.309	-1.011	-0.641	240.03	-4.108	5.602	0.47	19.2	1.31	0.03	29.208	251.31	0.00
22:37:30	547.5	9.939	9.856	-1.024	-0.776	232.74	36.413	25.714	0.41	19.6	1.3	0.04	28.791	252.84	0.00
22:52:30	562.5	9.05	8.995	-0.628	-0.771	223.69	238.08	226.78	0.36	17.4	1.33	0.04	27.657	257.23	0.00
23:07:30	577.5	8.391	8.346	-0.63	-0.593	210.59	536.18	533.51	0.34	18	1.54	0.02	26.411	262.38	0.00

23:22:30	592.5	6.09	6.073	-0.222	-0.408	199.63	614.16	523.51	0.34	15.7	1.59	0.01	26.166	263.45	0.00
23:52:30	622.5	3.193	3.085	-0.796	-0.207	190.96	-192.45	-130.48	0.33	27.5	1.48	0.01	25.237	267.61	0.00
0:07:30	637.5	1.824	1.778	-0.298	-0.277	185.4	-356.67	-288.57	0.33	23.8	1.5	0.01	25.37	267	0.00
0:22:30	652.5	0.308	0.235	-0.171	-0.103	181.42	-315.09	-265.9	0.33	40.3	1.57	0.01	25.657	265.7	0.00
0:37:30	667.5	1.878	-1.806	-0.466	-0.223	177.85	-279.68	-151	0.33	177.5	1.53	0.01	26.931	260.18	0.00
0:52:30	682.5	2.619	-2.533	-0.522	-0.413	175.05	-245.11	-121.62	0.33	181.7	1.59	0.01	27.691	257.07	0.00
1:07:30	697.5	1.585	-1.561	-0.152	-0.234	172.51	-216.08	-73.908	0.34	189	1.42	0.02	27.934	256.11	0.00
1:22:30	712.5	3.697	-3.655	-0.209	-0.516	172.12	-299.49	-269.74	0.38	189.5	1.31	0.03	28.007	255.82	0.00
1:37:30	727.5	3.405	-3.332	0.378	-0.594	173.93	-306.64	-218.58	0.42	199.2	1.34	0.02	28.072	255.57	0.00
1:52:30	742.5	3.912	-3.827	0.359	-0.728	174.33	-312.26	-252.79	0.48	198.4	1.35	0.02	28.116	255.4	0.00
2:07:30	757.5	3.912	-3.821	0.604	-0.587	174.1	-295.64	-151.54	0.53	201.4	1.4	0.02	28.183	255.14	0.00
2:22:30	772.5	4.502	-4.414	0.39	-0.797	174.05	-355.6	-259.16	0.6	198.2	1.45	0.02	28.213	255.02	0.00
2:37:30	787.5	3.694	-3.415	1.237	-0.676	172.9	-296.45	-175.56	0.66	212	1.47	0.02	28.253	254.86	0.00
2:52:30	802.5	2.797	-2.74	0.14	-0.542	171.71	-199.58	-91.012	0.71	196.7	1.46	0.03	28.294	254.71	0.00
3:07:30	817.5	2.945	-2.82	0.639	-0.56	170.8	-400.8	-185.88	0.78	207.1	1.48	0.03	28.311	254.64	0.00
3:22:30	832.5	2.557	-2.289	0.985	-0.574	171.78	-308.93	-134.47	0.85	216.4	1.5	0.03	28.353	254.48	0.00
3:37:30	847.5	2.48	-2.417	-0.277	-0.484	173.22	-298.68	-88.106	0.94	186.9	1.59	0.03	28.343	254.52	0.00
3:52:30	862.5	2.553	-2.265	1.111	-0.392	177.84	-304.13	-213.55	1.01	219.5	1.43	0.09	28.325	254.59	0.00
4:07:30	877.5	0.94	-0.681	-0.61	-0.218	182.6	-152.31	-28.672	1.07	153.5	1.47	0.1	28.291	254.72	0.00
4:22:30	892.5	1.564	-1.301	0.788	-0.366	185.06	-346.51	-54.756	1.13	224	1.53	0.1	28.272	254.79	0.00
4:37:30	907.5	0.404	-0.118	-0.214	-0.322	186.66	-432.11	-65.962	1.16	145.9	1.53	0.1	28.246	254.89	0.00
4:52:30	922.5	1.02	-0.846	-0.395	-0.409	191.35	-374.41	-106.15	1.19	164.5	1.49	0.11	28.218	255	0.00
5:07:30	937.5	0.361	0.138	-0.182	-0.28	192.05	-7.969	-36.576	1.25	56.9	1.52	0.11	28.199	255.07	0.00
5:37:30	967.5	0.946	-0.87	0.273	-0.249	193.63	-287.66	-18.528	1.33	210.6	1.62	0.1	28.173	255.17	0.00
5:52:30	982.5	2.023	0.942	-1.752	-0.368	193.84	-66.255	-37.797	1.32	75	1.66	0.06	28.116	255.4	0.00
6:07:30	997.5	1.96	0.842	-1.72	-0.417	194.75	-81.193	-27.759	1.29	76.9	1.53	0.12	27.944	256.07	0.00
6:22:30	1012.5	3.47	1.896	-2.84	-0.616	187.61	-37.135	-9.392	1.25	69	1.54	0.13	27.75	256.83	0.00
6:37:30	1027.5	3.607	2.64	-2.393	-0.558	178.73	85.603	54.567	1.21	56	1.5	0.14	27.569	257.55	0.00
6:52:30	1042.5	3.094	2.155	-2.154	-0.535	170.83	56.456	29.075	1.17	58.4	1.5	0.14	27.379	258.32	0.00
7:07:30	1057.5	3.43	2.616	-2.141	-0.581	164.78	0.741	2.15	1.12	52.5	1.47	0.14	27.25	258.85	0.00
7:22:30	1117.5	6.562	6.086	-2.333	-0.754	153.36	70.792	59.185	0.89	34.6	1.43	0.14	27.338	258.49	5.26
8:22:30	1132.5	6.889	6.657	-1.639	-0.674	154.52	118.08	106.95	0.82	26.9	1.37	0.14	27.467	257.96	8.61
8:37:30	1147.5	7.548	7.378	-1.415	-0.734	158.83	143.86	84.976	0.75	24.4	1.49	0.07	27.556	257.61	14.28
8:52:30	1162.5	7.576	7.427	-1.297	-0.746	166.23	107.2	86.871	0.69	23.1	1.42	0.07	27.618	257.36	23.37
9:07:30	1177.5	8.173	8.065	-1.097	-0.738	171.07	195.94	190.89	0.64	21.2	1.4	0.07	27.634	257.29	23.51
9:22:30	1192.5	8.038	7.905	-1.295	-0.667	177.07	67.568	57.695	0.58	22.3	1.37	0.06	27.658	257.2	34.42

9:37:30	1207.5	8.77	8.713	-0.754	-0.661	185.23	3.913	34.209	0.52	18.2	1.34	0.05	27.75	256.83	52.65
9:52:30	1222.5	8.975	8.858	-1.298	-0.628	189.56	91.825	49.203	0.46	21.4	1.3	0.06	27.793	256.66	69.92
10:07:30	1237.5	8.503	8.445	-0.726	-0.68	197.3	38.461	21.699	0.41	18.6	1.27	0.06	27.189	259.12	92.19

Table A3g. 15-min average data eddy correlation deployment vegetated site – deployment 6 – July 16- 17, 2007

Real Time	Time	U	Ux	Uy	Uz	O2	LD DO Flux	RA DO Flux	Depth	CurDir	ZeroPd	Hs	Temp	O2 Sat	Light Intensity
	min	cm s-1	cm s-1	cm s-1	cm s-1	uM	mmol O2 m-2 d-1	mmol O2 m-2 d-1	m	degrees	s	m	C	uM	lum m-2
18:07:30	7.50	4.09	3.71	1.70	-0.10	293.25	724.45	621.14	0.35	173.90	1.34	0.02	27.52	257.78	1263.30
18:22:30	22.50	4.22	4.00	1.31	-0.21	266.00	735.85	526.23	0.42	171.30	1.27	0.05	28.55	253.74	675.04
18:37:30	37.50	3.33	3.31	0.33	-0.10	253.03	95.23	78.46	0.52	183.30	1.31	0.05	28.51	253.87	294.20
18:52:30	52.50	4.06	4.04	0.15	-0.32	247.43	34.93	36.19	0.61	186.50	1.34	0.06	28.45	254.12	159.39
19:07:30	67.50	3.59	3.58	-0.13	-0.18	242.34	75.51	31.05	0.70	192.80	1.38	0.05	28.38	254.39	168.78
19:37:30	97.50	3.89	3.86	-0.46	-0.23	244.10	167.51	151.62	0.89	196.30	1.36	0.10	28.23	254.94	61.68
19:52:30	112.50	2.31	2.31	-0.13	-0.07	237.32	118.79	97.88	0.96	192.90	1.38	0.10	28.15	255.28	21.29
20:07:30	127.50	1.98	1.97	-0.11	-0.18	232.94	-50.85	2.31	1.05	192.10	1.58	0.06	28.08	255.54	5.32
20:22:30	142.50	1.34	1.28	-0.38	0.02	226.00	-35.29	-34.67	1.13	205.70	1.43	0.13	28.02	255.77	0.95
20:37:30	157.50	0.57	0.56	-0.12	0.00	220.63	-170.13	-143.58	1.19	200.90	1.53	0.11	27.97	255.96	0.00
20:52:30	172.50	0.80	0.62	0.42	-0.28	215.35	-156.00	-133.19	1.26	158.40	1.49	0.11	27.93	256.12	0.00
21:07:30	187.50	0.97	0.90	-0.34	-0.12	209.86	-91.97	-60.60	1.32	207.70	1.71	0.06	27.90	256.26	0.00
21:22:30	202.50	1.50	1.45	-0.35	-0.15	203.99	-55.07	-64.52	1.40	203.50	1.83	0.05	27.85	256.45	0.00
22:22:30	262.50	1.50	1.48	0.21	-0.16	170.39	3.99	-15.02	1.58	181.30	2.18	0.04	27.20	259.07	0.00
22:37:30	277.50	1.50	1.42	-0.46	-0.17	166.01	-14.73	-11.38	1.59	208.10	2.64	0.03	27.02	259.81	0.00
22:52:30	292.50	0.63	0.55	-0.25	-0.17	164.05	-44.99	-12.55	1.59	214.20	3.15	0.03	26.90	260.31	0.00
23:37:30	337.50	0.56	0.49	0.24	-0.14	156.79	-98.80	-24.37	1.53	164.70	3.63	0.02	26.83	260.59	0.00
23:52:30	352.50	0.52	-0.49	0.16	-0.10	153.20	-32.30	-22.25	1.47	25.60	3.75	0.02	27.03	259.77	0.00
0:07:30	367.50	1.34	-1.17	0.61	-0.22	156.98	-200.49	-131.57	1.41	37.10	3.18	0.02	27.20	259.07	0.00
0:22:30	382.50	3.77	-3.27	1.77	-0.59	158.69	-815.55	-731.08	1.34	38.30	2.33	0.02	27.40	258.24	0.00
0:37:30	397.50	5.46	-4.86	2.31	-0.92	161.55	-523.13	-444.13	1.27	35.00	1.95	0.01	27.55	257.63	0.00
0:52:30	412.50	6.14	-5.60	2.34	-0.92	160.86	-887.26	-815.69	1.19	32.70	1.80	0.01	27.59	257.46	0.00
1:07:30	427.50	7.46	-7.03	2.19	-1.19	163.97	-611.70	-580.54	1.12	26.90	1.85	0.01	27.62	257.37	0.00
1:37:30	457.50	7.69	-7.45	1.52	-1.18	167.38	-328.78	-301.78	0.97	21.00	1.74	0.01	27.64	257.29	0.00
1:52:30	472.50	8.86	-8.63	1.37	-1.46	168.02	-589.76	-558.80	0.89	18.70	1.71	0.01	27.65	257.23	0.00
2:07:30	487.50	8.65	-8.49	0.87	-1.43	166.49	-377.20	-367.90	0.81	15.30	1.68	0.01	27.65	257.25	0.00
2:22:30	502.50	9.02	-8.86	0.69	-1.52	164.51	-367.21	-297.75	0.74	14.00	1.69	0.01	27.62	257.34	0.00
2:37:30	517.50	9.15	-9.01	0.34	-1.55	162.92	-384.11	-364.32	0.67	12.40	1.68	0.01	27.59	257.48	0.00
2:52:30	532.50	9.81	-9.64	0.02	-1.79	161.59	-152.55	-196.15	0.60	9.60	1.65	0.01	27.55	257.65	0.00
3:22:30	562.50	9.03	-8.90	-0.46	-1.48	157.98	-107.21	-127.09	0.48	7.00	1.46	0.01	27.42	258.15	0.00
3:37:30	577.50	8.80	-8.69	-0.47	-1.28	155.75	-554.98	-445.36	0.42	6.80	1.44	0.01	27.04	259.72	0.00
3:52:30	592.50	7.58	-7.48	-0.52	-1.14	152.08	-242.09	-233.22	0.38	5.60	1.44	0.03	25.72	265.43	0.00
4:07:30	607.50	6.50	-6.42	-0.82	-0.63	147.78	-283.06	-281.51	0.37	2.40	1.57	0.01	25.18	267.89	0.00

4:22:30	622.50	6.17	-6.10	-0.69	-0.61	144.37	-390.90	-371.71	0.36	3.30	1.55	0.01	25.09	268.31	0.00
4:37:30	637.50	5.36	-5.28	-0.75	-0.57	140.61	-293.45	-265.42	0.36	1.50	1.60	0.01	25.13	268.11	0.00
4:52:30	652.50	3.98	-3.94	-0.37	-0.37	136.06	-581.70	-554.56	0.36	4.80	1.54	0.01	25.39	266.93	0.00
5:07:30	667.50	3.58	-3.58	-0.03	-0.19	132.93	-331.84	-274.86	0.36	8.90	1.53	0.01	25.67	265.64	0.00
5:22:30	682.50	1.58	-1.47	0.52	-0.20	129.37	-413.44	-330.64	0.37	26.90	1.60	0.01	25.72	265.41	0.00
5:37:30	697.50	1.60	1.16	1.10	-0.11	124.42	-8.08	-47.94	0.37	146.40	1.58	0.01	25.67	265.65	2.32
5:52:30	712.50	2.29	2.02	1.06	-0.15	122.24	-50.35	-83.46	0.37	161.80	1.56	0.01	25.56	266.16	33.80
6:07:30	727.50	3.05	2.77	1.28	-0.14	120.25	-163.81	-133.31	0.37	165.70	1.53	0.01	26.45	262.21	143.01
6:22:30	742.50	4.35	4.10	1.43	-0.14	119.76	-154.68	-116.20	0.37	170.80	1.55	0.02	26.69	261.19	392.22
6:52:30	772.50	5.42	5.39	0.56	-0.09	123.37	-56.40	-45.28	0.49	184.40	1.40	0.02	26.74	260.99	401.69
7:07:30	787.50	5.98	5.97	-0.04	-0.40	127.83	-158.57	-149.34	0.57	190.30	1.45	0.02	26.74	260.98	493.38
7:22:30	802.50	4.51	4.51	-0.16	-0.23	130.47	-101.08	-121.44	0.64	192.20	1.42	0.02	26.76	260.87	593.11
7:37:30	817.50	3.97	3.96	-0.02	-0.27	132.15	-31.66	-13.32	0.72	189.60	1.45	0.02	26.81	260.67	649.86
7:52:30	832.50	3.74	3.73	-0.21	-0.22	134.59	-4.17	-41.98	0.80	192.90	1.49	0.03	26.86	260.45	717.93
8:07:30	847.50	2.73	2.71	-0.22	-0.16	136.59	-34.44	-9.43	0.88	194.10	1.59	0.03	26.90	260.28	743.20
8:52:30	892.50	1.56	1.55	-0.07	-0.20	137.99	-42.22	-2.39	1.10	191.90	1.72	0.03	27.04	259.71	728.42
9:07:30	907.50	1.90	1.77	-0.67	-0.16	139.89	-76.53	-40.16	1.18	210.20	1.74	0.04	27.09	259.51	701.38
9:22:30	922.50	2.02	2.01	-0.26	-0.10	142.51	-82.69	-70.59	1.25	197.50	2.04	0.03	27.15	259.27	663.58
9:37:30	937.50	1.35	1.31	-0.26	-0.17	141.12	-106.72	-59.71	1.32	200.30	2.35	0.03	27.19	259.12	638.11
9:52:30	952.50	1.45	1.29	-0.64	-0.16	141.42	-32.28	-28.26	1.38	214.90	2.30	0.03	27.20	259.05	612.05
10:07:30	967.50	0.59	0.41	-0.40	-0.13	140.73	-30.21	-26.21	1.43	232.60	3.02	0.03	27.21	259.03	599.60
10:22:30	982.50	1.16	0.99	-0.57	-0.22	140.98	-15.25	-11.91	1.48	220.30	2.95	0.03	27.19	259.09	605.35
10:37:30	997.50	0.60	0.44	-0.39	-0.14	140.77	-16.82	-16.22	1.50	231.90	3.12	0.03	27.23	258.94	642.32
10:52:30	1012.50	1.02	0.87	-0.49	-0.18	141.97	-57.94	-24.63	1.52	218.60	2.98	0.03	27.25	258.84	703.68
11:07:30	1027.50	0.14	0.12	0.03	-0.06	142.97	-50.15	-9.27	1.52	163.80	3.01	0.03	27.31	258.60	780.05
11:22:30	1042.50	0.36	0.23	0.20	-0.18	146.38	15.25	-5.17	1.51	151.50	2.70	0.03	27.38	258.32	824.83
11:37:30	1057.50	0.56	0.44	0.27	-0.24	150.26	-31.49	-23.08	1.49	163.60	2.74	0.02	27.42	258.15	863.87
11:52:30	1072.50	0.36	0.05	0.34	-0.10	151.05	-42.62	-9.74	1.47	107.80	2.43	0.03	27.46	258.01	891.06
12:07:30	1087.50	0.65	0.32	0.54	-0.15	151.07	41.84	12.07	1.44	129.40	2.63	0.02	27.55	257.62	979.91
12:22:30	1102.50	0.81	-0.46	0.64	-0.20	154.48	103.44	52.53	1.38	65.50	2.55	0.02	27.83	256.52	1142.10
12:37:30	1117.50	1.52	-1.29	0.76	-0.27	162.18	211.87	133.64	1.32	40.40	2.38	0.02	28.04	255.71	1275.87
12:52:30	1132.50	3.70	-3.16	1.85	-0.55	156.15	13.99	46.82	1.25	40.10	2.07	0.02	28.15	255.27	1469.81
13:07:30	1147.50	6.31	-5.76	2.41	-0.92	164.28	90.48	73.64	1.18	33.00	1.82	0.01	28.19	255.11	1629.51
13:22:30	1162.50	6.89	-6.58	1.75	-1.06	173.93	96.74	96.28	1.11	25.20	1.78	0.01	28.23	254.95	1873.10
13:37:30	1177.50	7.59	-7.37	1.45	-1.12	181.38	130.45	109.96	1.04	21.20	1.73	0.01	28.28	254.75	2159.46
13:52:30	1192.50	7.47	-7.35	0.72	-1.11	189.32	164.22	144.47	0.96	15.50	1.77	0.01	28.35	254.51	2500.90

14:07:30	1207.50	8.99	-8.84	0.74	-1.44	196.45	237.57	213.33	0.89	14.80	1.70	0.01	28.44	254.14	2933.57
14:22:30	1222.50	9.19	-9.06	0.30	-1.52	202.63	396.12	352.39	0.82	12.20	1.74	0.01	28.56	253.71	3310.80
14:37:30	1237.50	8.67	-8.54	0.37	-1.43	209.11	308.47	287.58	0.75	12.30	1.58	0.01	28.67	253.30	3697.50
14:52:30	1252.50	8.33	-8.19	0.08	-1.51	213.69	437.06	370.91	0.68	10.50	1.42	0.02	28.75	252.98	3959.80
15:07:30	1267.50	9.50	-9.34	-0.42	-1.70	214.43	519.10	514.81	0.62	7.20	1.46	0.01	28.82	252.73	4614.02
15:22:30	1282.50	8.29	-8.16	-0.59	-1.33	212.44	509.94	469.21	0.55	5.20	1.40	0.02	28.72	253.09	4645.15

Table A3h. 15-min average data eddy correlation deployment vegetated site – deployment 7 – July 18- 19, 2007

Real Time	Time	U	Ux	Uy	Uz	O2	LD DO Flux	RA DO Flux	Depth	CurDir	ZeroPd	Hs	Temp	O2 Sat	Light Intensity
	min	cm s-1	cm s-1	cm s-1	cm s-1	uM	mmol O2 m-2 d-1	mmol O2 m-2 d-1	m	degrees	s	m	C	uM	lum m-2
19:07:30	7.5	2.987	-2.865	-0.71	-0.459	257.89	-111.79	-80.626	0.34	196.3	1.36	0.02	27.8	256.64	69.76
19:22:30	22.5	3.548	-3.487	-0.364	-0.546	257.12	-63.928	-58.922	0.4	191.5	1.32	0.02	27.925	256.14	37.23
19:37:30	37.5	3.357	-3.304	-0.094	-0.584	254.99	-64.448	-65.455	0.46	196	1.35	0.02	27.904	256.22	19.97
19:52:30	52.5	2.939	-2.884	-0.269	-0.496	252.28	-21.745	-15.733	0.53	193.7	1.32	0.04	27.871	256.35	10.47
20:22:30	82.5	2.43	-2.379	0.035	-0.495	242.04	-31.281	9.146	0.66	199.3	1.37	0.06	27.783	256.7	0.80
20:37:30	97.5	2.334	-2.296	-0.055	-0.411	239.18	-81.612	-27.478	0.74	196.8	1.4	0.06	27.767	256.77	0.05
20:52:30	112.5	2.265	-2.206	0.324	-0.399	237.41	-129.98	-124.83	0.81	207.4	1.44	0.05	27.742	256.86	0.00
21:07:30	127.5	2.231	-2.157	0.389	-0.414	237.47	-217.08	-179.03	0.88	208.4	1.51	0.04	27.713	256.98	0.00
21:37:30	157.5	1.17	-1.105	0.308	-0.23	227.23	-41.436	-12.281	1	213.6	1.56	0.04	27.668	257.16	0.00
21:52:30	172.5	0.869	-0.846	-0.035	-0.196	222.75	-28.131	-17.219	1.06	196	1.61	0.04	27.654	257.22	0.00
22:07:30	187.5	0.788	-0.762	0.068	-0.185	220.9	-1.664	-4.827	1.12	203.3	1.67	0.04	27.637	257.28	0.00
22:22:30	202.5	1.082	-1.028	0.181	-0.283	215.94	-62.277	-11.279	1.18	209.2	1.66	0.05	27.619	257.35	0.00
22:37:30	217.5	1.121	-1.065	0.235	-0.26	211.56	-96.48	-14.41	1.23	212.1	1.68	0.05	27.606	257.41	0.00
23:07:30	247.5	0.637	-0.602	0.1	-0.183	205.04	-78.538	-32.541	1.32	210.4	1.59	0.09	27.599	257.43	0.00
23:22:30	262.5	0.902	-0.839	0.214	-0.254	202.69	-36.492	-7.727	1.36	212.6	1.64	0.07	27.593	257.46	0.00
23:37:30	277.5	0.956	-0.919	0.044	-0.261	199.16	-130.76	-75.146	1.39	201.2	1.67	0.06	27.589	257.47	0.00
23:52:30	292.5	0.264	-0.116	-0.21	-0.111	197.23	-16.428	-7.363	1.41	151.4	1.59	0.08	27.592	257.46	0.00
0:07:30	307.5	0.566	-0.411	-0.339	-0.193	195.61	-81.082	-38.609	1.41	157.5	1.77	0.05	27.605	257.41	0.00
0:22:30	322.5	1.063	0.118	-1.04	-0.187	195.01	-159.72	-112.42	1.4	100.9	1.77	0.04	27.618	257.36	0.00
0:37:30	337.5	1.56	0.252	-1.507	-0.315	195.22	-256	-98.533	1.39	98.7	1.82	0.03	27.616	257.37	0.00
0:52:30	352.5	2.519	0.465	-2.439	-0.428	196.16	-254.8	-176.73	1.35	96.5	1.69	0.04	27.582	257.5	0.00
1:07:30	367.5	1.796	0.356	-1.736	-0.287	194.83	-57.652	-33.736	1.32	96.1	1.71	0.03	27.557	257.6	0.00
1:22:30	382.5	3.108	1.446	-2.686	-0.595	190.08	-33.495	-35.326	1.28	79.9	1.61	0.05	27.534	257.7	0.00
2:37:30	457.5	5.987	5.756	-1.476	-0.729	177.94	-100.67	-28.537	0.96	32.8	1.49	0.05	27.338	258.49	0.00
3:07:30	487.5	6.647	6.555	-0.823	-0.728	174.92	-161.07	-150.16	0.82	25.7	1.47	0.03	27.231	258.93	0.00
3:52:30	532.5	6.943	6.891	-0.525	-0.667	152.54	-36.37	-45.447	0.63	23.1	1.37	0.04	27.08	259.55	0.00
4:07:30	547.5	5.868	5.838	-0.011	-0.588	142.7	-124.29	-117.74	0.58	18.7	1.34	0.04	26.99	259.92	0.00
4:37:30	577.5	7.33	7.292	-0.308	-0.673	129.76	-85.484	-69.469	0.47	21	1.32	0.03	26.791	260.76	0.00
5:07:30	607.5	6.496	6.462	0.1	-0.658	125.78	-249.06	-185.12	0.38	17.5	1.32	0.04	26.566	261.71	0.00
6:07:30	667.5	2.815	2.777	-0.35	-0.298	124.11	-69.671	-39.854	0.32	26.2	1.6	0.01	25.618	265.87	13.52
6:52:30	712.5	1.471	-1.398	-0.439	-0.129	125.66	-36.773	-8.019	0.32	183	1.62	0.01	26.4	262.42	84.78
7:22:30	742.5	1.978	-1.924	-0.357	-0.292	127.86	-25.851	-19.026	0.35	186.7	1.32	0.03	26.475	262.1	128.75
7:37:30	757.5	2.69	-2.596	-0.583	-0.399	130.41	-11.079	-15.586	0.39	184.6	1.35	0.02	26.531	261.86	111.00

7:52:30	772.5	4.011	-3.876	-0.799	-0.655	134.27	56.469	45.137	0.44	186.6	1.34	0.02	26.587	261.62	112.25
8:07:30	787.5	3.518	-3.434	-0.249	-0.719	138.72	74.45	66.731	0.5	195	1.34	0.02	26.655	261.33	106.66
8:22:30	802.5	4.405	-4.336	-0.206	-0.748	143.88	118.83	105.47	0.57	195.8	1.38	0.02	26.738	260.98	100.15
8:37:30	817.5	3.868	-3.776	0.035	-0.837	147.69	153.74	133.08	0.64	199.1	1.37	0.04	26.823	260.62	100.97
8:52:30	832.5	2.905	-2.836	0.27	-0.568	153.1	231.25	172.14	0.71	204.3	1.42	0.04	26.915	260.23	102.82
9:07:30	847.5	2.207	-2.162	0.294	-0.334	158.13	212.52	148.06	0.77	206.4	1.45	0.04	27.016	259.81	112.16
9:22:30	862.5	2.612	-2.555	0.172	-0.514	162.75	321.32	235.34	0.85	203.2	1.48	0.05	27.113	259.41	118.62
9:37:30	877.5	1.899	-1.874	0.052	-0.302	169.57	83.74	100.45	0.91	201.2	1.53	0.04	27.204	259.04	119.70
9:52:30	892.5	2.263	-2.186	0.376	-0.445	175.72	144.31	122.98	0.99	208.2	1.57	0.04	27.284	258.71	113.77
10:07:30	907.5	1.459	-1.42	0.238	-0.235	180.37	83.509	70.622	1.06	207.8	1.65	0.04	27.358	258.41	107.96
10:22:30	922.5	1.294	-1.273	0.082	-0.216	183.68	48.878	56.931	1.14	201.4	1.74	0.03	27.414	258.18	103.39
10:37:30	937.5	1.074	-0.981	0.392	-0.193	186.46	80.35	59.371	1.19	220.6	1.88	0.03	27.454	258.02	99.06
10:52:30	952.5	0.668	-0.61	0.209	-0.174	189.56	43.902	39.119	1.25	218.4	2.15	0.03	27.497	257.84	95.46
11:07:30	967.5	0.891	-0.541	0.668	-0.237	193.01	126.42	73.952	1.31	249.2	2.7	0.02	27.54	257.67	90.17
11:22:30	982.5	0.952	-0.858	0.356	-0.207	192.77	135.58	29.786	1.36	219.8	2.14	0.03	27.577	257.52	89.90
11:37:30	997.5	0.471	-0.375	0.262	-0.111	197.07	-5.831	6.401	1.39	235.1	1.9	0.04	27.61	257.39	89.28
11:52:30	1012.5	0.436	-0.335	0.211	-0.181	200.71	14.287	12.505	1.41	232.1	1.95	0.03	27.652	257.22	89.16
12:07:30	1027.5	0.731	-0.576	0.412	-0.182	206.18	15.576	37.291	1.43	233.4	2.15	0.03	27.711	256.99	84.80
12:22:30	1042.5	0.511	-0.473	-0.059	-0.184	214.77	71.955	5.115	1.45	192.7	2.29	0.03	27.884	256.3	80.48
12:37:30	1057.5	0.419	-0.38	-0.011	-0.178	219.79	18.721	-1.307	1.46	198.6	2.29	0.03	28.128	255.35	80.83
12:52:30	1072.5	0.663	-0.024	-0.653	-0.115	224.77	-32.044	-13.28	1.44	110.2	2.32	0.02	28.352	254.48	85.61
13:07:30	1087.5	1.109	0.222	-1.046	-0.294	230.41	11.734	5.721	1.41	95.6	2.27	0.02	28.447	254.13	88.63
13:22:30	1102.5	1.487	0.358	-1.436	-0.143	227.18	62.978	119.4	1.39	94.2	1.74	0.04	28.511	253.88	101.10
13:37:30	1117.5	3.321	1.979	-2.639	-0.386	228.27	406.38	369.9	1.35	71.8	1.55	0.13	28.556	253.71	107.00
13:52:30	1132.5	5.028	4.072	-2.829	-0.83	231.42	88.369	73.671	1.29	52.8	1.56	0.13	28.584	253.61	98.38
14:22:30	1162.5	5.524	5.088	-1.999	-0.797	261.72	16.564	28.408	1.19	40.2	1.53	0.12	28.674	253.27	123.58
14:37:30	1177.5	5.109	4.772	-1.716	-0.62	277.4	128.5	166.77	1.12	38.7	1.46	0.14	28.619	253.48	164.02
14:52:30	1192.5	6.236	5.923	-1.781	-0.794	287.24	135.88	125.01	1.07	35.2	1.45	0.14	28.607	253.52	165.26
15:07:30	1207.5	7.196	6.979	-1.59	-0.739	290.38	1203.5	722.99	1	30.8	1.4	0.15	28.615	253.49	168.62
15:22:30	1222.5	7.158	6.933	-1.659	-0.64	286.32	696.76	666.64	0.93	32.2	1.38	0.16	28.63	253.44	172.23
15:37:30	1237.5	6.763	6.64	-1.159	-0.556	277.32	1030	1049.9	0.87	28.8	1.5	0.11	28.637	253.41	173.82
16:07:30	1267.5	8.697	8.646	-0.515	-0.788	304.45	1421.1	1147.7	0.74	21.4	1.43	0.08	28.681	253.24	188.57

Table 4a. 15-min average datasonde deployment data from the bare sediment site.

Time	TimeAdjust	DO	DO	DO	Temp	SpCond	Cond	Depth	pH	Sal	Turb	Chl	PAR1	PAR2
min	min	mg l-1	uM	% sat	C	mS	mS	m		ppt	NTU	ug l-1	uMol	uMol
8.25	10.31	9.65	268.90	150.68	29.14	50.07	54.03	0.15	7.96	32.67	1.97	2.62	-1447.24	-887.72
22.50	28.11	9.16	255.26	143.37	29.28	50.07	54.16	0.22	7.94	32.67	4.38	2.99	-1336.08	-977.86
37.50	46.86	8.60	239.63	134.68	29.32	50.05	54.19	0.30	7.90	32.66	7.59	3.34	-1349.64	-824.44
52.50	65.60	8.12	226.26	126.96	29.23	50.05	54.09	0.39	7.86	32.65	11.90	3.60	-1646.39	-808.26
67.50	84.34	8.08	225.18	126.54	29.32	50.08	54.21	0.50	7.86	32.68	13.71	4.06	-1368.64	-643.95
82.50	103.08	7.66	213.33	120.26	29.49	50.17	54.47	0.62	7.83	32.74	15.33	4.53	-987.04	-441.76
97.50	121.83	7.29	202.95	114.50	29.53	50.20	54.55	0.74	7.80	32.76	17.44	4.78	-706.27	-278.21
112.50	140.57	7.23	201.29	113.73	29.62	50.22	54.65	0.84	7.79	32.77	17.94	4.92	-510.92	-198.86
127.50	159.31	7.13	198.55	112.31	29.69	50.24	54.74	0.94	7.78	32.78	18.24	5.27	-377.68	-146.02
142.50	178.05	7.13	198.75	112.56	29.75	50.27	54.83	1.04	7.79	32.80	18.41	6.11	-211.90	-80.97
157.50	196.80	7.18	200.15	113.36	29.76	50.30	54.87	1.14	7.80	32.82	18.73	7.56	-57.67	-21.52
172.50	215.54	7.19	200.34	113.44	29.74	50.32	54.87	1.23	7.80	32.84	20.47	8.28	-86.82	-30.83
187.50	234.28	7.21	200.90	113.81	29.75	50.33	54.89	1.31	7.81	32.84	20.60	9.10	-72.24	-25.90
202.50	253.02	7.20	200.67	113.63	29.72	50.33	54.87	1.38	7.81	32.84	20.27	9.65	-42.88	-15.56
217.50	271.77	7.06	196.54	111.13	29.64	50.31	54.76	1.45	7.80	32.83	20.98	9.87	-30.68	-11.04
232.50	290.51	6.78	188.93	106.61	29.51	50.27	54.61	1.50	7.77	32.81	21.87	9.99	-25.60	-9.20
247.50	309.25	6.54	182.23	102.65	29.42	50.26	54.50	1.53	7.75	32.80	22.45	9.89	-17.22	-6.18
262.50	327.99	6.45	179.67	101.13	29.38	50.26	54.46	1.56	7.75	32.81	23.09	9.76	-10.74	-3.89
277.50	346.74	6.39	178.10	100.20	29.33	50.27	54.43	1.55	7.75	32.81	24.31	9.47	-7.50	-2.71
292.50	365.48	6.44	179.54	100.50	29.03	50.26	54.13	1.51	7.76	32.82	26.38	9.39	-0.15	-0.33
307.50	384.22	6.56	182.85	102.38	29.04	50.26	54.14	1.46	7.79	32.82	25.01	9.65	1.41	0.12
322.50	402.96	6.61	184.21	103.35	29.17	50.26	54.26	1.40	7.82	32.81	28.05	10.22	2.04	0.29
337.50	421.71	6.83	190.33	106.82	29.19	50.26	54.28	1.35	7.84	32.81	37.46	11.36	2.29	0.39
352.50	440.45	6.88	191.53	107.42	29.14	50.26	54.24	1.24	7.83	32.82	46.36	12.11	2.38	0.40
367.50	459.19	6.89	191.80	107.54	29.12	50.27	54.23	1.14	7.83	32.82	43.96	11.92	2.40	0.40
382.50	477.93	6.85	190.96	107.06	29.11	50.29	54.24	1.06	7.83	32.84	39.97	11.83	2.40	0.40
397.50	496.68	6.83	190.21	106.68	29.12	50.31	54.27	0.98	7.83	32.85	32.80	11.44	2.40	0.38
412.50	515.42	6.84	190.57	107.02	29.20	50.34	54.38	0.90	7.85	32.87	24.41	NaN	2.37	0.32
427.50	534.16	6.84	190.64	107.18	29.28	50.36	54.48	0.82	7.84	32.89	19.76	11.06	2.40	0.32
442.50	552.90	6.82	190.11	107.02	29.37	50.29	54.49	0.72	7.84	32.83	18.87	11.16	2.39	0.34
457.50	571.65	6.54	182.21	102.18	29.15	50.17	54.15	0.61	7.81	32.75	20.13	9.77	2.40	0.37
472.50	590.39	6.31	175.88	97.84	28.69	50.07	53.60	0.52	7.78	32.69	20.58	8.74	2.40	0.40
487.50	609.13	6.18	172.19	95.21	28.31	50.03	53.19	0.44	7.75	32.67	20.79	8.61	2.40	0.40
502.50	627.87	6.06	168.80	92.78	27.97	50.00	52.84	0.35	7.72	32.65	20.36	7.83	2.40	0.40

517.50	646.62	5.96	165.94	90.88	27.75	49.98	52.60	0.26	7.70	32.65	18.34	7.07	2.40	0.38
532.50	665.36	5.89	164.08	89.54	27.53	49.97	52.38	0.17	7.70	32.65	16.80	6.27	2.40	0.38
547.50	684.10	5.82	162.21	88.27	27.35	49.96	52.20	0.09	7.69	32.65	12.91	5.75	2.40	0.40
562.50	702.84	5.75	160.18	86.96	27.21	49.96	52.06	0.04	7.68	32.65	9.74	5.11	2.40	0.40
577.50	721.59	5.71	159.05	86.14	27.08	49.96	51.94	0.03	7.68	32.65	9.12	4.46	2.40	0.40
592.50	740.33	5.73	159.65	86.32	26.97	49.96	51.84	0.09	7.68	32.66	10.60	4.67	2.42	0.40
607.50	759.07	5.67	158.00	85.32	26.90	49.96	51.77	0.12	7.67	32.66	10.36	4.64	2.42	0.40
622.50	777.81	5.70	158.73	85.64	26.85	49.97	51.73	0.18	7.68	32.67	12.48	5.24	2.41	0.40
637.50	796.56	5.77	160.82	86.78	26.84	49.99	51.75	0.22	7.69	32.68	14.74	5.81	2.40	0.37
652.50	815.30	5.76	160.53	86.68	26.88	50.01	51.80	0.29	7.70	32.70	17.04	6.03	2.40	0.39
667.50	834.04	5.72	159.42	86.10	26.88	50.01	51.81	0.35	7.69	32.70	18.06	6.15	2.44	0.40
682.50	852.78	5.67	157.91	85.27	26.88	50.00	51.79	0.46	7.68	32.69	19.91	5.34	2.49	0.40
697.50	871.53	5.62	156.67	84.70	26.96	49.99	51.86	0.58	7.67	32.68	17.29	5.31	2.45	0.40
712.50	890.27	5.60	155.99	84.53	27.09	50.01	52.01	0.67	7.67	32.69	15.24	5.22	2.44	0.40
727.50	909.01	5.53	154.16	83.68	27.19	50.03	52.12	0.73	7.67	32.70	14.15	5.22	2.40	0.40
742.50	927.75	5.50	153.21	83.31	27.27	50.06	52.23	0.80	7.69	32.72	13.74	5.31	2.40	0.40
757.50	946.50	5.50	153.25	83.46	27.37	50.10	52.37	0.88	7.70	32.75	14.27	5.46	2.40	0.39
772.50	965.24	5.63	156.70	85.49	27.47	50.16	52.53	0.94	7.74	32.79	16.92	6.43	2.40	0.38
787.50	983.98	5.79	161.19	87.99	27.49	50.19	52.58	1.02	7.79	32.82	19.07	6.42	2.40	0.38
802.50	1002.72	5.90	164.38	89.69	27.47	50.19	52.56	1.09	7.82	32.81	21.09	6.19	2.32	0.36
817.50	1021.47	6.12	170.41	93.01	27.49	50.15	52.54	1.13	7.90	32.79	20.32	4.66	1.19	-0.04
832.50	1040.21	6.19	172.45	94.01	27.43	50.15	52.47	1.15	7.93	32.78	22.82	4.23	-0.76	-0.61
847.50	1058.95	6.06	168.95	91.37	26.92	50.20	52.04	1.16	7.84	32.83	22.22	4.35	-5.25	-2.27
862.50	1077.69	6.00	167.15	89.73	26.50	50.16	51.59	1.17	7.77	32.82	19.48	4.50	-8.02	-3.41
877.50	1096.44	6.01	167.56	89.64	26.29	50.14	51.37	1.18	7.75	32.81	21.17	4.52	-13.40	-5.19
892.50	1115.18	6.06	168.93	90.23	26.20	50.11	51.26	1.18	7.75	32.79	20.56	4.75	-36.03	-13.21
907.50	1133.92	6.11	170.16	90.91	26.16	50.32	51.44	1.14	7.76	32.95	20.85	4.65	-48.30	-16.95
922.50	1152.66	6.17	171.76	91.86	26.16	50.55	51.67	1.09	7.77	33.11	23.96	4.82	-61.28	-19.18
937.50	1171.41	6.21	172.90	92.49	26.18	50.56	51.70	1.02	7.77	33.13	26.33	5.08	-80.98	-22.88
952.50	1190.15	6.32	176.04	93.97	26.04	50.59	51.60	0.94	7.77	33.15	26.00	5.26	-130.95	-37.93
967.50	1208.89	6.33	176.30	94.32	26.17	50.64	51.76	0.86	7.77	33.18	27.95	5.31	-185.38	-50.00
982.50	1227.63	6.40	178.22	95.42	26.21	50.65	51.82	0.78	7.78	33.19	27.77	5.28	-275.78	-73.92
997.50	1246.38	6.39	178.10	95.74	26.45	50.68	52.08	0.69	7.78	33.20	28.40	5.56	-406.71	-107.79
1012.50	1265.12	6.46	179.89	96.87	26.56	50.58	52.08	0.61	7.79	33.13	26.77	5.94	-590.84	-161.68
1027.50	1283.86	6.55	182.60	98.44	26.66	50.51	52.11	0.53	7.79	33.07	25.13	5.92	-849.48	-245.67
1042.50	1302.60	6.68	186.15	100.56	26.83	50.30	52.06	0.43	7.80	32.92	22.96	6.09	-1236.51	-387.95
1057.50	1321.35	6.88	191.55	103.88	27.06	50.29	52.27	0.36	7.82	32.90	19.72	5.70	-1564.62	-580.05

1072.50	1340.09	7.23	201.29	109.65	27.33	50.31	52.55	0.28	7.86	32.90	14.77	4.82	-1830.00	-845.69
1087.50	1358.83	7.69	214.16	116.96	27.49	50.32	52.72	0.23	7.89	32.91	11.64	4.07	-1984.22	-1092.73

Table 4b. 15-min average datasonde deployment data from the vegetated site.

Time	TimeAdjust	DO	DO	DO	Temp	SpCond	Cond	Depth	pH	Sal	Turb	Chl	PAR1	PAR2
min	min	mg l-1	uM	% sat	C	mS	mS	m		ppt	NTU	ug l-1	uMol	uMol
8.25	10.31	9.65	268.90	150.68	29.14	50.07	54.03	0.15	7.96	32.67	1.97	2.62	-1447.24	-887.72
22.50	28.11	9.16	255.26	143.37	29.28	50.07	54.16	0.22	7.94	32.67	4.38	2.99	-1336.08	-977.86
37.50	46.86	8.60	239.63	134.68	29.32	50.05	54.19	0.30	7.90	32.66	7.59	3.34	-1349.64	-824.44
52.50	65.60	8.12	226.26	126.96	29.23	50.05	54.09	0.39	7.86	32.65	11.90	3.60	-1646.39	-808.26
67.50	84.34	8.08	225.18	126.54	29.32	50.08	54.21	0.50	7.86	32.68	13.71	4.06	-1368.64	-643.95
82.50	103.08	7.66	213.33	120.26	29.49	50.17	54.47	0.62	7.83	32.74	15.33	4.53	-987.04	-441.76
97.50	121.83	7.29	202.95	114.50	29.53	50.20	54.55	0.74	7.80	32.76	17.44	4.78	-706.27	-278.21
112.50	140.57	7.23	201.29	113.73	29.62	50.22	54.65	0.84	7.79	32.77	17.94	4.92	-510.92	-198.86
127.50	159.31	7.13	198.55	112.31	29.69	50.24	54.74	0.94	7.78	32.78	18.24	5.27	-377.68	-146.02
142.50	178.05	7.13	198.75	112.56	29.75	50.27	54.83	1.04	7.79	32.80	18.41	6.11	-211.90	-80.97
157.50	196.80	7.18	200.15	113.36	29.76	50.30	54.87	1.14	7.80	32.82	18.73	7.56	-57.67	-21.52
172.50	215.54	7.19	200.34	113.44	29.74	50.32	54.87	1.23	7.80	32.84	20.47	8.28	-86.82	-30.83
187.50	234.28	7.21	200.90	113.81	29.75	50.33	54.89	1.31	7.81	32.84	20.60	9.10	-72.24	-25.90
202.50	253.02	7.20	200.67	113.63	29.72	50.33	54.87	1.38	7.81	32.84	20.27	9.65	-42.88	-15.56
217.50	271.77	7.06	196.54	111.13	29.64	50.31	54.76	1.45	7.80	32.83	20.98	9.87	-30.68	-11.04
232.50	290.51	6.78	188.93	106.61	29.51	50.27	54.61	1.50	7.77	32.81	21.87	9.99	-25.60	-9.20
247.50	309.25	6.54	182.23	102.65	29.42	50.26	54.50	1.53	7.75	32.80	22.45	9.89	-17.22	-6.18
262.50	327.99	6.45	179.67	101.13	29.38	50.26	54.46	1.56	7.75	32.81	23.09	9.76	-10.74	-3.89
277.50	346.74	6.39	178.10	100.20	29.33	50.27	54.43	1.55	7.75	32.81	24.31	9.47	-7.50	-2.71
292.50	365.48	6.44	179.54	100.50	29.03	50.26	54.13	1.51	7.76	32.82	26.38	9.39	-0.15	-0.33
307.50	384.22	6.56	182.85	102.38	29.04	50.26	54.14	1.46	7.79	32.82	25.01	9.65	1.41	0.12
322.50	402.96	6.61	184.21	103.35	29.17	50.26	54.26	1.40	7.82	32.81	28.05	10.22	2.04	0.29
337.50	421.71	6.83	190.33	106.82	29.19	50.26	54.28	1.35	7.84	32.81	37.46	11.36	2.29	0.39
352.50	440.45	6.88	191.53	107.42	29.14	50.26	54.24	1.24	7.83	32.82	46.36	12.11	2.38	0.40
367.50	459.19	6.89	191.80	107.54	29.12	50.27	54.23	1.14	7.83	32.82	43.96	11.92	2.40	0.40
382.50	477.93	6.85	190.96	107.06	29.11	50.29	54.24	1.06	7.83	32.84	39.97	11.83	2.40	0.40
397.50	496.68	6.83	190.21	106.68	29.12	50.31	54.27	0.98	7.83	32.85	32.80	11.44	2.40	0.38
412.50	515.42	6.84	190.57	107.02	29.20	50.34	54.38	0.90	7.85	32.87	24.41	NaN	2.37	0.32
427.50	534.16	6.84	190.64	107.18	29.28	50.36	54.48	0.82	7.84	32.89	19.76	11.06	2.40	0.32
442.50	552.90	6.82	190.11	107.02	29.37	50.29	54.49	0.72	7.84	32.83	18.87	11.16	2.39	0.34
457.50	571.65	6.54	182.21	102.18	29.15	50.17	54.15	0.61	7.81	32.75	20.13	9.77	2.40	0.37
472.50	590.39	6.31	175.88	97.84	28.69	50.07	53.60	0.52	7.78	32.69	20.58	8.74	2.40	0.40
487.50	609.13	6.18	172.19	95.21	28.31	50.03	53.19	0.44	7.75	32.67	20.79	8.61	2.40	0.40
502.50	627.87	6.06	168.80	92.78	27.97	50.00	52.84	0.35	7.72	32.65	20.36	7.83	2.40	0.40

517.50	646.62	5.96	165.94	90.88	27.75	49.98	52.60	0.26	7.70	32.65	18.34	7.07	2.40	0.38
532.50	665.36	5.89	164.08	89.54	27.53	49.97	52.38	0.17	7.70	32.65	16.80	6.27	2.40	0.38
547.50	684.10	5.82	162.21	88.27	27.35	49.96	52.20	0.09	7.69	32.65	12.91	5.75	2.40	0.40
562.50	702.84	5.75	160.18	86.96	27.21	49.96	52.06	0.04	7.68	32.65	9.74	5.11	2.40	0.40
577.50	721.59	5.71	159.05	86.14	27.08	49.96	51.94	0.03	7.68	32.65	9.12	4.46	2.40	0.40
592.50	740.33	5.73	159.65	86.32	26.97	49.96	51.84	0.09	7.68	32.66	10.60	4.67	2.42	0.40
607.50	759.07	5.67	158.00	85.32	26.90	49.96	51.77	0.12	7.67	32.66	10.36	4.64	2.42	0.40
622.50	777.81	5.70	158.73	85.64	26.85	49.97	51.73	0.18	7.68	32.67	12.48	5.24	2.41	0.40
637.50	796.56	5.77	160.82	86.78	26.84	49.99	51.75	0.22	7.69	32.68	14.74	5.81	2.40	0.37
652.50	815.30	5.76	160.53	86.68	26.88	50.01	51.80	0.29	7.70	32.70	17.04	6.03	2.40	0.39
667.50	834.04	5.72	159.42	86.10	26.88	50.01	51.81	0.35	7.69	32.70	18.06	6.15	2.44	0.40
682.50	852.78	5.67	157.91	85.27	26.88	50.00	51.79	0.46	7.68	32.69	19.91	5.34	2.49	0.40
697.50	871.53	5.62	156.67	84.70	26.96	49.99	51.86	0.58	7.67	32.68	17.29	5.31	2.45	0.40
712.50	890.27	5.60	155.99	84.53	27.09	50.01	52.01	0.67	7.67	32.69	15.24	5.22	2.44	0.40
727.50	909.01	5.53	154.16	83.68	27.19	50.03	52.12	0.73	7.67	32.70	14.15	5.22	2.40	0.40
742.50	927.75	5.50	153.21	83.31	27.27	50.06	52.23	0.80	7.69	32.72	13.74	5.31	2.40	0.40
757.50	946.50	5.50	153.25	83.46	27.37	50.10	52.37	0.88	7.70	32.75	14.27	5.46	2.40	0.39
772.50	965.24	5.63	156.70	85.49	27.47	50.16	52.53	0.94	7.74	32.79	16.92	6.43	2.40	0.38
787.50	983.98	5.79	161.19	87.99	27.49	50.19	52.58	1.02	7.79	32.82	19.07	6.42	2.40	0.38
802.50	1002.72	5.90	164.38	89.69	27.47	50.19	52.56	1.09	7.82	32.81	21.09	6.19	2.32	0.36
817.50	1021.47	6.12	170.41	93.01	27.49	50.15	52.54	1.13	7.90	32.79	20.32	4.66	1.19	-0.04
832.50	1040.21	6.19	172.45	94.01	27.43	50.15	52.47	1.15	7.93	32.78	22.82	4.23	-0.76	-0.61
847.50	1058.95	6.06	168.95	91.37	26.92	50.20	52.04	1.16	7.84	32.83	22.22	4.35	-5.25	-2.27
862.50	1077.69	6.00	167.15	89.73	26.50	50.16	51.59	1.17	7.77	32.82	19.48	4.50	-8.02	-3.41
877.50	1096.44	6.01	167.56	89.64	26.29	50.14	51.37	1.18	7.75	32.81	21.17	4.52	-13.40	-5.19
892.50	1115.18	6.06	168.93	90.23	26.20	50.11	51.26	1.18	7.75	32.79	20.56	4.75	-36.03	-13.21
907.50	1133.92	6.11	170.16	90.91	26.16	50.32	51.44	1.14	7.76	32.95	20.85	4.65	-48.30	-16.95
922.50	1152.66	6.17	171.76	91.86	26.16	50.55	51.67	1.09	7.77	33.11	23.96	4.82	-61.28	-19.18
937.50	1171.41	6.21	172.90	92.49	26.18	50.56	51.70	1.02	7.77	33.13	26.33	5.08	-80.98	-22.88
952.50	1190.15	6.32	176.04	93.97	26.04	50.59	51.60	0.94	7.77	33.15	26.00	5.26	-130.95	-37.93
967.50	1208.89	6.33	176.30	94.32	26.17	50.64	51.76	0.86	7.77	33.18	27.95	5.31	-185.38	-50.00
982.50	1227.63	6.40	178.22	95.42	26.21	50.65	51.82	0.78	7.78	33.19	27.77	5.28	-275.78	-73.92
997.50	1246.38	6.39	178.10	95.74	26.45	50.68	52.08	0.69	7.78	33.20	28.40	5.56	-406.71	-107.79
1012.50	1265.12	6.46	179.89	96.87	26.56	50.58	52.08	0.61	7.79	33.13	26.77	5.94	-590.84	-161.68
1027.50	1283.86	6.55	182.60	98.44	26.66	50.51	52.11	0.53	7.79	33.07	25.13	5.92	-849.48	-245.67
1042.50	1302.60	6.68	186.15	100.56	26.83	50.30	52.06	0.43	7.80	32.92	22.96	6.09	-1236.51	-387.95
1057.50	1321.35	6.88	191.55	103.88	27.06	50.29	52.27	0.36	7.82	32.90	19.72	5.70	-1564.62	-580.05

1072.50	1340.09	7.23	201.29	109.65	27.33	50.31	52.55	0.28	7.86	32.90	14.77	4.82	-1830.00	-845.69
1087.50	1358.83	7.69	214.16	116.96	27.49	50.32	52.72	0.23	7.89	32.91	11.64	4.07	-1984.22	-1092.73